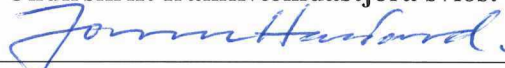


Preliminary tephra fallout hazard assessment for selected eruptive scenarios in Iceland

Sara Barsotti
Sigrún Karlsdóttir
Anna María Ágústsdóttir
Björn Oddsson
Íris Marelsdóttir
Þorvaldur Þórðarson
Þórólfur Guðnason
Bogi B. Björnsson

Preliminary tephra fallout hazard assessment for selected eruptive scenarios in Iceland

Sara Barsotti, Veðurstofa Íslands
Sigrún Karlsdóttir, Veðurstofa Íslands
Anna María Ágústsdóttir, Landgræðslan
Björn Oddsson, Almannavarnadeild Ríkislögreglustjóra
Íris Marelsdóttir, Embætti landlæknis
Þorvaldur Þórðarson, Jarðvísindastofnun Háskólans
Þórólfur Guðnason, Embætti landlæknis
Bogi B. Björnsson, Veðurstofa Íslands

Skýrsla nr. VÍ 2020-004	Dags. Júní 2020	ISSN 1670-8261	Opin <input checked="" type="checkbox"/> Lokuð <input type="checkbox"/> Skilmálar:
Heiti skýrslu / Aðal- og undirtitill: Preliminary tephra fallout hazard assessment for selected eruptive scenarios in Iceland			Upplag: 20 Fjöldi síðna: 119
Höfundar: Sara Barsotti, Sigrún Karlsdóttir, Anna María Ágústsdóttir, Björn Oddsson, Íris Marelsdóttir, Þorvaldur Þórðarson, Þórólfur Guðnason & Bogi B. Björnsson			Framkvæmdastjóri sviðs: Jórunn Harðardóttir
Þýðing myndatexta og útdráttur: Bergrún Arna Óladóttir			Verkefnisstjóri: Sara Barsotti
Gerð skýrslu/verkstíg:			Verknúmer: 3721-0-0003
Unnið fyrir:			Málsnúmer: 2020-0151
Samvinnuaðilar: Almannavarnadeild ríkislögreglustjóra, Embætti landlæknis, Jarðvísindastofnun Háskólans, Landgræðslan			
Útdráttur: Í sprengigosum myndast gjóska sem hefur margvísleg og breytileg áhrif á umhverfið nær og fjær. Með því að skoða hegðun eldstöðva í fortíð má spá fyrir um hegðun þeirra í framtíð. Hér hafa þrjár sviðsmyndir gosa verið dregnar upp og notaðar til að svara spurningum um þau áhrif sem gos gætu haft á umhverfi sitt. Heklugosið 1980 er látið vera fyrirmynd lítilla gosa; Kötlugosið 1918 er notað fyrir meðalstór gos; og Örafajökulsgosið 1362 fyrir stór gos. Gjóskafall var hermt með gjóskudreifingarlíkaninu VOL-CALPUFF en það tekur tillit til goslengdar, hæðar gosmakkar, magns gosefna og kornastærðardreifingar þeirra, auk veðurfræðigagna frá tímabilum af afmarkaðri lengd. Niðurstöður hermanna eru notaðar til þess að meta líkur á gjóskufalli á ólíkum stöðum og áhrif gjóskufalls á innviði s.s. vegi, flugvelli og raforkuflutningskerfi. Heklugos sambærilegt gosinu 1980 mundi hafa staðbundin áhrif, akstursskilyrði yrðu varhuga-verð á köflum og hugsanlega mundi rafmagni slá út vegna áhrifa á rafmagnsinnviði. Kötlugos sambærilegt gosinu 1918 gæti valdið þykku gjóskufalli á stóru landsvæði, það stæði yfir í daga eða vikur og gæti haft áhrif á samgöngur í töluverðan tíma. Ef gos yrði í Örafajökli sambærilegt því sem átti sér stað árið 1362 gæti gjóska fallið um allt land en gjóskupykkt í 25 km fjarlægð frá gosstöðvum gæti náð 1 m, akstursskilyrði yrðu skert á löngum köflum og raforkuflutningskerfi gæti orðið fyrir skemmdum.			
Lykilorð: Sprengigos, sviðsmyndir, gjóska, hættumat Eruptive scenarios, tephra fallout, hazard assessment		Undirskrift framkvæmdastjóra sviðs:  Undirskrift verkefnisstjóra:  Yfirfarið af: SG	

Contents

Figures	6
Tables	8
Abstract.....	9
Ágrip.....	11
1 General introduction.....	13
1.1 Main aim of the project.....	13
1.2 Type of results	15
1.3 Expected usage of the results	15
1.4 Icelandic volcanoes ranking.....	17
2 Selected volcanoes and selected scenarios	20
2.1 Hekla	21
2.2 Katla.....	22
2.3 Örfajökull	23
3 Volcanic hazard considered and selected infrastructure at risk	25
3.1 Volcanic tephra fallout	25
3.2 Human health	27
3.3 Roads.....	27
3.4 Airports	28
3.5 Power lines.....	29
3.6 Impact at selected locations	30
4 Methodology.....	31
4.1 General approach	31
4.2 Numerical model.....	32
4.2.1 Plume rise model	33
4.2.2 VOL-CALPUFF	34
4.3 Meteorological data.....	34
4.4 Monte-Carlo simulation	37
4.5 Event tree	38
5 Results	39
5.1 How to read a probabilistic hazard map.....	39
5.2 Hekla	41
5.2.1 Input parameters and synthetic scenario.....	41
5.2.2 Validating model results with real deposit map	43
5.2.3 Probabilistic hazard maps	45
5.2.4 Towards Impact-based maps.....	50
5.2.5 Probability of exceedance and accumulation rate.....	53
5.3 Katla.....	60
5.3.1 Input parameters and synthetic scenario.....	60

5.3.2	Probabilistic hazard maps	62
5.3.3	Towards Impact-based maps.....	69
5.4	Öræfajökull.....	72
5.4.1	Input parameters and synthetic scenario	72
5.4.2	Validating model results with real deposit map	73
5.4.3	Probabilistic hazard maps	76
5.4.4	Towards Impact-based maps.....	81
5.4.5	Probability of exceedance and accumulation rate.....	87
5.5	Towards an integration of the three explosive eruptive scenarios.....	93
6	Main conclusions and next steps	94
6.1	Tephra fallout impact during an eruption at Hekla, like 1980.....	94
6.2	Tephra fallout impact during an eruption at Katla, like 1918.....	94
6.3	Tephra fallout impact during an eruption at Öræfajökull, like 1362.....	95
6.4	Recommendations and next steps.....	96
	Note on maps and graphical tools.....	97
	Acknowledgements.....	97
	APPENDIX 0. Volcano hazard index	99
	APPENDIX I. Daily tephra dispersal simulation.....	102
	APPENDIX II. HEKLA 1980 – The likelihood of receiving tephra at different locations ...	104
	APPENDIX III. KATLA 1918 – The likelihood of receiving tephra at different locations ...	107
	APPENDIX IV. ÖRÆFAJÖKULL 1362 – The likelihood of receiving tephra at different locations	110
7	Bibliography	113

Figures

Figure 1	Risk matrix for Icelandic volcanoes.	18
Figure 2	The locations of the three volcanoes considered in this report.....	19
Figure 3	Repose time at Hekla volcano.	21
Figure 4	Timeline of VEI for the eruptions occurred at Hekla volcano.....	22
Figure 5	Statistics of eruptive style for Katla volcano.....	23
Figure 6	Isopach maps of the largest known eruption at Öræfajökull in 1362 CE.....	24
Figure 7	Examples of tephra deposits	26
Figure 8	Selected locations investigated for the Hekla eruptive scenario	30
Figure 9	Selected locations investigated for the Öræfajökull eruptive scenario.....	31
Figure 10	Basic structure of the methodology adopted for this study	32
Figure 11	Vertical profile of the vertical velocity of the volcanic mixture.	33
Figure 12	Wind roses for Hekla volcano.	35
Figure 13	Wind roses for Katla volcano.	36

Figure 14 Wind roses for Öräfajökull volcano.	37
Figure 15 Example of probabilistic tephra-fallout hazard map at Hekla volcano.	40
Figure 16 Total Grain Size Distribution (TGSD) for Hekla and Katla scenarios.....	41
Figure 17 Probabilistic hazard map for an event like 1980 at Hekla.....	42
Figure 18 Wind analysis for Hekla volcano.....	44
Figure 19 Probabilistic hazard map for a tephra load ≥ 0.1 kg/m ² (Hekla).....	45
Figure 20 Probabilistic hazard map for a tephra load ≥ 10 kg/m ² (Hekla).....	46
Figure 21 Probabilistic hazard map for a tephra load ≥ 100 kg/m ² (Hekla).....	47
Figure 22 Seasonal analysis of tephra load probability exceeding 0.1 kg/m ² (Hekla).....	48
Figure 23 Seasonal analysis for tephra probability exceeding 1 kg/m ² (Hekla).....	49
Figure 24 Seasonal analysis for tephra probability exceeding 10 kg/m ² (Hekla).....	50
Figure 25 Probabilistic hazard maps for a load ≥ 3 kg/m ² (Hekla).	51
Figure 26 Probabilistic hazard maps for a load ≥ 1 kg/m ² (Hekla).	52
Figure 27 Probabilistic hazard maps for a load ≥ 10 kg/m ² (Hekla).....	53
Figure 28 Probability of exceedance graph at key locations (Hekla).....	54
Figure 29 Tephra accumulation rate on the ground on 11 June 1984 (Hekla).....	56
Figure 30 Tephra accumulation rate on the ground on 21 September 1983 (Hekla).....	57
Figure 31 Tephra accumulation rate on the ground on 9 June 1986 (Hekla).....	58
Figure 32 Tephra accumulation rate on the ground in Geysir (Hekla).....	59
Figure 33 Event Tree for Katla volcano.	60
Figure 34 Probabilistic hazard map for a tephra load ≥ 0.1 kg/m ² (Katla).....	62
Figure 35 Probabilistic hazard map for a tephra load ≥ 1 kg/m ² (Katla).....	63
Figure 36 Probabilistic hazard maps for a tephra load ≥ 10 kg/m ² (Katla).....	64
Figure 37 Probabilistic hazard maps for a tephra load ≥ 100 kg/m ² (Katla).....	65
Figure 38 Seasonal analysis for tephra probability exceeding 1 kg/m ² (Katla).....	66
Figure 39 Seasonal analysis for tephra probability exceeding 10 kg/m ² (Katla).....	67
Figure 40 Seasonal analysis for tephra probability exceeding 100 kg/m ² (Katla).....	68
Figure 41 Impact map for road network in case of an eruption like 1918 at Katla.	69
Figure 42 Impact map for airports in case of an eruption like 1918 at Katla.	70
Figure 43 Impact map for power line in case of an eruption like 1918 at Katla.	71
Figure 44 Reconstructed Total Grain Size Distribution for the Öräfajökull scenario.....	73
Figure 45 Model results over-laid with the deposit isopach for the 1362 eruption.	74
Figure 46 Vertical velocity profile for the eruptive mixture (Öräfajökull).....	75
Figure 47 Probabilistic hazard map for a load ≥ 1.0 kg/m ² (Öräfajökull).....	76
Figure 48 Probabilistic hazard map for a load ≥ 100 kg/m ² (Öräfajökull).....	77
Figure 49 Probabilistic hazard map for a load ≥ 1000 kg/m ² (Öräfajökull).....	78
Figure 50 Seasonal analysis for 1 kg/m ² (~1mm) tephra ground load (Öräfajökull).	79
Figure 51 Seasonal analysis for 10 kg/m ² (~1 cm) tephra ground load (Öräfajökull).....	80
Figure 52 Impact map for roads in case of an eruption like 1362 at Öräfajökull.....	81
Figure 53 Impact map for airports in case of an eruption like 1362 at Öräfajökull.....	82
Figure 54 Impact map for power lines in case of an eruption like 1362 at Öräfajökull.....	83
Figure 55 5% PM ₁₀ probability map for an eruption like 1362 at Öräfajökull.....	84
Figure 56 25% PM ₁₀ probability map for an eruption like 1362 at Öräfajökull.....	85

Figure 57 50% PM ₁₀ probability map for an eruption like 1362 at Öräfajökull	86
Figure 58 The probability of exceedance curve at key locations (Öräfajökull).....	87
Figure 59 Tephra accumulation rate on the ground on 7 May 1982 (Öräfajökull)	88
Figure 60 Tephra accumulation rate on the ground on 5 May 1981 (Öräfajökull)	89
Figure 61 Tephra accumulation rate on the ground on 8 October 1982 (Öräfajökull).....	90
Figure 62 Tephra accumulation rate on the ground in Skaftafell (Öräfajökull).....	91
Figure 63 Preliminary intersectional map	93
Figure 65 Initial user-interface of the public web-site dispersion.vedur.is	102
Figure 66 Example of visualization	103
Figure 67 Example of visualization of ground loading.....	103

Tables

Table 1 List of scenarios that have been investigated in this project.	14
Table 2 Representation of the evolution with time of volcanic hazard assessment.	16
Table 3 Monitoring level assigned to each of the active Icelandic volcanoes	19
Table 4 Summary of reference volcanological scenarios.....	20
Table 5 Terminology used for pyroclastic material and its size.....	25
Table 6 Tephra fallout conditions investigated to cause insulator flashover.....	28
Table 7 Tephra fallout conditions investigated to cause electrical tower, pole and line damage. 29	
Table 8 Conversion between tephra load and tephra deposit thickness.	40
Table 9 Worst-case scenario at several locations in Iceland	55
Table 10 Total mass and volume calculations summary.	73
Table 11 Worst-case scenario of tephra load after 40 hours.....	92
Table 12 Scoring system developed by Auker et al	99
Table 13 Volcano Hazard Index calculated for Hekla, Katla and Öräfajökull	101

Abstract

When a volcano erupts several phenomena may accompany the progression of the event. If the eruption is explosive, it may feature the production of tephra and the generation of pyroclastic flows; if effusive, it may feature lava flows and gas pollution. In few instances, the transitory behavior of an eruption might produce a mix of phenomena covering the entire range of possible volcanic outcomes.

Prior an eruption it is very difficult to anticipate how the event will evolve, where it will take place, how big it will be and how it will impact the surroundings. It is, however, often the case that a question asked, mainly by Civil Protection authorities, is: what might happen if *this or that* volcano will erupt? It is possible to constraint the expected scenario by looking into what happened in the past and learn from the volcano's history as an example of its possible behavior in the future.

This report summarizes the results we obtained trying to answer the question: “which national level impact might have the tephra fallout generated by an explosive eruption occurring at Hekla, Katla or Öräfajökull?”

We provide a preliminary answer to this question by quantifying the volcanic hazard associated to tephra fallout from a predetermined eruption scenario using the VOL-CALPUFF numerical model that simulates the dispersal of volcanic material in the atmosphere. For each volcano a specific volcanological scenario (typified by mass of erupted magma, the plume height, the dimension of tephra, duration of the event) was chosen and simulated by using a large data set of meteorological conditions. For Hekla the scenario is the 1980 eruption, for Katla it is the 1918 eruption and for Öräfajökull it is the 1362 eruption. Input parameters for the dispersal model have been defined in order to reproduce these scenarios and simulate the total tephra deposits.

This report contains several maps illustrating the likelihood of tephra fall and that it exceeds critical loads of potential danger for sensitive infrastructure (like airports, powerline, roads). Each map refers to a specific eruption scenario and the likelihood is calculate as *conditional probability*, i.e. it assumes that the probability of the eruption itself is equal to 100%. Critical conditions for different infrastructure have been defined based on available data. In this sense a threshold of ~1mm of tephra deposit has been considered as critical for airport functionality, ~3 mm of tephra is the threshold adopted for critical driving conditions assessment and ~10 cm of tephra is the threshold used to evaluate impact on powerlines.

The results show that for an eruption like the 1980 event at Hekla the impact on the ground would be quite local due to short duration (≤ 2 hours). Heavy tephra fallout is expected within few kilometers from the summit. The worst-case modelled outcomes for touristic areas, such as Landmannalaugar, Þórsmörk and Gullfoss, is of a deposit over 10 kg/m^2 (~1 cm), i.e. 37, 25 and 17 cm, respectively. The results also indicate that for up to 10 km of road the conditions would be critical with a probability $> 75\%$. No airports would be directly affected by tephra fall on the ground with a likelihood higher than 5%. Around 95 km of power line network may be impacted by heavy load from tephra fallout and potential flashover, although the probability is lower than 25%.

An eruption like 1918 at Katla would have an intermediate impact on the ground where several inhabited or touristic areas, such as Þórsmörk, Vík, Landmannalaugar Skógar, could be affected by a fallout greater than 100 kg/m^2 (~10 cm). No part of the road system falls into the category of high probability ($>75\%$) for critical driving conditions. However, more than 150 km can may fall in the category of dangerous driving conditions with likelihood higher than 25%. These

results imply that an eruption in Katla might cause disruption to the commutation in the southern part of the country (including the possible impact of a jökulhlaup that will destroy entire sectors of the road). A prolonged eruption may extend the impact significantly in terms of time.

In case of an eruption like 1362 at Öräfajökull there are no places in the country completely exempt from tephra fall. In addition, the resulting tephra fallout will have a very severe impact in the proximity of the volcano with loads up to 1000 kg/m^2 , equivalent to thickness of 100 cm, expected up to a distance of about 25 km the vent. The worst-case scenario for Fagurhólsmýri and Skaftafell is tephra fallout reaching thicknesses up to 260 and 100 cm, respectively. A long sector of the Highway 1 is prone to unsafe driving conditions and, given that the road will be most likely impassable due to jökulhlaup impact, very popular localities of Höfn, Skaftafell and Jökulsarlón will be cut off the main viable connections. The airports in Hornafjörður (next to Höfn) and Egilsstaðir have the likelihood of disruption greater than 50% due to tephra fallout. This may reduce further the capability of maintaining an open connection between the capital area and the East part of the country. A large section of electricity distribution system in the area might be disrupted due to damages to power lines located southeast of the volcano.

In case of the scenarios investigated for Katla and Öräfajökull, the results indicate that inhabited regions might be exposed to heavy tephra fallout. In the light of this outcome it is recommended that exposed regions have in place plans to implement regular roof cleaning to avoid accumulation of critical load potentially causing collapse and damages to house and buildings.

Ágrip

Eldgos eru margvísleg og geta þróast á mismunandi hátt. Í sprengigosi myndast gjóska og jafnvel gjóskuflóð en hraungos mynda hraunstrauma og jafnvel töluverða gasmengun. Í gosum af báðum tegundum myndast því bæði hraun og gjóska sem skapa margvíslega eldgosavá. Fyrir upphaf eldgoss er erfitt að segja fyrir um hvar eldsupptök verða, hversu stórt gos verður, hvernig gosið mun þróast, og hvaða áhrif það mun hafa á umhverfi sitt. Með því að skoða hegðun eldgosa í fortíð og þau áhrif sem þau höfðu má draga upp líklegar sviðsmyndir þess sem búast má við í framtíðinni. Þessar sviðsmyndir má nota til að reyna að svara spurningum um það hvað mun gerast og hvaða áhrif gos í ákveðnu eldstöðvum munu hafa á nær og fjær umhverfi sitt.

Í þessari skýrslu eru sýndar niðurstöður sem fengust þegar reynt var að svara þeirri spurning hvaða áhrif gjóskufall úr sprengigosum í Heklu, Kötlu og Örfafjökli hefði á landsvísu. Gjóskudreifingarlíkan sem kallast VOL-CALPUFF var notað til að herma gjóskufall frá þremur eldstöðvum. Líkanið notast við fyrirfram skilgreindar sviðsmyndir eldgosa (s.s. lengd goss, magn og kornastærðardreifing gosefna, hæð gosmakkar) og stórt gagnasett veðurfræðigagna til að fá raunhæfa mynd af gjóskudreifingu í framtíðinni en ómögulegt er að segja hvernig vindar blása þegar næst fer að gjósa. Þrjú gos voru notuð sem fyrirmyndir, Heklugosið árið 1980 var notað sem sviðsmynd lítils Heklugoss, Kötlugosið árið 1918 var fyrirmynd meðalstórs Kötlugoss og Örfafjökulsgosið árið 1362 var notað sem sviðsmynd stórs Örfafjökulsgoss. Í upphafi var gjóskudreifingarlíkanið stillt á þann hátt að það endurskapaði gjóskudreifingu frá þessum gosum og gjóskudreifing framtíðarinnar var svo hermd með stærra veðurfræðigagnasetti til að meta líkur á gjóskufalli á mismunandi stöðum og áhrif gjóskufalls á innviði landsins (vegir, flugvellir, raforkuflutningskerfi).

Ýmis hættumatskort sem sýna líkur á að ákveðnir fyrirfram skilgreindir atburðir gerist hafa verið teiknuð miðað við þær sviðsmyndirnar sem voru skilgreindar. Hvert kort byggir á einni sviðsmynd og líkur á að ákveðnum þröskuldum sé náð eru reiknaðar. Þröskuldarnir eru a) 1 mm gjóskuþykkt á flugvöllum, en sýnt hefur verið fram á að við meiri gjóskuþykkt fer að draga úr öryggi við landing flugvéla, b) 3 mm gjóskuþykkt á vegum en þá fara akstursskilyrði að dvína og c) 10 cm þykk gjóska er viðmið fyrir áhrif á tengivirki og flutningsgetu rafmagnslína.

Niðurstöður sýna að Heklugos sambærilegt því sem átti sér stað árið 1980 myndi aðallega hafa áhrif nærri upptökum vegna þess hve stutt það stendur yfir (um 2 klst). Gert er ráð fyrir töluvert miklu gjóskufalli nærri gosupptökum (nokkrir km). Versta mögulega sviðsmynd á vinsælum ferðamannastöðum sýnir að búast má við að gjóskufall fari yfir 10 kg/m² (sambærilegt ~1 cm þykku gjóskulagi), en hermanir benda til þess að í Landmannalaugum nái gjóskuþykkt 37 cm, í Þórsmörk 25 cm og við Gullfoss má búast við 17 cm þykku gjóskulagi. Niðurstöður sýna einnig að meira en 75% líkur eru á að allt að 10 km vegakafli verði fyrir það miklu gjóskufalli að akstursskilyrði verði mjög varhugaverð. Flugvellir væru allir utan áhrifasvæðis frá gosi sambærilegu því sem varð árið 1980 sé miðað við 5% líkur. Hins vegar er töluvert af rafmagnslínum (~95 km) sem geta orðið fyrir áhrifum gjóskufalls, en líkur á útslætti rafmagns eru þó minni en 25%.

Verði gos í Kötlu sambærilegt því sem átti sér stað árið 1918 myndi það hafa áhrif á nokkur byggð svæði og vinsæla ferðamannastaði (Vík, Skógar, Þórsmörk, Landmannalaugar,) en hermt gjóskufall sýnir 100 kg/m² eða um 10 cm. Engir vegir hafa miklar líkur (>75%) á að akstursskilyrði verði mjög slæm en meira en 25% líkur eru á því að akstursskilyrði verði skert á um 150 km vegakafli. Gjóskufall vegna goss í Kötlu getur því haft áhrif á samgöngur um

Suðurland en líklega munu jökulhlaup hafa meiri áhrif á vegi en gjóskufallið sjálft. Kötlugos standa oft í nokkrar vikur og því er líklegt að áhrif á samgöngur standi í töluverðan tíma.

Komi til þess að gos svipað Öräfajökulsgosinu 1362 eigi sér stað í Öräfajökli sýna gjóskudreifingarhermanir að gjóska getur fallið um allt land. Áhrif gjóskufalls í nágrenni eldstöðvarinnar geta orðið mjög mikil en gjóskuþungi í hermunum ná 1000 kg/m^2 sem jafngildir 100 cm þykku gjóskulagi í allt að 25 km fjarlægð frá eldsupptökum. Versta mögulega sviðsmynd á Fagurhólsmýri sýnir 260 cm þykkt gjóskufall og í Skaftafelli gæti gjóska náð 100 cm þykkt. Langir vegakaflar verða þakktir gjósku sem gera aksturskilyrði ótrygg og að auki er líklegt að hluti vegakerfisins sunnan Öräfajökuls verði fyrir miklum áhrifum af jökulhlaupum sem veldur því að samgöngur um svæðið raskast mikið. Meira en 50% líkur eru á að flugvellirnir á Höfn í Hornafirði og Egilsstöðum verði fyrir áhrifum af gjóskufalli sem dregur enn úr samgöngum milli höfuðborgarsvæðisins og Austurlands. Eins er viðbúið að flutningskerfi rafmagns verði fyrir áhrifum og jafnvel skemmdum á meðan á gosi stendur og í einhvern tíma eftir að því líkur.

Sviðsmyndir frá Kötlu og Öräfajökli sýna að byggð svæði geta orðið fyrir miklu gjóskufalli. Því er mikilvægt að viðbragðsaðilar hafi getu til að hreinsa gjósku af þökum til að koma í veg fyrir að þau láti undan gjóskuþunga.

1 General introduction

This study is part of the risk assessment of Icelandic volcanoes. The overall project started in 2012 and goes by the name of GOSVÁ. The project is led by the Icelandic Meteorological Office (IMO) and its steering committee is composed by IMO, the Institute of Earth Sciences (IES, University of Iceland), the Department of Civil Protection and Emergency Management of the National Commissioner of the Icelandic Police (NCIP-DCPEM), the Soil Conservation Service of Iceland (SCSI), and the Icelandic Road and Coastal Administration (IRCA).

The main aim of the risk assessment projects is to minimize loss of lives, minimize impact on society and thereby critical infrastructure and to make the society better prepared to deal with volcanic hazards. From the onset of this risk assessment, several projects are being conducted and/or have been finalized. Overall, it is estimated that it will take 15 to 20 years to complete the whole project, and it will require a joint effort and collaboration between various institutions. The projects cover hazard assessment and where needed risk assessment for: glacial outburst in relation to sub-glacial eruptions, eruptions in vicinity of urban areas, ash- and gas-rich eruptions, pyroclastic flows, volcanic firebombs. In addition research will be conducted where necessary to fill in knowledge gaps and strengthen the hazard and risk assessment, those include estimation of eruption at sea, modelling of sub-glacial thermal activity and link to unexpected and fast glacial outburst, grain-size distribution of Icelandic eruptions, effect of ash on ecosystems and how ecosystems can act as mitigation especially for resuspension of ash. In the start of the overall project a web-browser was created, that includes all available information about the 32 active volcanoes in Iceland (www.icelandicvolcanoes.is/ www.islenskeldfjoll.is). All results obtained in the GOSVÁ project will be available at that site.

The study presented here goes under the name “Preliminary tephra fallout hazard assessment for selected eruptive scenarios in Iceland”.

1.1 Main aim of the project

There are about 30 active volcanic systems in Iceland and more than half of them have produced explosive eruptions in the past (Thordarson & Höskuldsson, 2008). Basaltic eruptions are the most common volcanic events in Iceland, and among them explosive subglacial eruptions are most frequent because many of the active central volcanoes are capped by glaciers (e.g. Katla, Grímsvötn, Bárðarbunga). Less frequent are explosive eruptions featuring more evolved magmas, such as dacite and rhyolite, that typify central volcanoes such as Öraefajökull and Hekla (Gudmundsson et al., 2008; Thordarson & Höskuldsson, 2008; Thordarson & Larsen, 2007). Highly active volcanic systems as Hekla, Katla, Bárðarbunga and Grímsvötn, have explosive eruptions rates of 82%, 97%, 90% and 95%, respectively (Gudmundsson & Larsen, 2016; Larsen & Gudmundsson, 2016b, 2016a; Larsen & Thordarson, 2016). Volcanic eruptions are quite common in Iceland and occur on average every two to five years (Larsen & Eiríksson, 2008; Thordarson & Höskuldsson, 2008; Thordarson & Larsen, 2007).

Volcanogenic floods (Pagneux et al., 2015), lava flows (Sólnes et al., 2013; T Thordarson & Höskuldsson, 2007), tephra fallout (Gudnason et al., 2017, 2018; Janebo et al., 2016; Larsen, 2002; Moles et al., 2019; Óladóttir et al., 2011), lightning (Behnke et al., 2014; Bennett et al., 2010), pyroclastic density currents (PDCs) (Jørgensen, 1981; Thordarson & Höskuldsson, 2007; Tomlinson et al., 2010; Walker, 1962), gas pollution (Gíslason et al., 2015; Thordarson & Self, 1996, 2003) are phenomena associated with past eruptions in Iceland.

Tephra dispersal and fallout is by far the most widespread hazard affecting local as well as distal regions during explosive eruptions (Folch, 2012). Ash clouds and tephra fallout can cause severe health issue (Baxter, 1990; Horwell & Baxter, 2006), affect important infrastructure like electricity supply systems (Wilson et al., 2012), the national and international transportation network (Guffanti et al., 2009; Wilson et al., 2012), sensitive buildings (Spence et al., 2005), human health and life stock, vegetation and eco-system (Ágústsdóttir, 2015; Wilson et al., 2012).

This project aims at investigating and quantifying hazard at the ground due to tephra released during explosive eruptions in Iceland. Hazard and potential impact are assessed for selected eruption scenarios.

Table 1. List of scenarios that have been investigated in this project. — *Sviðsmyndir sem notaðar eru við hermanir og útreikninga.*

Scenario	Eruption type	Volcanic eruption of reference
1	Large explosive eruption	Öræfajökull 1362 CE
2	Mid-size frequent explosive eruption	Hekla 1980 CE
3	Mid-size un-frequent explosive eruption	Katla 1918 CE

At the start of this study the aim was to focus on large explosive eruptions. However, as they occur with low frequency it was decided to add scenarios of more frequent mid-sized explosive eruptions (Table 1).

The methodology adopted in this project relies on two main steps: 1) the definition of volcanological scenarios primarily characterized by duration of the event, erupted volume, plume height (Mastin et al., 2009) and 2) the choice of a numerical model to simulate the dispersal of tephra and ash to calculate the impact on the ground. The VOL-CALPUFF model (Barsotti, Neri, et al., 2008) was used for the simulations of the selected explosive eruptive scenarios.

This report presents the three investigated scenarios and all the results obtained, providing an overview of the potential impact that some eruptions, occurring at Hekla, Katla and Öræfajökull, might have at national level when they will occur.

In all cases the results have been represented through probabilistic hazard maps to allow a long-term planning evaluation. For all investigated eruptive scenarios, the spatial extent of critical tephra deposit over the country, the disruption to roads, airports and powerlines, are assessed. For the Öræfajökull case the impact due to dangerous level of volcanic PM₁₀ has also been assessed. Analysis of the worst-case scenarios is also provided, together with probability of exceedance curves for specific sensitive sites. It is worth mentioning that this study does not provide evaluation on the potential impact induced by these events on society, population centers or humans, such an assessment needs to be further investigated in a separate project. In chapter 6.4, recommendations for further studies are given.

In addition to the results for the three scenarios, an example of an Event Tree for Katla volcano is presented to address the importance of a long-term hazard assessment based on the background knowledge of a volcano.

1.2 Type of results

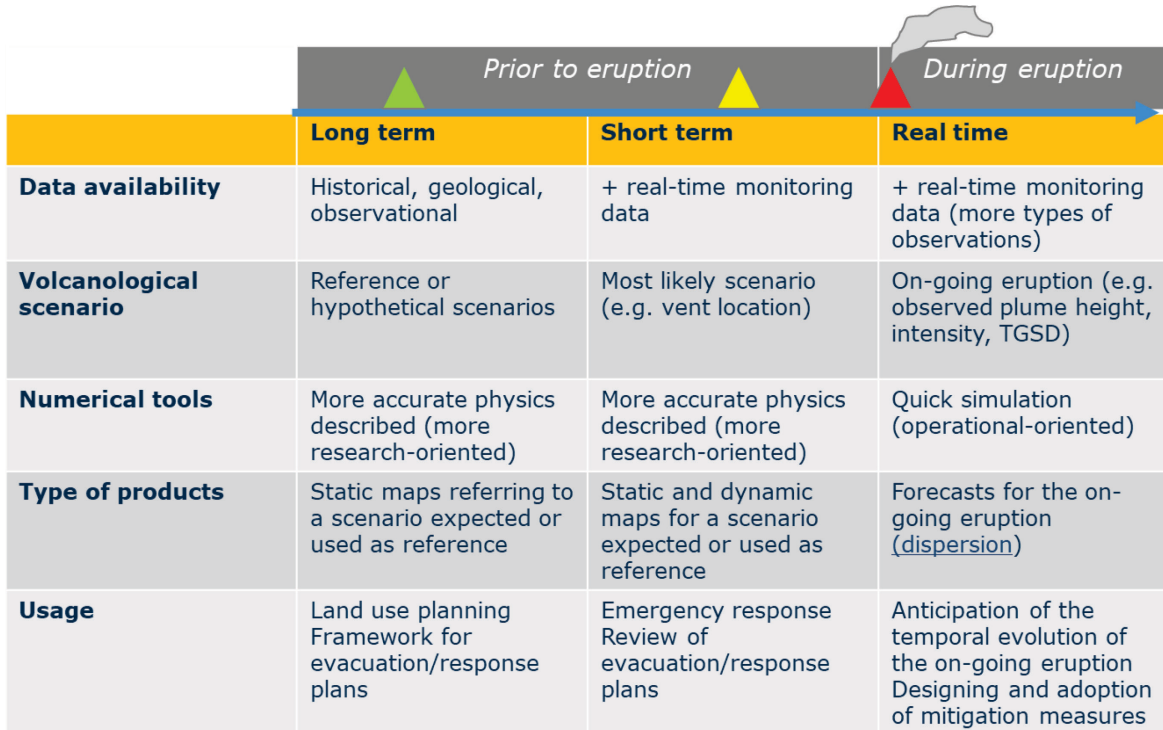
A common and well-established way to represent volcanic hazards is through maps (Calder et al., 2015; Loughlin, Vye-Brown, et al., 2015; Pallister et al., 2019). A map can visualize the spatial extent of volcanic phenomena potentially impacting the surroundings of a volcano. Different types of maps exist in the literature and are currently used by volcano monitoring institutions to communicate to their stakeholders (e.g., decision makers institutions, general public, emergency managers, land-plan managers) those areas prone to be affected by specific hazards in case of an eruption. Through a map it is possible to visualize extension of borders, sensitive infrastructures, roads, towns and villages and put the hazard into a spatial context that can be perceived in a more effective way by the users. The information contained in a hazard map can be adopted by decision-makers to evaluate and assess the risk associated to a potential eruption. Hazard maps can be produced on the basis of geological data, historical records and/or numerical model results (Mandeville et al., 2015). They can refer to a past eruption, to a specific hypothetical eruptive scenario or to a distribution of scenarios. If based on numerical results they can show the results from a single specific simulation (deterministic map) or from a multitude of scenarios. In the latter case the maps often represent the impact of a specific hazard as a spatial probability and we refer to them as “probabilistic hazard maps”. Volcanic hazard maps have been produced for several volcanoes in the world to evaluate a long-term assessment by using numerical models and several examples exist in literature. Deterministic hazard maps have been produced for pyroclastic density currents at Mt. Vesuvius (Esposti Ongaro et al., 2002), lava flows at Etna (Favalli et al., 2009) and Fogo Volcano (Richter et al., 2016); for volcanogenic floods at Öraefajökull volcano (Pagneux et al., 2015). Probabilistic hazard maps for tephra fallout have been produced for Mt. Etna (Scollo et al., 2013), Campi Flegrei (Costa et al., 2009), Ruapehu (Bonadonna et al., 2005; Hurst & Smith, 2004), Indonesian volcanoes (Jenkins et al., 2012), Santorini volcano (Jenkins et al., 2015). A multi-scale volcanic risk assessment for tephra fallout and airborne concentration was done for Hekla, Katla, Eyjafjallajökull and Askja (Biassé et al., 2014; Scaini et al., 2014). Most recently probabilistic maps for hazard due to ejection of ballistic have been produced for Etna volcano (Osman et al., 2019).

In this report we have produced probabilistic hazard maps and hazard graphs to investigate the potential impact of specific scenario-based events on ground-based infrastructure. GIS-layers containing information on power line network, roads, airport locations have been added to estimate potential disruptions to some services.

1.3 Expected usage of the results

The volcanic hazard assessment is a quantitative expression of the potential danger associated with renewed activity at a specific volcano. This information should be *functional* to selected end-users (e.g. civil protection, aviation authorities, private companies) and, as much as possible, *dynamic* to reflect the changes in the status of a volcano, e.g. quiet time, unrest time or eruption time. In this perspective a volcanic hazard assessment should be reviewed regularly whenever new data are available. Most importantly it needs to be updated as soon as the newest data coming from the monitoring suggest possible evolution from a given status of the volcano that might indicate a higher likelihood that an eruption will occur.

Table 2. Representation of the evolution with time of volcanic hazard assessment. — *Taflan sýnir hvernig mat á eldfjallavá breytist með tíma, langtímagreining (long term) felur í sér þá vinnu sem á sér stað þegar elfjall sýnir engin merki um virkni, bráðagreining (short term) tekur að auki tillit til niðurstaðna eftirlitskerfa og í rauntíma (real time) er upplýsingum úr gosinu bætt inn í mat á þeirri vá sem gos veldur.*



	Long term	Short term	Real time
Data availability	Historical, geological, observational	+ real-time monitoring data	+ real-time monitoring data (more types of observations)
Volcanological scenario	Reference or hypothetical scenarios	Most likely scenario (e.g. vent location)	On-going eruption (e.g. observed plume height, intensity, TGSD)
Numerical tools	More accurate physics described (more research-oriented)	More accurate physics described (more research-oriented)	Quick simulation (operational-oriented)
Type of products	Static maps referring to a scenario expected or used as reference	Static and dynamic maps for a scenario expected or used as reference	Forecasts for the on-going eruption (<u>dispersion</u>)
Usage	Land use planning Framework for evacuation/response plans	Emergency response Review of evacuation/response plans	Anticipation of the temporal evolution of the on-going eruption Designing and adoption of mitigation measures

A possible summary of a temporal evolution of volcanic hazard assessment is presented in Table 2. The table shows which type of data would be available during the different phases of a volcano reactivation timeline. Which type of products would be produced according to the data and the usage of these products is also reported as function of time.

In this representation a long-term hazard assessment evolves into a short-term hazard assessment and possibly even further into a real-time hazard assessment, whenever a volcano will start to show signs of reactivation and the unrest will evolve into an eruptive phase. The usage of these results moves from land-use planning and designing of a general framework for evacuation and response plans, to immediate decision-making driven by the hour-by-hour observation of the real scenario and the possible anticipation of its evolution (Marzocchi et al., 2004).

This project only investigates the *long-term hazard assessment* and the results presented here should be considered for this type of application only. The short-term and real-time assessment are dealt with in a different project (see Appendix I – Daily tephra dispersal simulations).

The main expectation from the long-term hazard assessment is that the provided results will have direct implication:

- to design and revise evacuation and response plans (e.g. spatial and temporal scales of the hazard)
- to identify critical areas exposed to a multitude of hazards that, when summed up, might create critical conditions (e.g. low air quality conditions, no transportation working, resuspended material, low visibility, areas where ecosystems might be more vulnerable due to repeated tephra fallout events)
- to identify and create other products that could support decision makers in both crises and non-eruptive time (e.g. the new PM₁₀ maps)
- to improve land-use planning (e.g. new constructions, sensitive infrastructures),
- to support further studies in other disciplines (e.g. environmental impact of the eruptions)

1.4 Icelandic volcanoes ranking

32 volcanic systems in Iceland are considered active (<http://icelandicvolcanos.is/>) and potential sources of new eruptions in the future. IMO has worked on assessing the threat associated with all these volcanoes to identify those that would need high priority either in the monitoring implementation and the hazard assessment. In order to do this IMO adopted the approach proposed by Mandeville et al. (2015) that is based on the definition and quantification of two main parameters: the Volcanic Hazard Index (VHI) and the Population Exposure Index (PEI). For each volcano these two parameters have been calculated and the results have been plotted over a matrix. VHI and PEI are defined as follows:

- VHI characterizes hazard at volcanoes based on their recorded eruption frequency, modal and maximum recorded VEI levels and occurrence of pyroclastic density currents, lahars and lava flows.
- PEI is based on populations within 10, 30 and 100 km of a volcano, which are then weighted according to evidence on historical distributions of fatalities with distance from volcanoes.

The VHI is here combined with the PEI to provide an indicator of risk, which is divided into Risk Levels I to III with increasing risk (Auker et al., 2015; Loughlin et al., 2015).

Following is the risk matrix for Icelandic volcanoes:

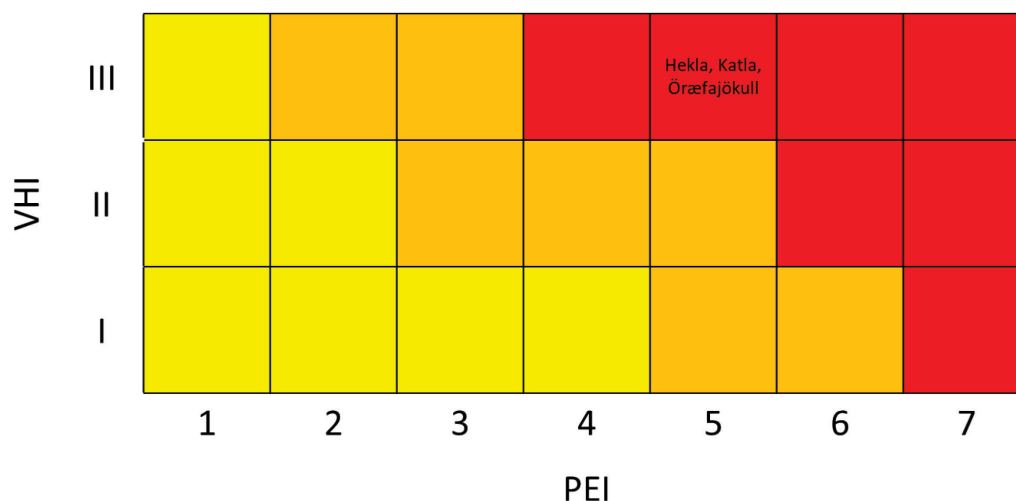


Figure 1. Risk matrix for Icelandic volcanoes. Volcanic Hazard Index (VHI) vs. Population Exposure Index (PEI) based on the methodology of Auken et al. (2015). See further discussion in the text. — *Áhættutafli íslenskra eldstöðva byggist á samspili eldfjallavár (VHI) og því hve berskjaldaður almenningur í landinu (PEI) er fyrir áhrifum af gosvá (sjá frekari umfjöllun í texta, Viðauka 0 og skýringar í grein Auken o.fl., 2015).*

To each volcano a specific category is assigned and defined by three different colors (yellow, orange and red) reflecting the level of risk. It is worth to mention here that PEI for Iceland has been calculated considering both the number of inhabitants and of visitors in the high-season. Data from inhabitants have been acquired by the Register of Iceland in 2017, whereas data from visitors at key touristic destinations have been estimated from the documents provided by the Icelandic Tourist Board (2016 and 2017). The PEI scale has been then adjusted from the original one to fit the Icelandic standards in terms of population numbers and it ranges from <200 (2) to > 10000 (7). In this way the analysis between the Icelandic volcanoes is still consistent, but the results here shown are not directly comparable with those produced for volcanoes worldwide as in the original formulations the population categories are designed to be valid for very highly-inhabited regions (Mandeville et al., 2015). More details about how the volcano hazard index (VHI) has been calculated for the three volcanoes considered in this report, are available in the Appendix 0.

Hekla, Katla and Öraefajökull, all in the highest level of risk, are treated and investigated within this project (Figure 2).

A complementary evaluation has been done to determine how to prioritize the monitoring level at different volcanoes. Three categories have been defined as: Level III (which need the more extended monitoring network), Level II (intermediate level of monitoring), Level I (minimum level of monitoring). In order to assign volcanoes into different categories two main criteria have been considered: the frequency of eruption and the potential for large eruption. In this way those volcanoes that are frequently erupting and with potential for large eruption belong to Level III; those that are frequently erupting or have potential for large eruption belong to Level II and, finally, all the remaining volcanoes belong to Level I. It was established that whenever a volcano will show signs of unrest, it will be moved directly to Level III. The results from this analysis are shown in Table 3.

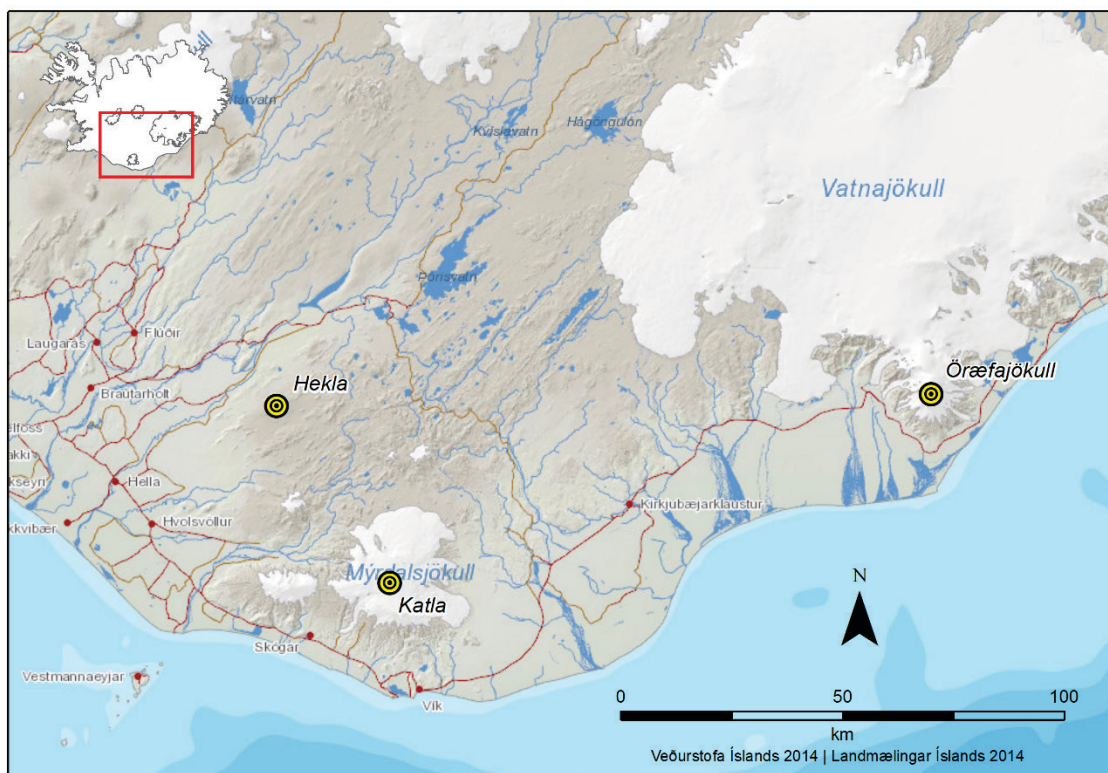


Figure 2. The locations of the three volcanoes considered in this report. — *Staðsetning þeirra þriggja megineldstöðva sem fjallað er um í þessari skýrslu.*

Table 3. Monitoring level assigned to each of the active Icelandic volcanoes. — *Vöktunarstig íslenskra eldstöðva. Stig 1: allar eldstöðvar sem ekki eru tilgreinar á stigi 2 eða 3. Stig 2: eldfjöll sem gjósa oft eða gos getur haft mikil áhrif. Stig 3: eldfjöll sem gjósa oft og geta haft mikil áhrif, og eldfjöll sem bæra á sér.*

Monitoring level 1 (all volcanoes not in level 2 and 3)	Monitoring level 2 (volcanoes either frequently erupting or with potential for large impact)	Monitoring level 3 (volcanoes frequently erupting and with potential for large impact (essentially occurrence of large eruption in the past); volcanoes in unrest)
Eldey, Esjufjöll, Fremrinámar, Grímsnes, Heiðarsporðar, Helgrindur, Hofsjökull, Hrómundartindur, Ljósufjöll, Langjökull, Prestahnúkur, Snæfell, Tungnafellsjökull, Þeistareykir	Askja, Eyjafjallajökull, Kverkfjöll, Snæfellsjökull, Tindfjallajökull, Torfajökull, Krafla, Reykjanes, Hengill, Krýsuvík, Brennisteinsfjöll, Vestmannaeyjar	Hekla, Katla, Grímsvötn/Þórðarhryna, Bárðarbunga, Öraefajökull

2 Selected volcanoes and selected scenarios

To assess the impact of an eruption it is necessary to identify *which eruption* we want to investigate. This means to identify those basic parameters that characterize the volcanological scenario we are interested in. For ash-rich eruptions these parameters are: emission duration, plume height, mass flow rate, total grain-size distribution (Mastin et al., 2009). In the following sections we report those parameters chosen to simulate volcanic ash dispersal for some reference eruptions at Hekla, Katla and Öräfajökull volcanoes. Some of these parameters can be used directly into a dispersal model, some others need to be constrained and assessed by other information. For example, the VOL-CALPUFF model is not using plume height estimates as an input parameter. The model itself solves the equations describing the rising of the mixture in the atmosphere and calculates the top-plume height by using some physical parameters as the vertical mixture velocity (V) and the radius of the vent (R). Based on these two parameters, V and R, we get an estimate of the mass flow rate and we calculate the associated plume height. The need to numerically describe this process is because often the volcanic plume is bent by wind action. Neglecting this aspect would cause an underestimation of the mass flow rate. As a consequence, the way the plume model has been used has been by matching the reported plume height for the different scenarios and identifying those erupting conditions that would have been able to reproduce that height. Several plume model descriptions exist in the literature and the one implemented in VOL-CALPUFF is the 1,5D model based on the work by Bursik (2001). A study performed in 2016 (Costa et al., 2016) indicates consistency of the VOL-CALPUFF model with the results provided by other 1,5D models allowing us to rely on the inversion performed here to get the flux values. For the three volcanoes producing explosive eruptions the scenarios of reference are reported in Table 4.

Table 4. Summary of reference volcanological scenarios used for the simulations as they are reported in the Catalogue of Icelandic Volcanoes (<http://icelandicvolcanos.is>). — *Yfirlit sviðsmynda sem unnið er með við hermun sprengigosa. Notaðar eru sviðsmyndir af vefsíðunni www.islenskeldfjoll.is.*

Volcano	Volume uncompactd (km ³)	Tephra mass (kg)	Duration of tephra/gas emission (hrs)	Plume height (km above sea level)	Reference eruption
<i>Hekla</i>	~0.06	~3.9E10	2	~15	1980 ⁽¹⁾
<i>Katla</i>	~0.7	~4.9E11	24 (+ few weeks of low level activity)	~15	1918 ⁽²⁾
<i>Öräfajökull</i>	~10	~4.8E12 (6.9E12 ^{(5)*})	18–24	25–35	1362 ⁽³⁾

* this mass estimate has been produced by using a GIS-interpolation between the isopach contour instead of a step approach (see Section 5.4.1).

⁽¹⁾ (Grönvold et al., 1983); ⁽²⁾ (Larsen, 2002; Thorarinsson, 1981); ⁽³⁾ (Thorarinsson, 1958).

2.1 Hekla

In this project we choose the 1980 CE eruption at Hekla as a reference for the frequent (1 eruption per 10 years) medium-sized (VEI = 3) eruption with a limited impact on the ground due to its short duration (few hours for the Sub-Plinian phase).

Hekla is one of the most active volcanoes in Iceland with about 18 eruptions since 1104 CE (Larsen & Thordarson, 2016). In the last century it erupted 6 times producing predominantly VEI=3 eruptions (VEI, Volcanic Explosivity Index, is a way to classify eruptions based on amount of emitted material and extension of the plume height and was introduced by Newhall and Self in 1982 (Newhall & Self, 1982). Over the last decades it erupted with almost regular interval every 10 years with the last five eruptions occurring in the 1970, 1980–1981, 1991 and 2000. All these events have been characterized by a short-lived explosive phase prolonged over a couple of hours followed by an effusive phase. Despite this apparent regular trend of the most recent period of activity, Hekla has been showing longer repose time in the past. *Figure 3* shows the repose time plotted for each eruption interval from 2000 CE back to 1104 CE. Including all the eruptions produced in this time period the average repose time is of 42,6 years (Gudnason et al., 2017).

Hekla volcano also produced some of the largest eruptions in the country with VEI=5–6, characterized by plume heights up to 35 km. These large scenarios appear to be more frequent in the past (see *Figure 4*). This could be due to a natural behavior of the volcanic system that is experiencing a rather steadily decrease in the intensity of the events since 1104 CE (Larsen et al., 2019); in addition an explanation might be that old thin deposits (produced by small eruptions) have not been well preserved until today to be identified.

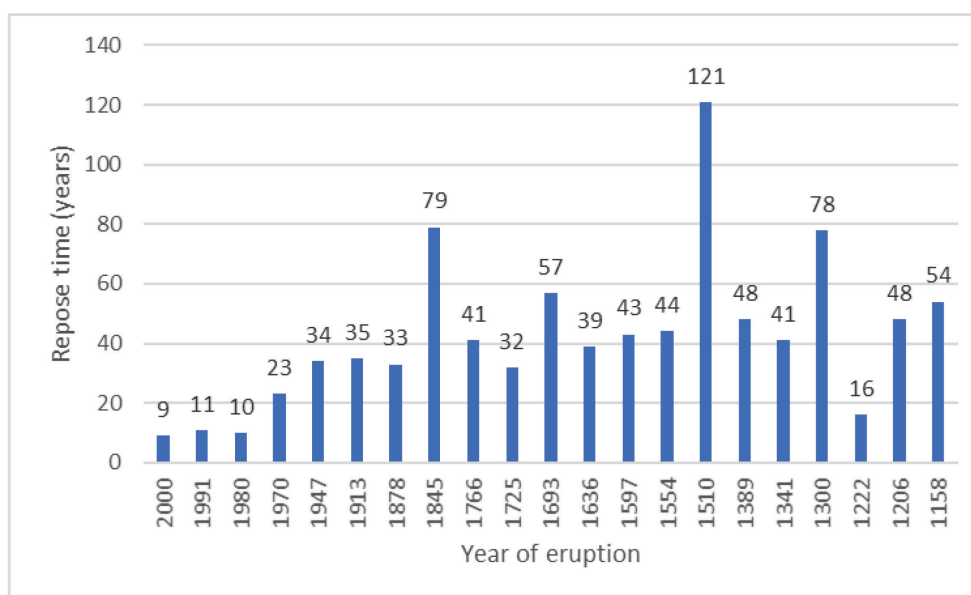


Figure 3. Repose time for Hekla volcano by considering all eruptions occurred since 1104CE til today (<http://icelandicvolcanos.is>). — *Hlé milli Heklugosa frá árinu 1104 til dagsins í dag (upplýsingar af vefsíðunni www.islenskeldfjoll.is/).*

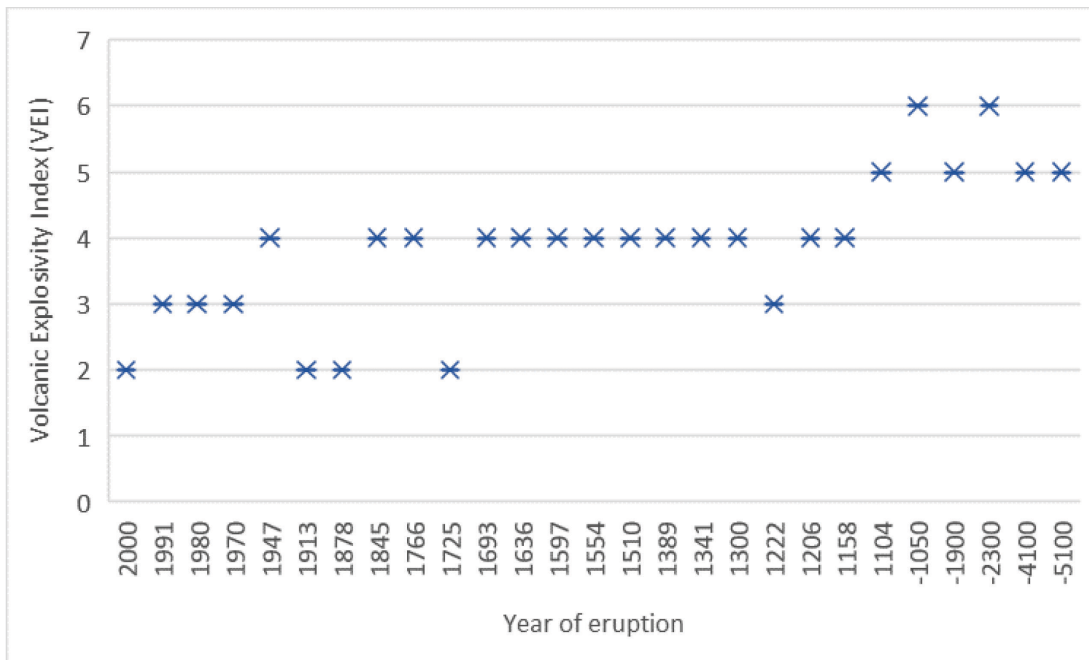


Figure 4. Timeline of VEI for the eruptions occurred at Hekla volcano. In the most recent years the most common VEI is equal to 3 (<http://icelandicvolcanos.is>). Negative years refer to BCE. — *Breytilegar stærðir Heklugosa með tíma. Stærðir eru sýndar á svokölluðum VEI kvarða (mælikvarði á sprengivirkni sem byggist á rúmmáli gjósku og hæð gosmakkar). Neikvæð ártöl tákna tímunn fyrir Krist.*

2.2 Katla

In this project we choose the 1918 CE eruption at Katla as a reference for infrequent (1 eruption per 50 years) medium-sized (VEI = 4) eruptions with a potential impact on the ground due to the eruption duration (hours to days).

As reported in the Catalogue of Icelandic Volcanoes (<http://icelandicvolcanos.is>), the partly ice covered Katla volcanic system has been highly active in the Holocene with at least 21 eruptions in the last 1100 years. The last eruption to break through the ice took place in 1918 CE. The Katla system lies on the Eastern Volcanic Zone and is about 80 km long, consisting of a central volcano rising to 1500 m a.s.l. and an active fissure extending towards northeast (Figure 2). The central volcano is partly covered by up to 700 m thick ice and has a 9x14 km ice-filled caldera. The characteristic activity is explosive basaltic eruptions at the Katla central volcano with tephra volumes (bulk volume) ranging from 0.02 to over 2 km³, accompanied by jökulhlaups with maximum discharge of up to 300,000 m³/s. Plume height ranges between 10 and 35 km. The largest eruptions are basaltic flood lava eruptions along the fissure with lava volumes up to 19.6 km³ and tephra volumes of 1.3 km³ DRE (Moreland et al., 2019). Eruption frequency during the last 1100 years is 1 eruption every 50 years.

As shown in Figure 5 the volcano has been erupting with an explosive style (generating ash cloud and tephra fallout) with a frequency up to 97%. During its last eruption in 1918 a plume reached an altitude of about 15 km for the first 24 hours. The eruption lasted for few weeks.

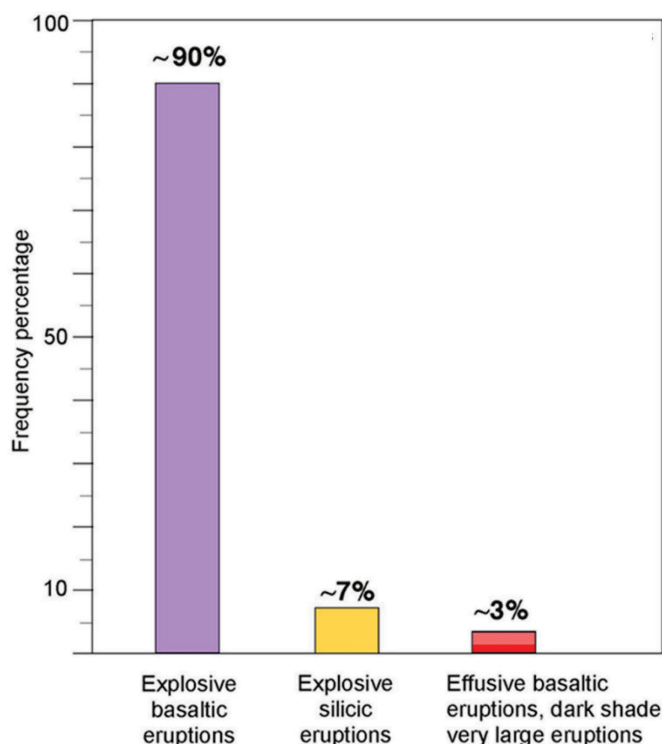


Figure 5. Statistics of eruptive style for Katla volcano. About 97% of ~330 eruptions in 8500 years have been explosive as specified in the Catalogue of Icelandic Volcanoes based on (Larsen, 2000; Óladóttir et al., 2005, 2008) (figure modified from Larsen & Thordarson, 2016). — *Gosgerðir Kötlu. Af áætluðum ~330 gosum síðustu ~8500 ára hafa um 97% verið sprengigos* (Larsen, 2000; Óladóttir o.fl., 2005, 2008). Mynd uppfærð af vefsíðunni www.islenskeldfjoll.is (Larsen & Thordarson, 2016).

2.3 Öräfajökull

In this project we choose the 1362 CE eruption at Öräfajökull. This event was chosen because it is characterized by a large explosive eruption (VEI = 6) with low frequency interval (1 eruption per 500 years) and high impact potential.

Öräfajökull is an ice-capped stratovolcano located in South-East Iceland on the southern margin of Vatnajökull glacier (Gudmundsson et al., 2008; Sharma et al., 2008; Thorarinnsson, 1958; Thordarson & Larsen, 2007). It is about 20 km in diameter with a 3x4 km ice-filled caldera which rises to a summit of 2110 m a.s.l. The volcano is part of the intraplate Öräfajökull Volcanic Belt, situated to the east of the current plate margins and possibly represents an embryonic rift (Thordarson & Höskuldsson, 2008; Thordarson & Larsen, 2007).

The Öräfajökull central volcano has only featured two explosive eruptions in historical times (Thorarinnsson, 1958). The most recent was in AD 1727–1728 with a small icelandite eruption of VEI=4 (e.g. Larsen et al., 1999, 2015). This was preceded by a much larger rhyolitic plinian eruption in 1362 CE of VEI=6. Tephrostratigraphy in soils around the volcano has identified other prehistoric silicic eruptions from the Öräfajökull volcano, all of which are assumed to be smaller in magnitude and intensity than the 1362 CE event (Gudmundsson, 1999). The plume heights may range between few kms up to 35 km.

The 1362 CE Öräfajökull eruption is the largest rhyolitic eruption in Iceland since settlement in Iceland in the 9th Century, despite the fact that the estimated volume of erupted tephra ranges from 1.2 to 2 km³, when calculated as Dense Rock Equivalent (DRE) (Selbekk & Trønnes, 2007; Sharma et al., 2008). The freshly fallen volume of the tephra deposit has been inferred to be up to 10 km³ (Thorarinsson, 1958). Early stage pyroclastic density currents and intercalated jökulhlaups, along with the subsequent tephra fall, inundated the then prosperous farming district “Litla Hérað” with associated fatalities (Jónsson, 2007; Thorarinsson, 1958; Thordarson & Höskuldsson, 2007). The reconstructed tephra dispersal is shown in Figure 6, where isopachs (i.e. lines of equal deposit thickness) for the 1362 CE eruptions are shown as black lines, and the dashed lines indicate the inferred dispersal over the sea. About half of the country received >1 mm of ash as a consequence of the tephra fall from this eruption. Close to the volcano up to 20 cm of ash accumulated over an area of 1000 km², peaks in the deposit thickness are found in Grófarlækur (40 cm) at about 10 km from the summit volcano (Thorarinsson, 1958) and between Hnappavellir and Fagurhólmsmýri where the thickness reached 2 m (Jónsson, 2007; Sharma et al., 2008). Ashes originating from 1362 CE eruption in Öräfajökull have been identified in Western Europe (Pilcher et al., 2005) and in Greenland ice cores (Palais et al., 1991). The AD 1362 event has been adopted by the Icelandic Civil Protection as the reference scenario for the hazard and risk assessment of Öräfajökull.

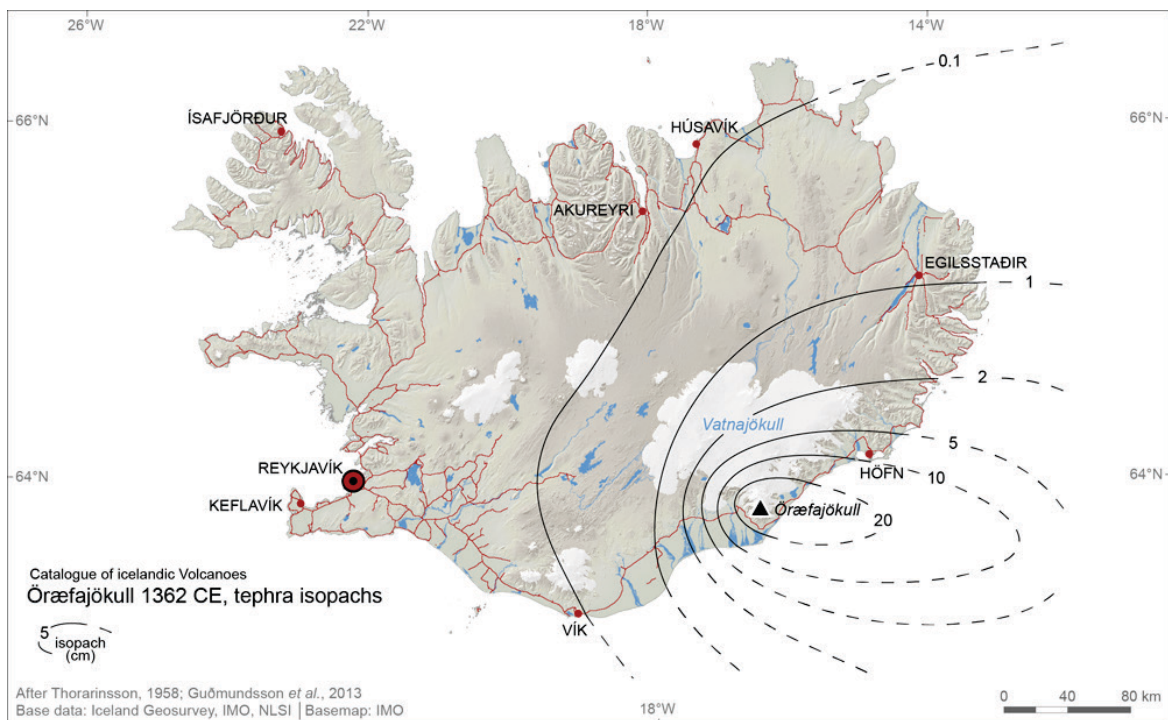


Figure 6. Isopach map of the largest known eruption at Öräfajökull in 1362 CE. It erupted 10 km³ of silicic tephra (eruption column height ~35 km) and caused a total devastation to the populated areas in its vicinity. Figure from the Catalogue of Icelandic Volcanoes (<http://icelandicvolcanos.is>). — *Jafnþykktarkort gjósku úr Öräfajökulsgosinu árið 1362. Gosið er stærsta þekktá gos í Öräfajökli en í því mynduðust um 10 km³ af kísilríkri (súrri) gjósku og hæð gosmakkar hefur verið metin ~35 km. Gosið olli miklum skemmdum í nágrenni gosstöðva og í kjölfar gossins breyttist nafn héraðsins úr Litla Hérað í Öräfi (mynd tekin af vefsíðunni www.islenskeldfjoll.is).*

3 Volcanic hazard considered and selected infrastructure at risk

During an explosive eruption several types of hazardous phenomena are concurring. The most common volcanic hazards in Iceland are: jökulhlaup, tephra fallout, lightning, pyroclastic flows, ballistic, volcanic gases, earthquakes, lahars (Gudmundsson et al., 2008; Thordarson & Höskuldsson, 2008). For the purpose of this project only two hazards have been taken into consideration, those characterized by airborne material, i.e. volcanic ash and gas clouds. Amongst all the hazards associated with explosive eruptions these two hazards have potential to affect both the ground and the atmosphere on the scale of days to few years. The eruption at Eyjafjallajökull in 2010 (Þorkelsson et al., 2012) revealed the potential of prolonged low-intensity explosive event to impact aviation and far field infrastructure. The impact on Iceland for the same scenario would have been significantly greater if the eruption would have been taking place during a southeasterly wind. In that scenario the entire country would have been affected by tephra fallout for several weeks. With this in mind, it is important to investigate the likelihood that a given eruption would produce tephra fall that may affect large part of the country.

Volcanic ash can affect different types of infrastructure and services that are vital for the daily social and economic life of a community. Within this pilot project we mainly look into three main infrastructures that, if damaged, can cause prolonged disruptions to services to the local population. The primary or direct hazards due to tephra fallout on airports, roads and power lines are here considered as they would be immediately affected by the presence of tephra and have *direct effect on the short-term*. Impact on health, in terms of exposure to the fine fraction of volcanic material is also considered for the Öräfajökull scenario.

3.1 Volcanic tephra fallout

With the term volcanic tephra we mean all the pyroclastic material released during an explosive eruption that is injected into the atmosphere. Tephra include blocks and bombs (everything larger than 64 mm in diameter), lapilli (2 mm < d < 64 mm) and ash (d < 2 mm) (Cashman & Scheu, 2015) (Table 5). Due to their small size *ash* can persist in the atmosphere for days and weeks and be transported far away from the eruptive source, whereas lapilli and bombs have a much more local impact falling closer to the vent.

Table 5. Terminology used for pyroclastic material and its size. — *Fræðiheiti gjósku og kornastærðir.*

Term	Grain diameter
Blocks and bombs	$d > 64 \text{ mm}$
Lapilli	$2 \text{ mm} < d < 64 \text{ mm}$
Ash	$d < 2 \text{ mm}$
Fine ash	$d < 0.063 \text{ mm}$

At ground level tephra can cause:

- Health issues (Baxter, 1990; Horwell & Baxter, 2006);
- Roofs/building collapse (Spence et al., 2005);
- Poor visibility conditions (Blong, 1996);
- Dangerous road conditions (Wilson et al., 2012);
- Contamination of water reservoirs and vegetation (Ágústsdóttir, 2015; Stewart et al., 2006; Wilson et al., 2012)
- Damages to electrical infrastructures (Wilson et al., 2012);
- Transportation system disruptions (Guffanti et al., 2009; Wilson et al., 2012);
- Impact on telecommunication networks (Wilson et al., 2012)

In the atmosphere volcanic ash represents a threat to aviation due to its possible ingestion by turbine engines and their potential failure (Casadevall, 1994; Prata & Tupper, 2009) (Casadevall, 1994; Guffanti et al., 2009; Prata & Tupper, 2009) as well as triggering factors for climate changes (Brasseur & Granier, 1992; Dlugokencky et al., 1996; Dutton & Christy, 1992; McCormick et al., 1995).

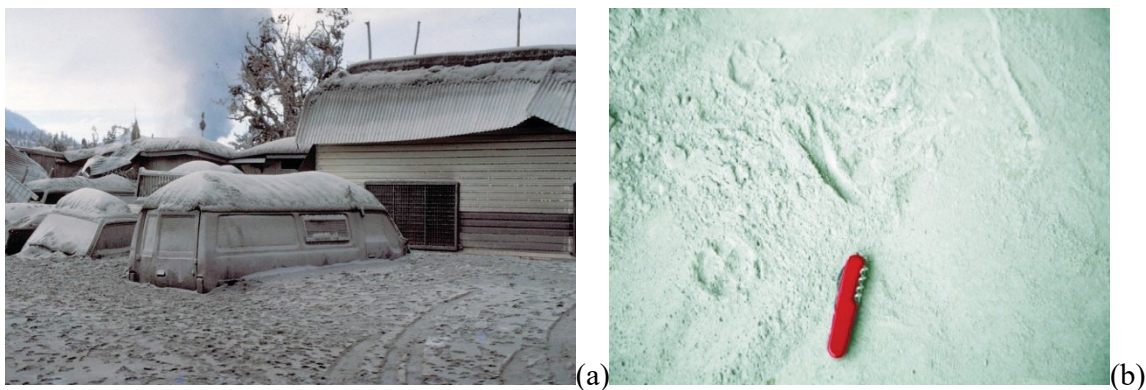


Figure 7. Examples of tephra deposits. Ash buries cars and buildings after the 1984 eruption of Rabaul, Papua New Guinea. Source: USGS; b) Ash deposit of about 8 mm thick found around Bekerah Village after the August 2010 Phreatic Eruption of Mount Sinabung, North Sumatra (Sutawidjaja et al., 2013). — *Dæmi um gjóskufall. (a) Bílar og byggingar grafin í gjósku frá eldgosi í fjallinu Rabaul á Papúa Nýju Gíneu árið 1984 (mynd frá USGS); (b) Um 8 mm þykkt gjóskufall í Beakerah Village eftir gufusprengingu í Sinabung fjalli á norður Sumötru í ágúst árið 2010 (Sutawidjaja o.fl., 2013).*

Composition of the ash, its grain-size distribution and presence of precipitation might enhance some of these hazards as for example roof collapse conditions, damages to electrical infrastructure and contamination of water and vegetation. Wet ash can reach higher load due to the contribution of rain that remains trapped in the ash deposit (Macedonio & Costa, 2012). This means that tephra fallout might have a different impact on buildings if it rains during the eruption or immediately after. Similarly, wet conditions might affect the conduction properties of ash enhancing its effect in flashover events (Wilson et al., 2012). Finally, silicic ashes are severely toxic for humans and they can have a toxic impact on water supplies and grazing animals (Stewart et al., 2006).

As a reference, two figures are reported showing a deposit of about 1 m of tephra as resulted after the eruption at Rabaul volcano, Indonesia, in 1984 (Figure 7a) and a 8-mm thick deposit measured after the eruption of Mount Sinabung in 2010 (Figure 7b).

The accumulation of tephra is a process that occurs over a period of time that starts immediately after the beginning of an eruption and lasts, often, several hours after the eruption is over (of course the finest fraction of ash can travel in the atmosphere for weeks without depositing). The initial hours after the eruption onset are often the most critical in terms of decisions and actions aimed to mitigate impact on population and infrastructure. Low visibility, severe air quality conditions and dangerous driving conditions are important factors to be considered in light of evacuation plans and identification of escaping routes. In the aftermath of an eruption, these hazards also need to be considered to assess whether and when occupants will be allowed to return into evacuated areas.

3.2 Human health

Humans can be exposed to low-quality air conditions when airborne material is contaminating the surrounding environment. Particulate matter less than 10 μm diameter (PM_{10}) is classed as thoracic, and respirable if less than 4 μm (Horwell & Baxter, 2006). During a volcanic eruption the amount of small pyroclastic material injected into the atmosphere can reach the ground and have a severe impact on air-quality level. For this purpose, the finest fraction of ash, with diameter smaller than 10 μm , has been here considered to investigate the potential impact on human health. International standards exist for daily average of exposure to critical concentration of PM_{10} and a wide literature is available for studies conducted for volcanic cases (IVHNN, 2008). The daily threshold assessed to be of a danger for humans is 50 $\mu\text{g}/\text{m}^3$. The effect of exposure to such concentration might vary and it depends on particle size, chemical content and the amount of exposure (Damby et al., 2017; Gudmundsson, 2011; Horwell & Baxter, 2006) in addition to the susceptibility of the subject itself. However, in this project the time frame of interest for the specific volcanological scenarios investigated is of the order of hours to days, with a particular interest in the period following immediately the onset of an eruption when mitigation measures, like evacuation procedures, could still be on-going. In this sense the 50 $\mu\text{g}/\text{m}^3$ threshold cannot be adopted for our purposes. As there are currently no clear standards for air-quality assessment when it goes to hourly PM_{10} concentration, it was decided to adopt a range of concentrations coming from independent studies performed in other volcanic areas. For example based on a study done for Montserrat it resulted that in a condition of hourly PM_{10} concentration higher than 300 $\mu\text{g}/\text{m}^3$ “Masks should be worn and efforts made to reduce exposure” (Horwell & Baxter, 2006). Other studies identify a threshold of 3000 $\mu\text{g}/\text{m}^3$ to be representative of a limit of concerns for human health. For the purpose of this project we investigated the effect on humans considering both thresholds.

3.3 Roads

The presence of volcanic ash on road surface is a threat for the safety of vehicular transportation. It can cause the reduction of tyres friction, obscure road markings, cause blockage of engine air intake filters, and reduce the visibility for drivers. Few studies have properly investigated the thresholds of ash deposit capable to create critical driving conditions. Recently, Blake et al. (2017) provided the results of laboratory experiments aimed to investigate how the properties of ash deposit (thickness, presence of precipitation, particle composition, particle size) can compromise skid resistance. These results showed that for a 1mm-thick ash deposit the skid resistance is below the safety level for difficult sites (even lower for dry conditions).

In most cases for thicker deposit (>5mm) the conditions are more favorable, with skid resistance above the value considered safe. The paper concludes by identifying an ash deposit thickness up to 5mm as a critical limit for which mitigation actions need to be taken to guarantee safe driving conditions on roads. At the same time Blake et al. (2017) presents a list of road disruptions occurred at volcanoes worldwide and shows how in several cases deposit several-tens-of-mm-thick has been causing difficulties to the ground transportation (Barnard, 2004). Considering these guidelines, a threshold of 3 mm has been used as a critical level in our analysis. For the analysis reported here we have been considering all the paved and unpaved roads according to the National Land Survey IS50V database (v3.4, 2012).

<i>Fine & Dry Ash</i>	Deposit Thickness < 5mm	Deposit Thickness > 5mm
Insulator Flashover (line voltage <33kV)	Low	Low
Insulator Flashover (line voltage >33kV)	Low	Low

<i>Fine & Wet Ash</i>	Deposit Thickness < 5mm	Deposit Thickness > 5mm
Insulator Flashover (line voltage <33kV)	High	High
Insulator Flashover (line voltage >33kV)	Medium	High

Table 6. Tephra fallout conditions investigated to cause insulator flashover for wet and dry ash (Wilson et al., 2012). — *Áætlaðar líkur á að gjóska (annars vegar þurr og hins vegar blaut) valdi skammhlaupi og útslætti á flutningskerfi rafmagns (Wilson o.fl., 2012).*

3.4 Airports

As reported by Guffanti et al (2009) the primary hazard to airports is ashfall, which can cause loss of visibility, create slippery runways, infiltrate communication and electrical systems, interrupt ground services, and damage buildings and parked airplanes. The skid resistance analysis performed by Blake et al (2017) can be partly applied to airfield and runways even though no clear thresholds exist for this environment with each airport operating authorities responsible for maintaining the runways functional and secure. Some critical conditions described for roads can also be applied to airfield and runways with few-mm ash deposit a condition that can be considered critical for safe operations. Here we consider 1 mm to be a critical limit for disruption to runways. For this report we have been considering all those airports for which there are scheduled flights (“Áætlunaryöllur” as based on data from the National Land Survey IS50V database (v3.4, 2012). In the maps produced for this report other locations are included as they correspond to what is referred to be “landing strips” (in Icelandic “lendingarstaður”) or more generally “a place to land”. The data originates from the National Land Survey IS50V cartographic database where a classification code for these areas exists. Even though there are no scheduled flights their location is mapped for reference.

3.5 Power lines

Wilson et al. (2012) was used to quantify specific thresholds of ash thickness and the level of impact (low, medium and high) it would have on critical infrastructure. Critical infrastructure as power lines have been investigated for what concerns damages due to:

- Insulator flashover
- Electrical tower and pole damage
- Electrical line damage

<i>Fine & Dry Ash</i>	Deposit Thickness < 100mm	Deposit Thickness > 100mm
Electrical Tower and Pole Damage	Low	Medium
Electrical Line Damage	Low	Medium

<i>Fine & Wet Ash</i>	Deposit Thickness < 5mm	Deposit Thickness > 5mm
Electrical Tower and Pole Damage	Low-Medium	Medium-High
Electrical Line Damage	Low-Medium	High

Table 7. Tephra fallout conditions investigated to cause electrical tower, pole and line damage for wet and dry ash (Wilson et al., 2012). — *Áætlaðar líkur á að gjóska (annars vegar þurr og hins vegar blaut) valdi skemmdum á flutningskerfi rafmagns (Wilson o.fl., 2012).*

The effect of volcanic ash on this type of infrastructure depends on three main factors: the grain-size, the amount of tephra load and if the deposition is occurring in wet conditions (either water vapor in the plume or meteorological precipitation). Table 6 and Table 7 summarize the results as reported in the mentioned paper. Some of these deposit thickness thresholds have been adopted to perform the analysis of impact on power lines.

It results that for a deposit larger than 5 mm in wet conditions there is a high likelihood of insulator flashover. Damages to tower, poles and lines are highly likely for thicknesses larger than 100 mm in dry conditions and 5 mm in wet conditions. In the following analysis we have been considering the likelihood to get deposit larger than 10 mm and 100 mm in dry conditions. The assumption is that these limits can be considered as of danger in wet condition for a fully wet deposit (i.e. all the voids in the deposit are full of water).

Only the national network owned by the principal Icelandic company Landsnet, which operates from 33 kV to 220 kV power transmission lines, has been considered in this analysis but no explicit references are done to the smaller lines responsible for the domestic distribution (11 kV to 33 kV). This was done to investigate the worst disruption in the electricity supply, but it is worth to mention that the national network is slightly less vulnerable than the domestic one (Wilson et al., 2012), this implies that whenever the large scale electric distribution line will be disrupted similar disruptions should be expected also on the smaller lines.

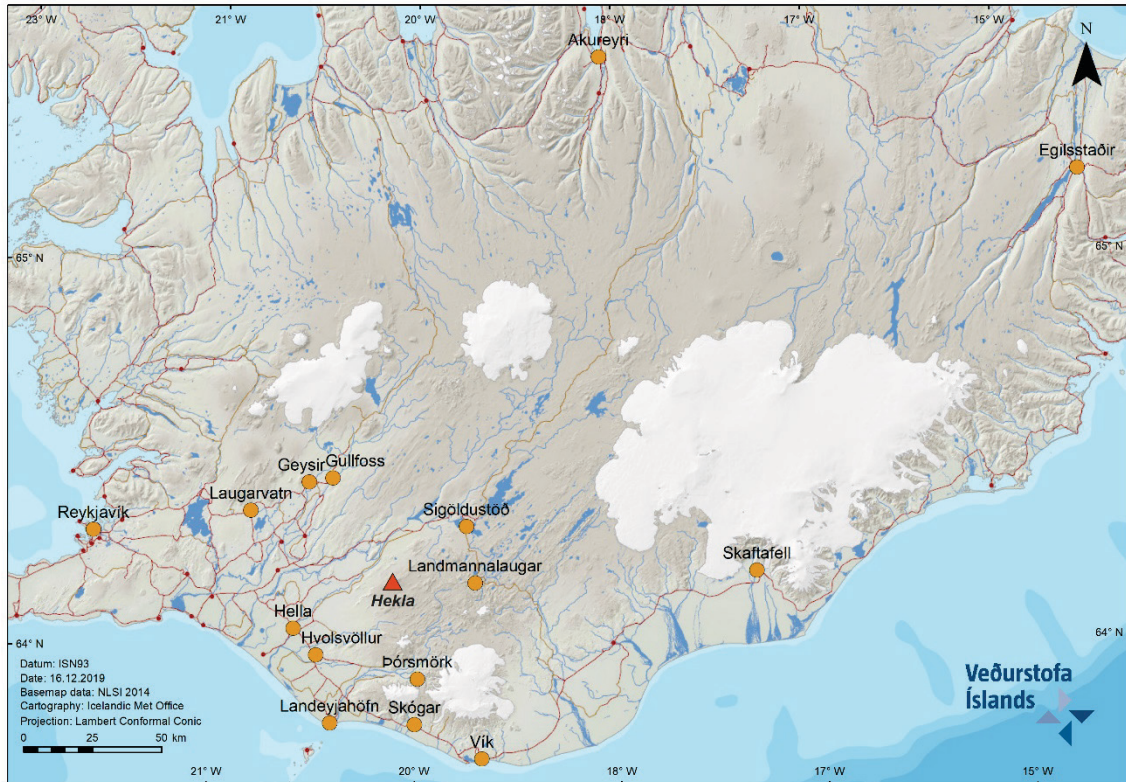


Figure 8. Selected locations to investigate tephra accumulation rate and worst-case scenario for the Hekla scenario. — *Valdar staðsetningar þar sem verstu mögulegu sviðsmyndir og upphleðsla gjósku var skoðuð fyrir sviðsmynd Heklugoss (sjá kafla 2.1).*

In addition, no special investigation has been done to assess the impact on the power plants (in Iceland mainly hydro and geothermal) but their spatial locations have been visualized on the maps for the power line as a reference. The type and location are provided by the National Energy Authority as in 2014.

3.6 Impact at selected locations

Some locations have been investigated all around the country and the hazards due to tephra fallout is reported for some of these locations. Some of these are cities or villages, some are touristic places and other are areas where important infrastructure exists (e.g. power plant). The list of these locations has been taken from the Road Authority Vegagerdin web-site and is available here: <http://www.vegagerdin.is/vegakerfid/vegalengdir/tafla-yfir-ymsar-leidir/>.

This list has also been used for reporting the likelihood of occurrence of specific tephra ground loading all over the country as reported in the three Appendices II, III and IV.

Some key locations have been selected to investigate the tephra accumulation rate for the Hekla (Figure 8) and Örafajökull (Figure 9) eruptive scenarios.



Figure 9. Selected locations to investigate tephra accumulation rate and worst-case scenario for the Örfajökull scenario. — *Valdar staðsetningar þar sem verstu mögulegu sviðsmyndir og upphleðsla gjösku var skoðuð fyrir sviðsmynd Örfajökulgoss (sjá kafla 2.3).*

4 Methodology

4.1 General approach

The basic structure of the methodology adopted to perform the hazard assessment presented in this study is shown in Figure 10. It consists of four main steps: 1) identification of the scenario of interest (this can be defined on the basis of an Event Tree outcomes or from literature); 2) initialization of VOL-CALPUFF model (Barsotti, Neri, et al., 2008) by using a *synthetic scenario* (selected eruption source parameters to be used as a model input) as well as a range of meteorological scenarios); 3) execution of several numerical runs by using different starting time; 4) statistical processing of the results from multiple runs. The obtained probabilities, as visualized in the final maps, are those called “conditional probabilities”, i.e. conditioned to the occurrence of that specific eruptive scenario.

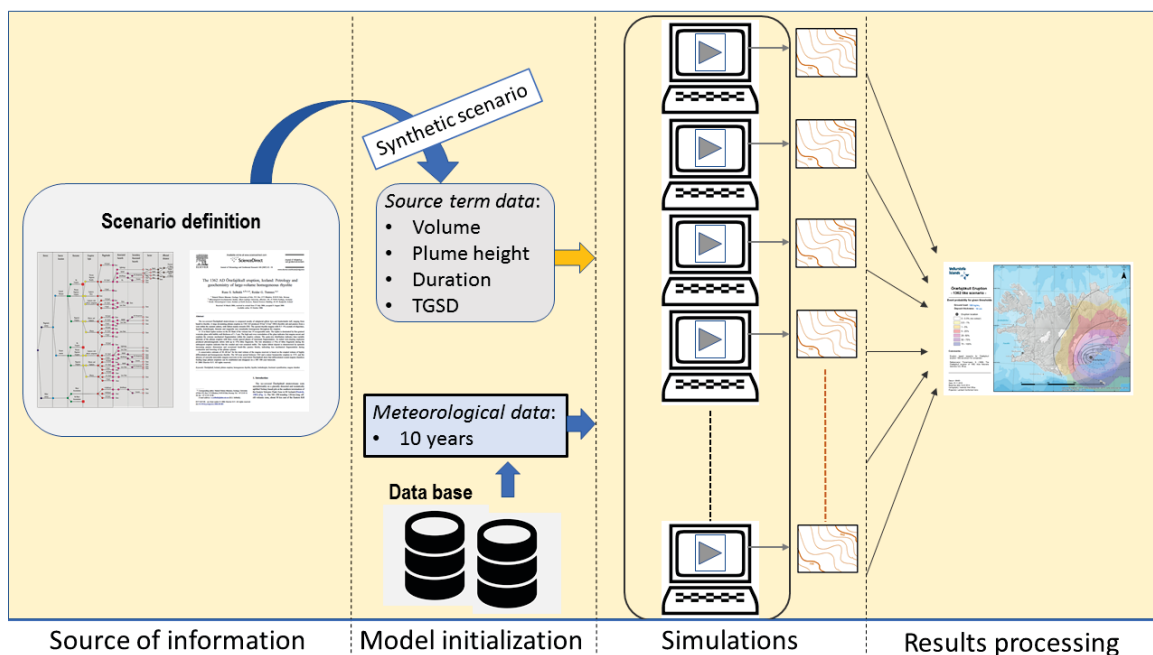


Figure 10. Basic structure of the methodology used to generate the probabilistic hazard maps. — *Aðferðafræði við gerð hættumatskorta sem sýna líkur á að ákveðinn atburður eigi sér stað.*

The identification of scenario has been already treated in Section 3. Here we explain the computational strategy once the model initialization has been done. Each specific source term data is described in more detail Section 5, where the results are presented volcano by volcano.

4.2 Numerical model

Over the last decades the use of numerical tools has increased and become a well- established approach to investigate the dynamics of natural phenomena. In volcanology there has been a full exploitation of this methodology to understand the physics, validate theories, compile laboratories experiments, provide forecast (Kavanagh et al., 2018). Numerical models try, through the definition of simplified physical/chemical equations, to reproduce and describe real complex processes occurring in nature. In this sense the simplified reality that is intrinsic in a model description leaves space for uncertainties in the quantitative results and the confidence in the model should always rely on a critical review of its performance. For this reason, numerical models are always verified over test beds or well-known cases for which input data and the output data are both known with good accuracy.

Here we introduce the main components of the dispersal model used to perform the simulations of tephra/gas dispersal. The model consists of two modules: 1) the plume description and 2) the dispersal (either gas or ash). In the following each phase is described in more details and references to published articles where the models have been already validated are mentioned.

For this specific study VOL-CALPUFF model has been validated against test cases selected for this project. In Section 5 the results from the comparison between modelled and observed ground deposits is provided.

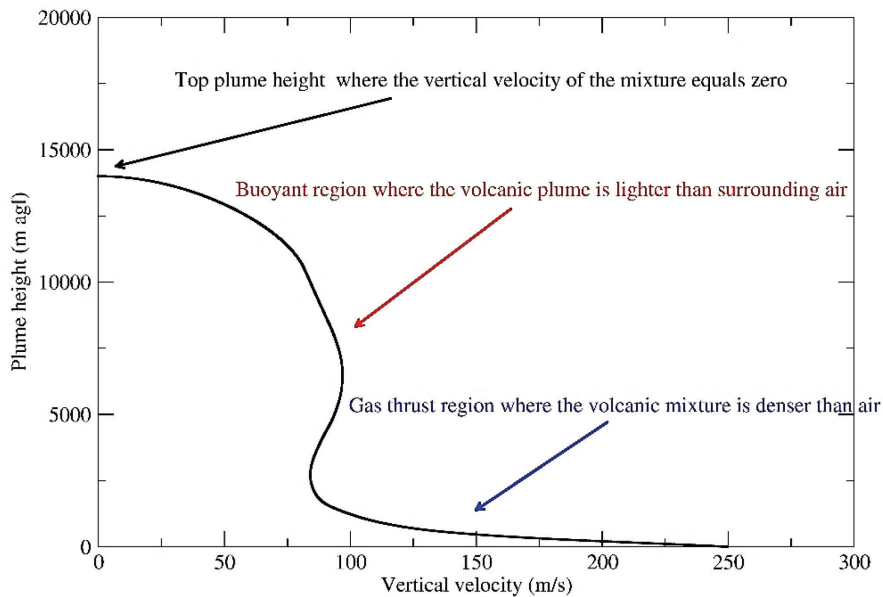


Figure 11. Vertical profile of the vertical velocity of the volcanic plume. Three areas are identifiable as the gas-thrust region, the buoyant region and the umbrella region. — *Lóðrétt snið í gegnum gosmökk sem sýnir breytilegan hraða gosefna. Gosmekki er skipt í þrjú svæði, gasspyrnuhluta (gas-thrust region), uppdrifshluta (buoyant region) og kúf (umbrella region). Í gasspyrnuhluta eru gosefni eðlisþyngri en loftið en skriðþungi efnisins nægir til að lyfta gosefnum; í uppdrifshluta draga gosefnin til sín kyrrstætt loft sem hitnar og þenst út vegna snertingar við heit gosefnin. Við þetta verður eðlisþyngd gosmakkar minni en loftsins umhverfis og því stígur hann vegna uppdrifskrafts. Í kúfnum verður mökkurinn jafnþungur andrúmsloftinu og gosefni falla til jarðar sem gjóskufall þegar skriðþungi þeirra er uppurinn.*

4.2.1 Plume rise model

Plume ascent is described solving plume theory equations (Bursik, 2001) to compute column height as function of volcanological source input data and wind field action. The latter is relevant for simulating weak plumes that are strongly affected by wind shearing. During plume ascent the heaviest particles fall from the column and a lighter mixture continues its upward motion, entraining air up to a null-vertical velocity altitude where only lateral dispersion takes place. The plume initially decelerates due to higher density compared to the surrounding atmosphere, but due to heating of entrained air (mixed by turbulent motions) the mixture can eventually become lighter than air. Buoyancy effect can cause the mixture to accelerate upward until an equilibrium is reached (Figure 11).

4.2.2 VOL-CALPUFF

The dispersal code VOL-CALPUFF originates from the CALPUFF model, a software package developed in the 1970's for air quality issues (Scire, Strimaitis, et al., 2000). The model describes the release of specific amounts of particles and gases, discretized as a series of packets, and their temporal advection and deposition within a 3D computational domain. It accounts for basic chemical reactions and different deposition schemes (either dry or wet). The code is directly linked with the meteorological processor CALMET (Scire, Robe, et al., 2000) which elaborates input data produced by meso-scale models and generates a refined analysis of the atmospheric circulation. This allows us to describe the dispersal phenomenon considering the effects of small-scale atmospheric dynamics. Strong vertical wind shears, boundary-layer dynamics, day/night weather variability, other than liquid and frozen precipitation are all phenomena reproduced and their effect on volcanic particles transport and deposition considered. VOL-CALPUFF is capable to reproduce some processes specific of a volcanic eruption, e.g. plume rise phase and a distribution of solid particles. It is a hybrid model in which the plume rise phase is described with a Eulerian approach, whereas the ash cloud transport is solved in a Lagrangian framework. Along the plume and at the top the material is released as a series of diffusing packets (puffs) containing an initially assigned amount of particulate matter which varies during the transport due to gravitational fallout. Since its development the VOL-CALPUFF model has been applied mostly at Mt. Etna to reconstruct past explosive events (Barsotti, Neri, et al., 2008; Barsotti & Neri, 2008), as an ash dispersal forecasting tool (Barsotti, Nannipieri, et al., 2008) and to estimate potential hazards posed by volcanic ash to human health and ground infrastructures (Barsotti et al., 2010). In the last years VOL-CALPUFF has also been applied to other active volcanoes to produce forecasting maps of ash dispersal during eruptive crises at Redoubt Volcano (Alaska) in 2009, Eyjafjallajökull (Iceland) and Mount Merapi (Indonesia) in 2010 (Barsotti et al., 2011; Spinetti et al., 2013) and Grímsvötn (Iceland) in 2011.

4.3 Meteorological data

Forecast data produced by the European Centre of Medium-range Weather Forecast have been used to run both CALPUFF and VOL-CALPUFF. The meteorological data for the probabilistic maps has been downloaded from the ERA-INTERIM archive (Berrisford et al., 2009) and cover a period of 10 years, from 1980 to 1991, with a temporal resolution of six hours. This data set is produced by re-analysing the forecast by adding the assimilation of observational data. This means that this data set provides quite complete and verified description of the 3D atmospheric fields. On the other side the horizontal resolution is of 0.7 degrees (i.e. about 35 km and 77 km in the longitude and latitude respectively) making the spatial resolution of this data set a bit coarse for the domain considered in this project. The wind statistics for the three volcanoes considered for the explosive scenarios is shown in Figure 12 (Hekla), Figure 13 (Katla) and Figure 14 (Öræfajökull). In each figure six wind roses corresponding to different pressure levels are shown. They are: 850 hPa (~1500 m asl), 700 hPa (~2800 m asl), 300 hPa (~9000 m asl), 100 hPa (~15000 m asl), 50 hPa (~20000 m asl) and 20 hPa (~25000 m asl).

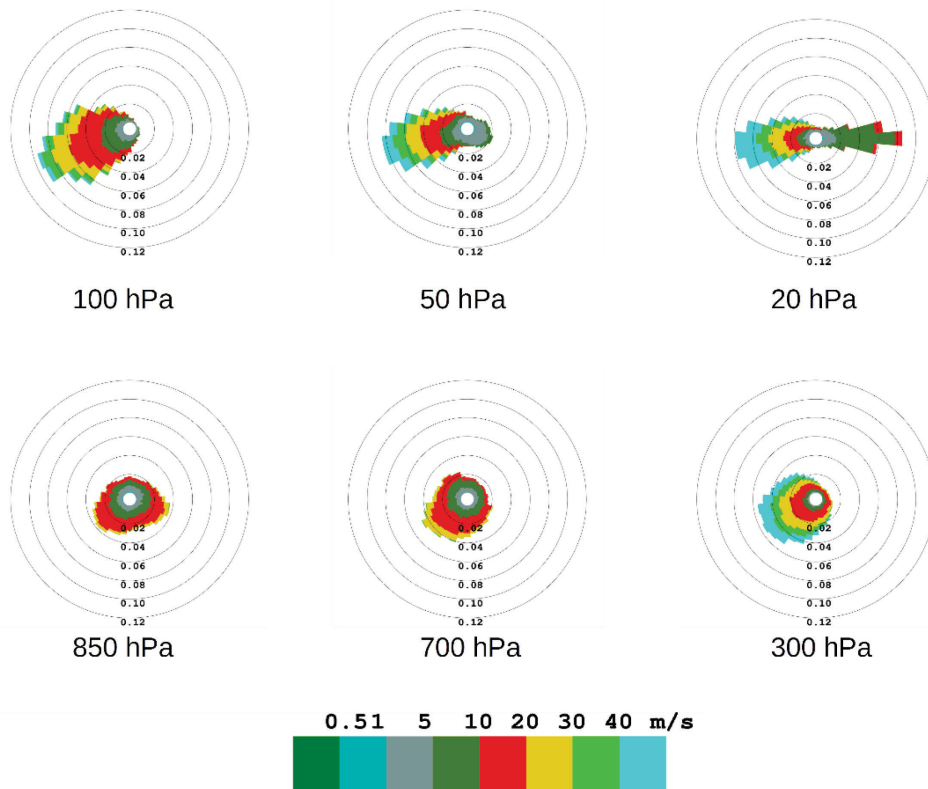


Figure 12. Wind roses for Hekla volcano. Each graph shows the distribution of wind direction provenance and the legend reports the wind speed. The wind data is provided by the ECMWF (ERA-INTERIM archive) with a frequency of six hours. — *Vindrósir sem sýna tíðni vindátta (stefna) og vindhraða (breytilegir litir) í mismunandi hæð yfir Heklu; 850 hPa jafngilda um 1500 m hæð yfir sjó og 20 hPa jafngilda um 25000 m hæð yfir sjó (sjá frekari umfjöllun í texta). Veðurgögn eru frá endurgreiningu Reikni-miðstöðvar evrópskra veðurstofa (ECMWF), ERA-Interim, tekin á 6 klst. fresti.*

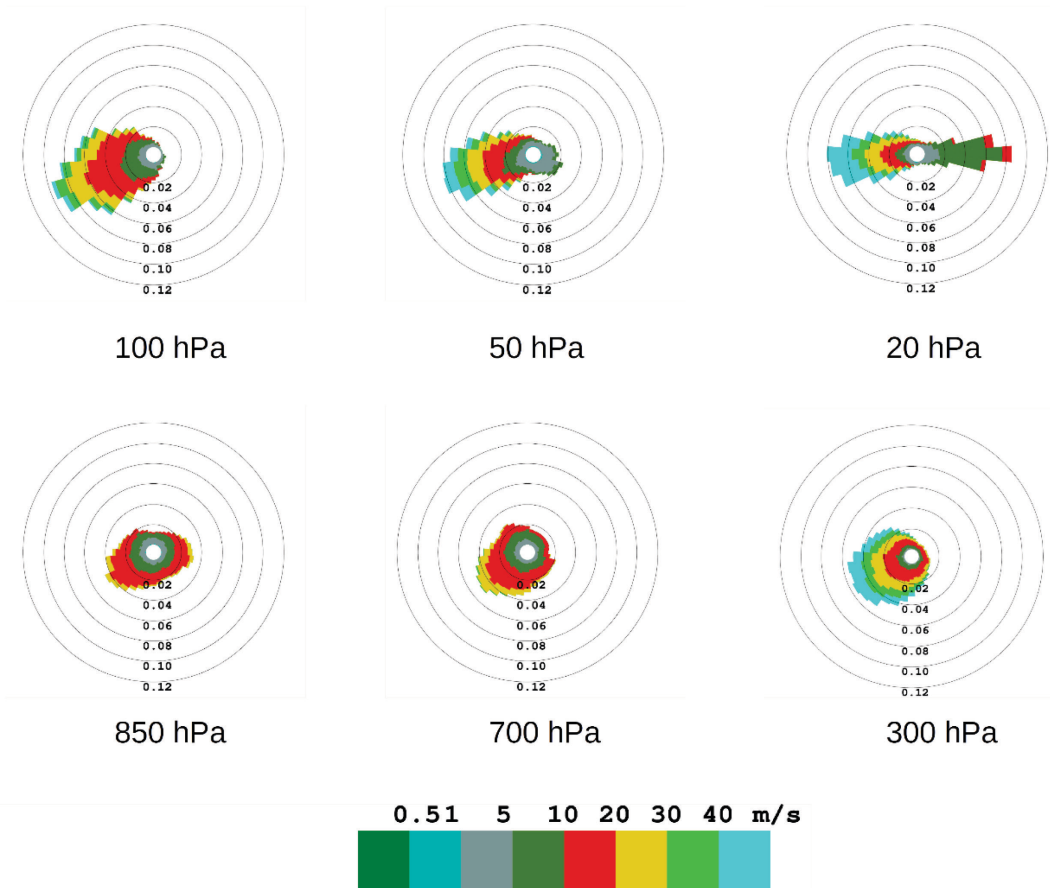


Figure 13. Wind roses for Katla volcano. Each graph shows the distribution of wind direction provenance and the legend reports the wind speed. The wind data is provided by the ECMWF (ERA-INTERIM archive) with a frequency of six hours. — *Vindrósir sem sýna tíðni vindátta (stefna) og vindhraða (breytilegir litir) í mismunandi hæð yfir Kötlu, 850 hPa jafngilda um 1500 m hæð yfir sjó og 20 hPa jafngilda um 25000 m hæð yfir sjó (sjá frekari umfjöllun í texta). Veðurgögn eru frá endurgreiningu Reiknimiðstöðvar evrópskra veðurstofa (ECMWF), ERA-Interim, tekin á 6 klst. fresti.*

The wind rose shows the direction of provenance of the wind (every 6 hours), identified by the sector, and the wind velocity, identified by the colors explained in the legend. At low levels (850 and 700 hPa) the wind is generally weaker than at higher levels, with most of velocities between 5–20 m/s. The prevailing direction at this altitude depend from place to place. A general W-E trend is observable at 850 hPa for all the three volcanic areas, but over Hekla volcano both SW and SE components are present whereas over Katla and Öräfajökull is also visible an ENE component. At 700 hPa the preferred direction is from SSW in all locations. Higher up in the atmosphere is more uniform over the country with less effect due to topographical factors. The velocity tends to increase moving higher up to 300 hPa. Further up the wind velocity decreases (100 and 50 hPa) to increase again at 20 hPa where there is a strong W-E directionality. With easterly winds weaker than westerly ones. Winds at this altitude have a strong seasonality with westerly winds blowing mainly in the winter time and easterly wind in the summer time.

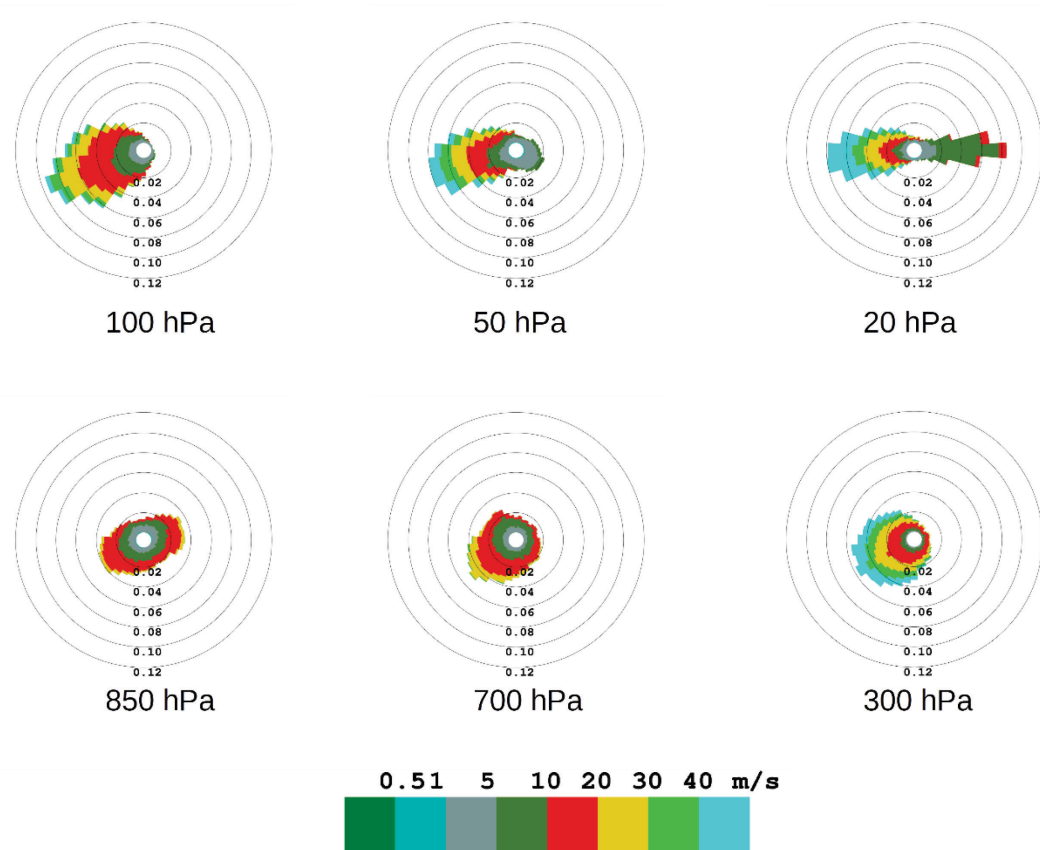


Figure 14. Wind roses for Öräfajökull volcano. Each graph shows the distribution of wind direction provenance and the legend reports the wind speed. The wind data is provided by the ECMWF (ERA-INTERIM archive) with a frequency of six hours. — *Vindrósir sem sýna tíðni vindátta (stefna) og vindhraða (breytilegir litir) í mismunandi hæð yfir Öräfajökli, 850 hPa jafngilda um 1500 m hæð yfir sjó og 20 hPa jafngilda um 25000 m hæð yfir sjó (sjá frekari umfjöllun í texta). Veðurgögn eru frá endurgreiningu Reiknimiðstöðvar evrópskra veðurstofa (ECMWF), ERA-Interim, tekin á 6 klst. fresti.*

The meteorological data, before being used by the dispersal models, are processed by a meteorological pre-processor called CALMET (Scire, Robe, et al., 2000) which refines the data in time and space. In this way the meteorology governing the simulation of the dispersal is corrected for topographical features and small-scale dynamics.

4.4 Monte-Carlo simulation

Numerical models can be used to investigate the behavior of a specific process (Kavanagh et al. 2018) as for example dispersal of ash (Bonadonna et al., 2011; Folch, 2012), lava flow invasion (Favalli et al., 2005, 2009; Negro et al., 2005), maximum distances of pyroclastic flow (Dufek, 2016; Esposti Ongaro et al., 2012). Each simulation needs specific input conditions to characterize the volcanological scenarios to investigate. For volcanic ash dispersal simulation, the eruptive source parameters as plume height, particle size distribution, mass flow rate need to be quantified (Mastin et al., 2009). As we do not know in advance about the next eruptive conditions, like the weather and the eruption source parameters, a way to treat this uncertainty

is to reflect this into a probabilistic analysis. Looking into a range of eruptive scenarios it is possible to get a statistic that would investigate and reflect the uncertainty in the assumption made analysing a single scenario. By running the model considering several initial conditions will allow to estimate the probability that a specific area will be affected by a specific hazard including the aleatoric uncertainty affecting the processes in place. A method widely used to achieve such a result is called Monte-Carlo approach and is based exactly on the assumption that a model could be executed a multitude of times for as many initial conditions by producing an ensemble modelling (Sparks et al., 2013).

Several examples exist already in the literature explaining and using this approach to get a probabilistic analysis of simulation of volcanic processes. When looking into tephra hazard studies treated by using Monte Carlo strategy we find amongst others: (Barsotti et al., 2010; Biasse et al., 2014; Bonadonna et al., 2005; Bonasia et al., 2014; Cioni et al., 2003; Costa et al., 2009; Hurst & Smith, 2004; Macedonio et al., 2008; Scaini et al., 2012; Scollo et al., 2013).

In this project a Monte-Carlo simulation has been performed by running several times the dispersal model VOL-CALPUFF (and CALPUFF) for a fixed volcanological scenario per volcano and by using several years of meteorological data. Each simulation has been performed by assuming the same input data as reported in Section 2. The simulations start at different starting times (day and hour of the day), over a period of 10 years, to reproduce the randomness of the process and to avoid bias in the results due to the daily variations of the atmospheric parameters. In this way we have investigated only the effect of the statistics of the wind field on the tephra dispersal pattern and not the whole range of variability possibly associated to the uncertainty in the volcanological scenario. A total of 500 simulations, per each scenario, have been performed in order to get a convergence of the dispersal results.

4.5 Event tree

A way to visualize the possible evolution of a volcano unrest is through the concept of Event Tree. With an Event Tree (ET) it is possible to represent the behavior of a volcano as a series of logical steps (from the unrest condition to the possible hazard extension) that follow each other as a sequence of arms of a tree. By using an ET is then possible to identify which hazardous behavior we can expect from a specific volcano and, eventually, quantify its likelihood (Newhall & Hoblitt, 2002). Each branch is initialized by a node that corresponds to a specific element in the definition of the unrest evolution (e.g. location of the vent, size of the eruption, type of hazards) and the tree builds on the logical possible steps from one node to the other. The preparation of an ET during non-eruptive time is an important step to identify the possible scenarios potentially associated to a new event of unrest. It has been demonstrated that the use of ET is an essential components of long-term hazard assessments and it represents an important step toward being prepared for future crises (Pallister et al., 2019).

In literature exist several examples of ET designed for volcanoes in the world. Here we used the type of ET as developed for Mt. Vesuvius in (Neri et al., 2008). An example of Event tree for Icelandic volcanoes is shown for the Katla case.

5 Results

In this section all the main results are shown. The section starts with a general explanation on how to read and interpret a probabilistic hazard map like those published in this report. Then other four sections follow, each section refers to a specific volcanological scenario (Hekla, Katla and Öräfajökull). The volcano sections have some parts in common, that are: 1) input parameter and synthetic scenario; 2) probabilistic hazard maps; 3) towards impact-based maps. The Hekla and Öräfajökull cases also contain two more sections called “Validating model results with real deposit” and “Probability of exceedance and accumulation rate”.

5.1 How to read a probabilistic hazard map

Figure 15 shows an example of a probabilistic hazard map. The map was done by simulating an eruption at Hekla volcano and has been obtained by following the approach showed in Figure 10. The map refers to the deposit of tephra on the ground in kg/m^2 and it contains two main parts: the legend and the visual display of colored contours on a geo-referenced map.

The legend contains:

- The title – which refers to the volcanological scenarios that the map is valid for (in this example – the 2000 eruption at Hekla)
- The parameter plotted in the map (in this case the probability for a given threshold of ground deposit)
- The threshold the map is valid for, in this example 0.1 kg/m^2 , that converted into a thickness is 0.01 cm (assuming a deposit density of 1000 kg/m^3)
- The contour levels (a color corresponds to a range in likelihood)

At each location the map shows:

- The conditional probability that, given an eruption at Hekla of a size comparable to the event in 2000, the tephra load at the end of the eruption will exceed a value of 0.1 kg/m^2 (i.e. the likelihood that the deposit will exceed 0.1 mm of thickness).

The numerical model provides the results as tephra load (t_l) but it is more common to see the tephra deposit as a thickness (t_t). In order to make the transition from kg/m^2 to centimeter, it is needed to make some assumptions on the deposit bulk density (ρ_d), so that:

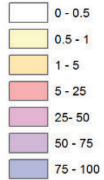
$$t_t = \frac{t_l}{\rho_d}$$

By assuming ρ_d to be 1000 kg/m^3 , the conversion results as in the following Table 8.

**Hekla Eruption
- 2000 like scenario -**

Event probability (%) for given thresholds

Deposit thickness: 0.01 cm
Ground load: 0.1 kg/m²



Comments:

Deposit density assumed as 1000 kg/m³.

Datum: ISN93
Date: 30.03.2016
Basemap data: NILSI 2014
Cartography: Icelandic Met Office
Projection: Lambert Conformal Conic

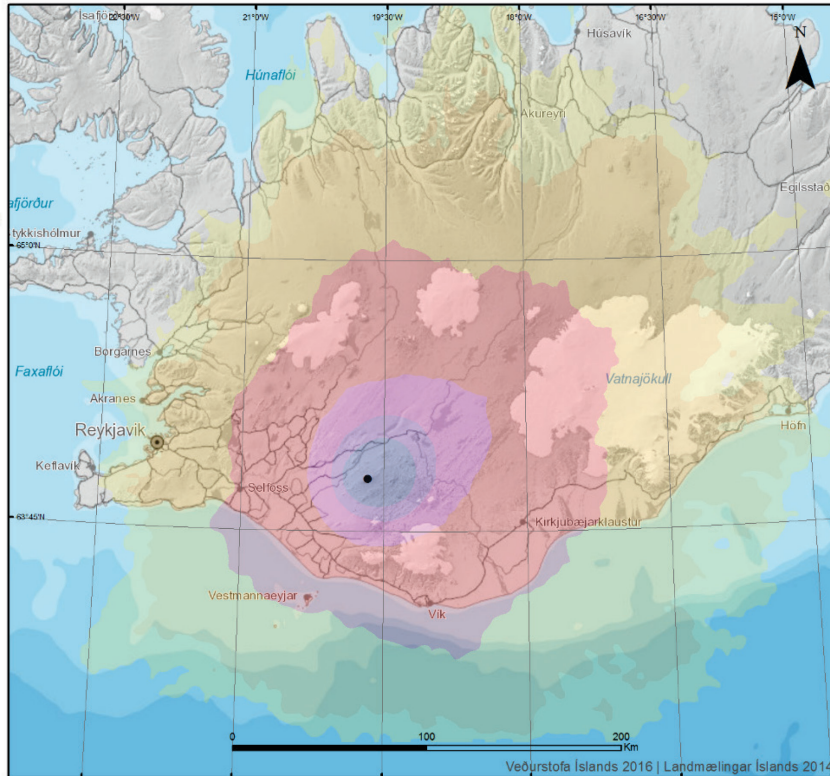


Figure 15. Example of probabilistic tephra-fallout hazard map at Hekla volcano. — *Dæmi um hættumatskort sem sýnir líkindi gjóskufalls af fyrirfram ákveðinni stærð. Í þessu tilfelli eru skoðaðar líkur á að gjóskufall í Heklugosi, sambærilegu því sem átti sér stað árið 2000, fari yfir 0,01 cm þykkt.*

Table 8. Conversion between tephra load and tephra deposit thickness as used for all scenarios presented in this report. — *Umbreyting gjóskuþyngdar á flatareiningu (t_l) í gjóskuþykkt (t_t).*

Tephra load (t_l) – kg/m ²	Tephra deposit thickness (t_t) – cm
1	0.1
10	1
100	10
1000	100

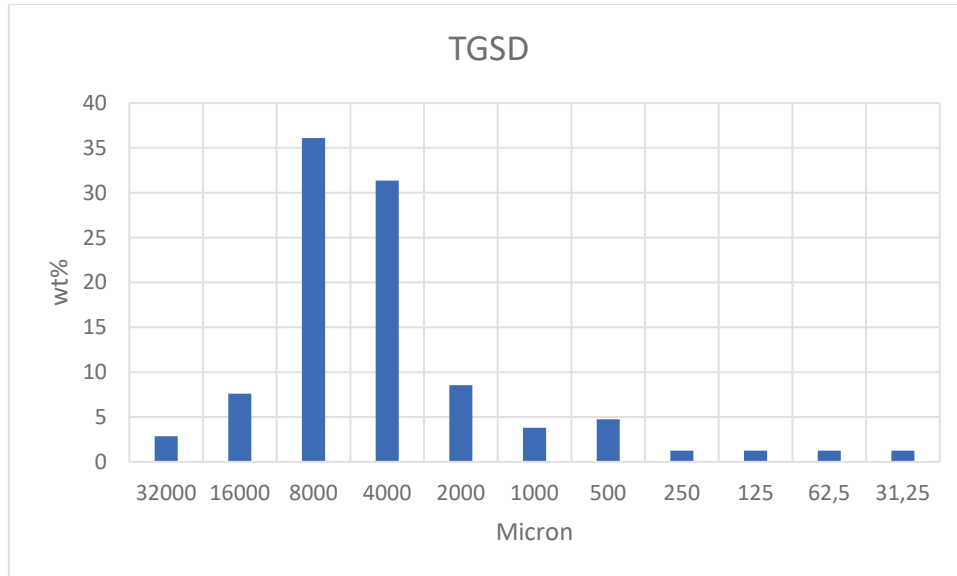


Figure 16. Total Grain Size Distribution (TGSD) used in input to the model to simulate the Hekla eruptive scenario. It derives from the reconstructed TGSD for the 1991 Hekla eruption as reported in (Höskuldsson, Janebo, et al., 2018). The same TGSD is used also for the Katla application. — *Heildarkornastærðardreifing Heklugossins 1991 (Höskuldsson o.fl., 2018) sem notuð var við líkanútreikninga á sviðsmynd Heklugoss og Kötlugoss.*

5.2 Hekla

5.2.1 Input parameters and synthetic scenario

In order to reproduce the scenario reported in Table 4, the VOL-CALPUFF dispersal model has been initialized by using the following input parameters (as obtained by a best-fitting procedure):

- Vertical velocity: 250 m/s
- Vent radius: 45 m
- Total Grain Size Distribution (TGSD) as shown in Figure 16
- Mass flow rate: 7×10^6 kg/s

Running the plume model with these input parameters allows to get the following quantities for plume height and tephra emitted mass (to be compared with those reported in Table 1):

- Plume height: 12.5 ± 5 km above ground level
- Total erupted tephra mass: 5×10^{10} kg

The real and the synthetic scenarios are in a reasonable agreement showing a larger mass in the synthetic scenario of a factor ~ 1.3 . This is an acceptable mismatch considering the uncertainties affecting the mass estimates based on field surveys and measurements.

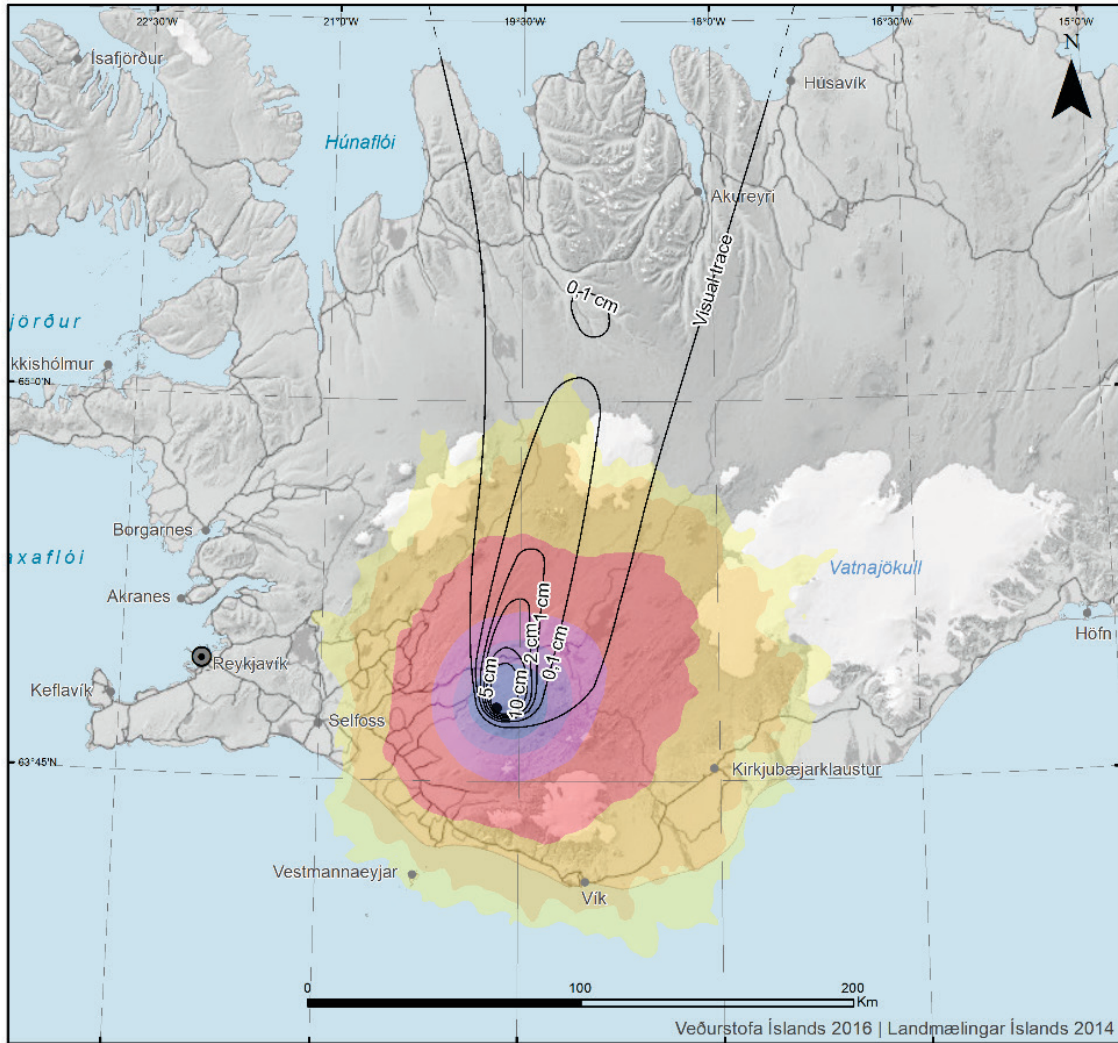


Figure 17. Probabilistic hazard map for an event like 1980 at Hekla. The map refers to a deposit of 1 kg/m^2 ($\sim 0.1 \text{ cm}$). The black contours correspond to the reconstructed deposit for the 1980 eruption (Grönvold et al., 1983). The color scale refers to the legend reported in Figure 15. — *Hættumatskort sem sýnir líkur á atburði sambærilegum Heklugosinu árið 1980 (sjá kafla 5.2.1). Kortið sýnir líkur á að þungi gjóskufalls á flatareiningu verið 1 kg/m^2 (sambærilegt $\sim 0,1 \text{ cm}$ þykku gjóskulagi). Svörtu líurnar sýna jafnþykktarlínur gjóskunnar úr Heklu 1980 (Grönvold o.fl. 1983). Litaskalinn er sá sami og á mynd 13.*

5.2.2 Validating model results with real deposit map

To validate the reliability of the model computation, the deposit reconstructed from the 1980 eruption has been plotted over on the produced maps. The probabilistic map shows the likelihood that at each specific location the deposit will exceed a defined threshold. The map showed in Figure 17 refers to a threshold of 1 kg/m^2 .

The isopachs reconstructed for this event are in cm and a direct comparison with model results is possible when the calculated deposit values (in kg/m^2) are converted using deposit bulk density. Here we assume 1000 kg/m^3 that is a good approximation of the real one of 700 kg/m^3 (Grönvold et al., 1983). In this way the map plotted in Figure 17 shows that the realization of 1980 falls quite well within the area with likelihood higher than 0.5% when looking at the 0.1 cm contour. One element to investigate for understanding why the 1980 event corresponds to such a low likelihood is the current weather condition at the time of the eruption. As shown in Figure 18a, at the time of the eruption the vertical wind profile shows a peak in the horizontal velocity up to 27 m/s at a height of 300 hPa (~9000 m asl). At 500 hPa (~5500 m asl) the velocity is about 7.5 m/s, whereas at a corresponding plume height of about 15 km asl (~120 hPa) the velocity has a value of 15 m/s. Figure 18b shows the statistics of wind velocity at three different heights (in hPa) by using the entire meteorological dataset. It results that on average the wind speed at 500 hPa is about 15 m/s, at 300 hPa it is 22 m/s and at 150 hPa it is about 16 m/s. A comparison of these values with the current wind speed at the time of the eruption, suggests that the volcanic plume during the 1980 eruption experienced a less intense bending at the low altitudes (~5500 m asl), allowing the volcanic mixture to raise up to about 9000 m (and further) where a stronger wind bent the plume and dispersed the volcanic cloud over a long distance.

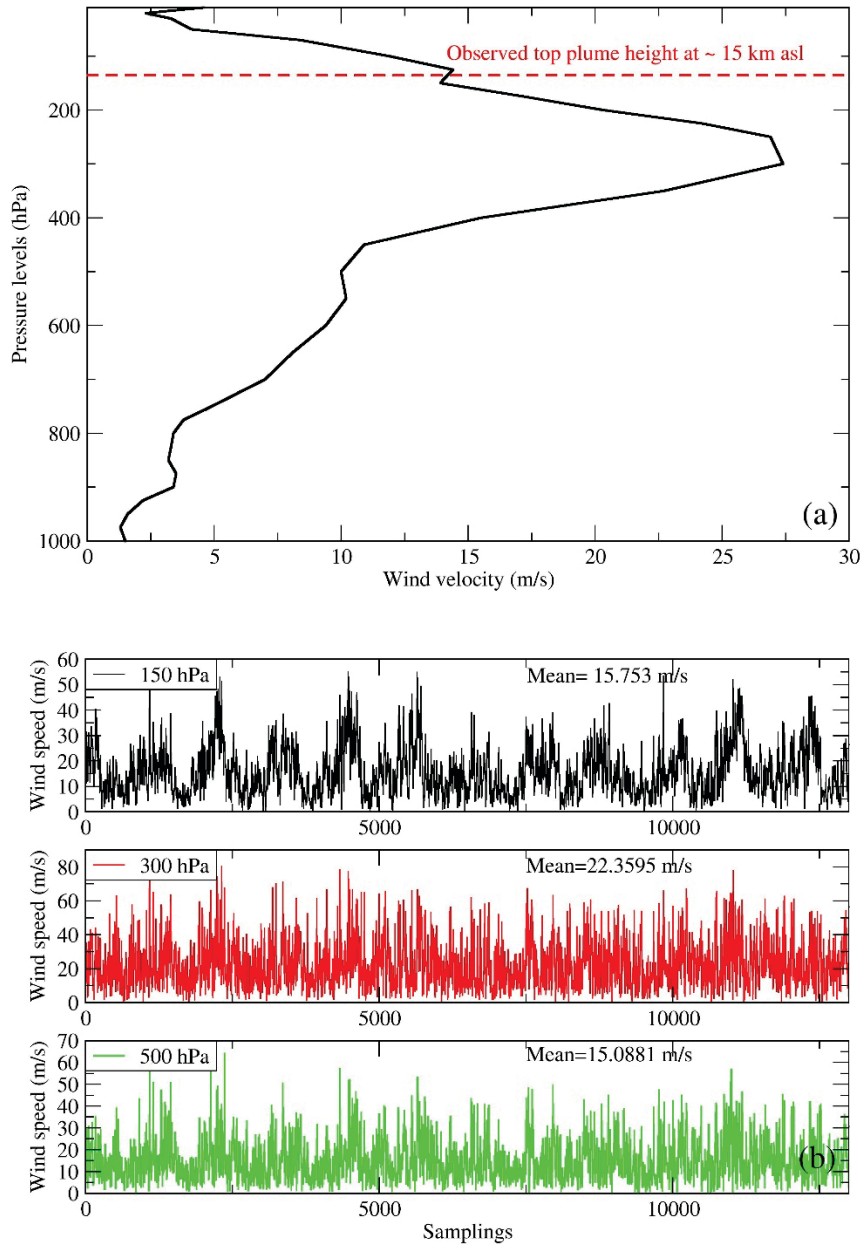


Figure 18. Wind analysis for Hekla volcano. a) Vertical profile of the wind speed for the 17 August 1980 (black curve) and the reported top plume height (dashed red line); b) Variability of wind speed at three different altitudes (150, 300 and 500 hPa) for a location close to the summit of Hekla over a period of ten years. Meteorological data are from the ECMWF ERA-INTERIM archive. — *Vindur við Heklu. a) Lóðrétt snið sem sýnir vindhraða og hvernig hann breyttist með hæð þann 17. ágúst 1980 (svört lína) og hæð gosmakkar sama dag (brotin rauð lína); b) Vindhraði nærri toppi Heklu í þremur mismunandi hæðum (150, 300 og 500 hPa). Veðurgögn eru frá endurgreiningu Reikni-miðstöðvar evrópskra veðurstofa (ECMWF), ERA-Interim.*

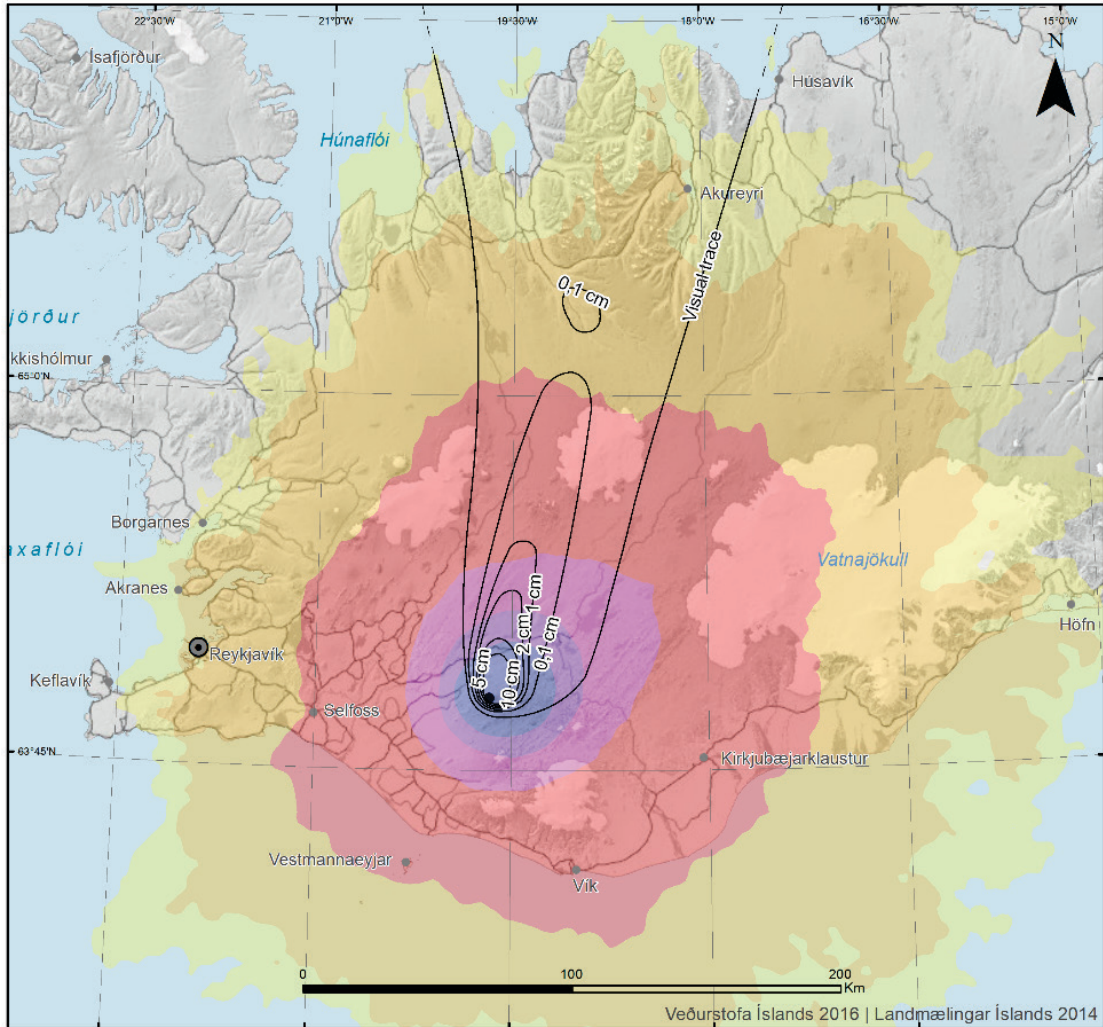


Figure 19. Probabilistic hazard map for a tephra load $\geq 0.1 \text{ kg/m}^2$ ($\sim 0.1 \text{ mm}$). The map is valid for an eruption at Hekla like 1980 event. The map shows the likelihood to exceed a tephra ground loading of 0.1 kg/m^2 . The continuous black lines are isopachs as reconstructed from ground observations for the 1980 eruption (Grönvold et al., 1983). The color scale refers to the legend reported in Figure 17. — *Hættumatskort sem sýnir líkindi þess að $\sim 0,1 \text{ mm}$ þykkt gjóskulag ($\geq 0,1 \text{ kg/m}^2$) myndist af völdum goss í Heklu sem hefur sömu einkenni og Heklugosið 1980 (sjá kafla 5.2.1). Litaskali líkinda er sá sami og á mynd 17. Svörtu líurnar eru jafnþykkjarlínur teiknaðar eftir þykktarmælingum sem gerðar voru á gjóskunni úr Heklugosinu 1980 (Grönvold o.fl., 1983).*

5.2.3 Probabilistic hazard maps

Several maps have been produced to investigate different tephra ground loads. Figure 19, Figure 20 and Figure 21 show a subset of them. These three maps have been produced for different tephra loads of, respectively, 0.1 (Figure 19), 10 (Figure 20) and 100 kg/m^2 (Figure 21). The three maps show a quite uniform pattern around the volcano summit, with a smooth trend toward the East. This elongation of deposit pattern toward the eastern side of the volcano is due to the prevailing wind pattern up to 100 mbar (Figure 12). The low tephra ground load could still be causing disruption of road traffic and the high values could potentially cause building damage or partial collapse.

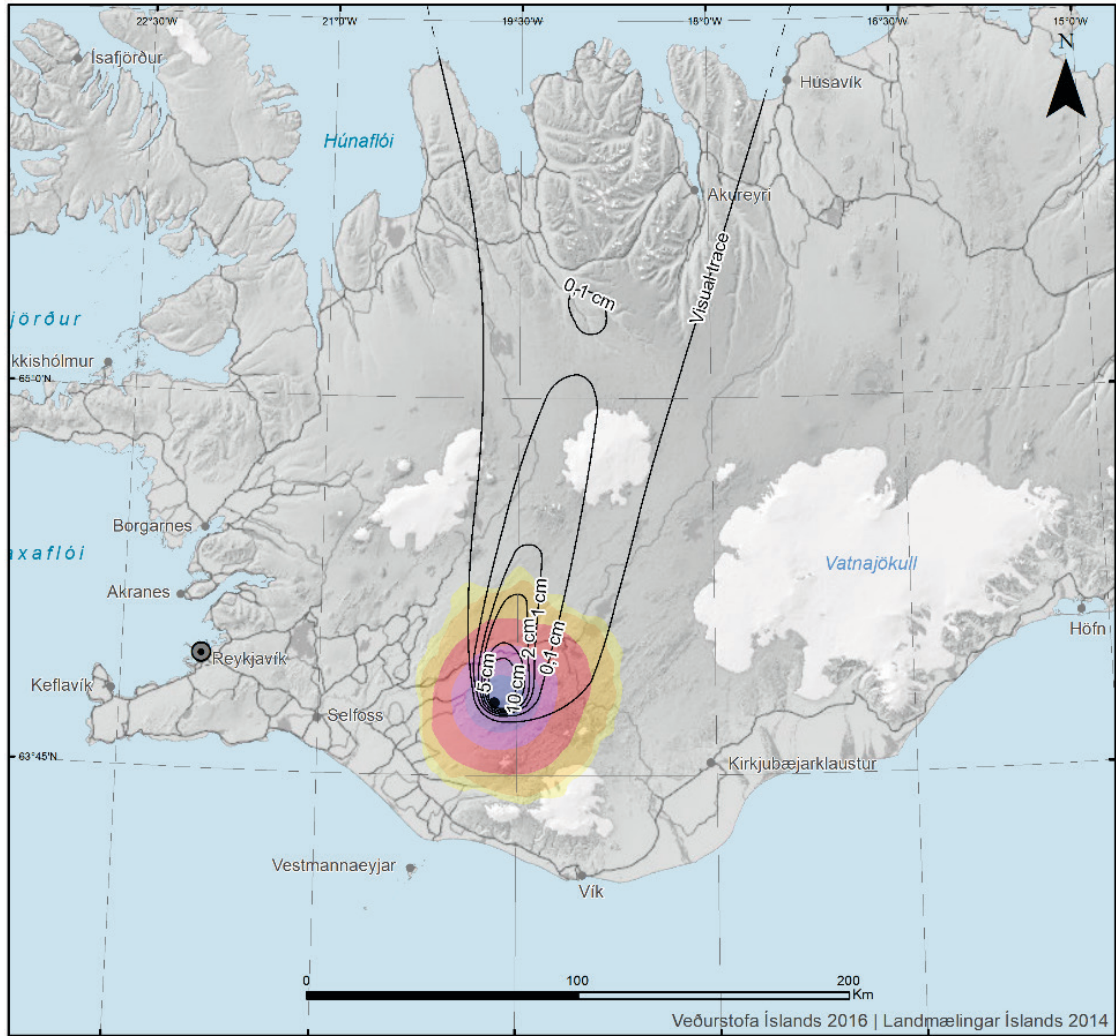


Figure 20. Probabilistic hazard map for a tephra load $\geq 10 \text{ kg/m}^2$ ($\sim 1 \text{ cm}$). The map is valid for an eruption at Hekla like 1980 event. The map shows the likelihood to exceed a tephra ground loading of 10 kg/m^2 . The continuous black lines are isopachs as reconstructed from ground observations for the 1980 eruption (Grönvold et al., 1983). The color scale refers to the legend reported in Figure 17. — *Hættumatskort sem sýnir líkindi þess að $\sim 1 \text{ cm}$ þykkt gjóskulag ($\geq 10 \text{ kg/m}^2$) myndist af völdum goss í Heklu sem hefur sömu einkenni og Heklugosið 1980 (sjá kafla 5.2.1). Litaskali líkinda er sá sami og á mynd 17. Svörtu línurnar eru jafnþykktarlínur teiknaðar eftir þykktarmælingum sem gerðar voru á gjóskunni úr Heklugosinu 1980 (Grönvold o.fl., 1983).*

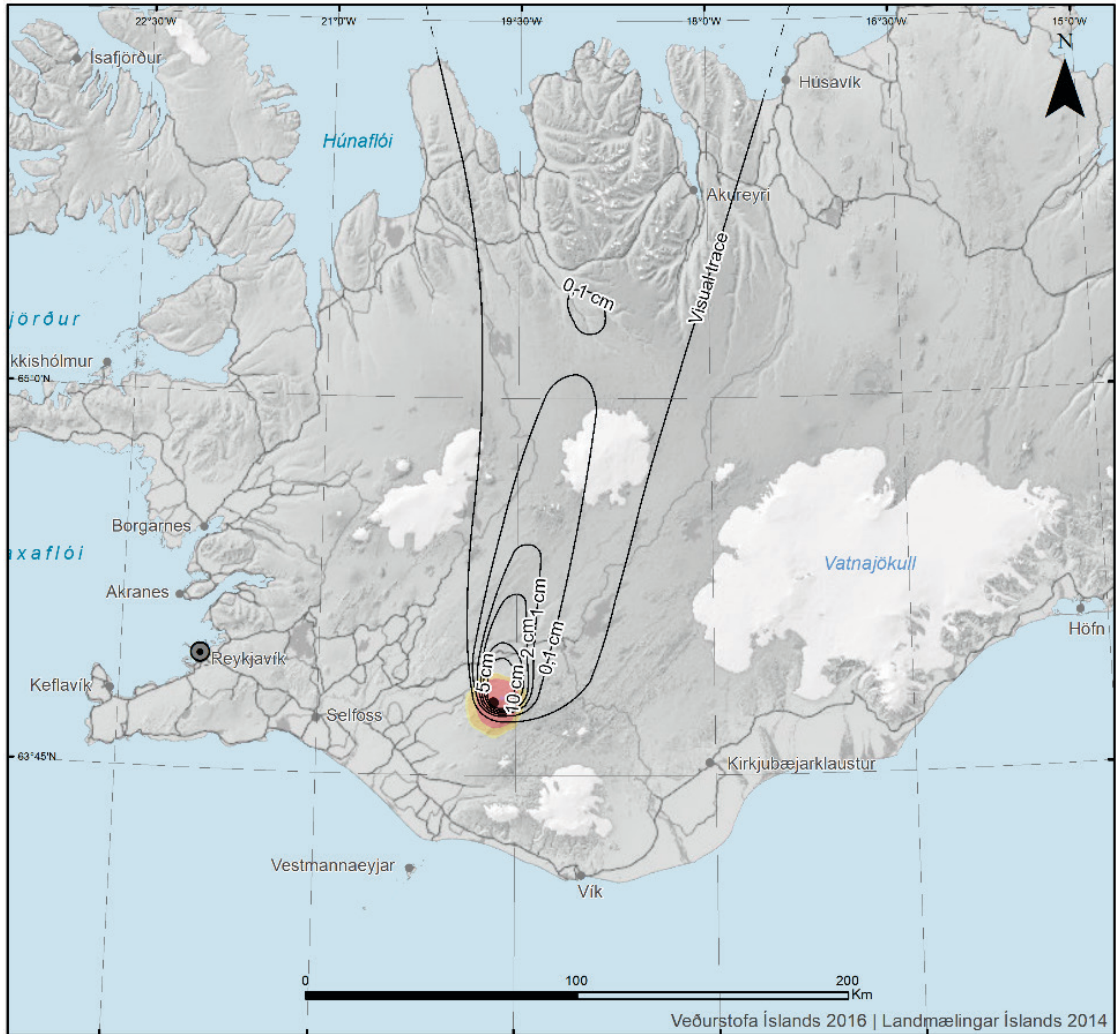


Figure 21. Probabilistic hazard map for a tephra load $\geq 100 \text{ kg/m}^2$ ($\sim 10 \text{ cm}$). The map is valid for an eruption at Hekla like 1980 event. The map shows the likelihood to exceed a tephra ground loading of 100 kg/m^2 . The continuous black lines are isopachs as reconstructed from ground observations for the 1980 eruption (Grönvold et al., 1983). The color scale refers to the legend reported in Figure 17. — *Hættumatskort sem sýnir líkindi þess að $\sim 10 \text{ cm}$ þykkt gjóskulag ($\geq 100 \text{ kg/m}^2$) myndist af völdum goss í Heklu sem hefur sömu einkenni og Heklugosið 1980 (sjá kafla 5.2.1). Litaskali líkinda er sá sami og á mynd 17. Svörtu línurnar eru jafnþykktarlínur teiknaðar eftir þykktarmælingum sem gerðar voru á gjóskunni úr Heklugosinu 1980 (Grönvold o.fl., 1983).*

Hekla eruption - 1980 like scenario

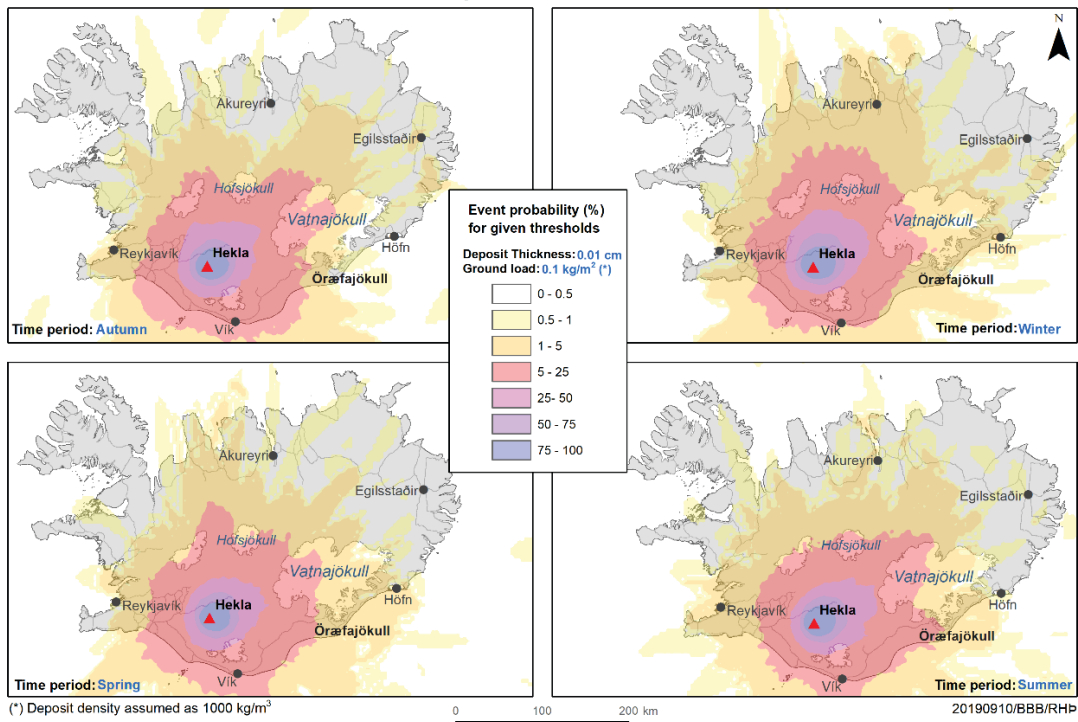


Figure 22. Seasonal analysis of tephra load probability exceeding 0.1 kg/m^2 (less than 0.1 mm of thickness). Few towns are reported as reference. — *Greining á árstíðabundnum líkindum þess að gjóskubýkkt fari yfir $0,1 \text{ mm}$ ($\geq 0,1 \text{ kg/m}^2$) í svipuðu Heklugosi og varð árið 1980 (sjá kafla 5.2.1). Haust: september, október, nóvember; Vetur: desember, janúar, febrúar; Vor: mars, apríl, maí; Sumar: júní, júlí, ágúst.*

Comparing the maps, we notice that for higher tephra ground load the area potentially affected by this amount of ash is becoming smaller. For a load of 1 kg/m^2 the contour of 0.5% and higher (light yellow) is extending to the south coast and reaches Langjökull in the north, Hofsjökull and the western part of Vatnajökull to distances up to 100 km far from the volcano summit (Figure 17). A smaller area is affected by this load with a higher probability, e.g. the 50% likelihood (light purple) is encompassed within an area of 50 km in radius. A load of 100 kg/m^2 or higher is possible only in the proximity of the volcano summit. The map in Figure 21 shows that this load is given with a likelihood up to 50% . Intermediate loads ($\geq 10 \text{ kg/m}^2$) are shown in Figure 20 and can affect an area of 50 km in radius with a likelihood higher than 0.5% . The likelihood rises to more than 75% within an area of about 10 km radius. Traces of ash ($\sim 0.01 \text{ cm}$) could be expected in Reykjavík with low probabilities (Figure 19).

Hekla eruption - 1980 like scenario

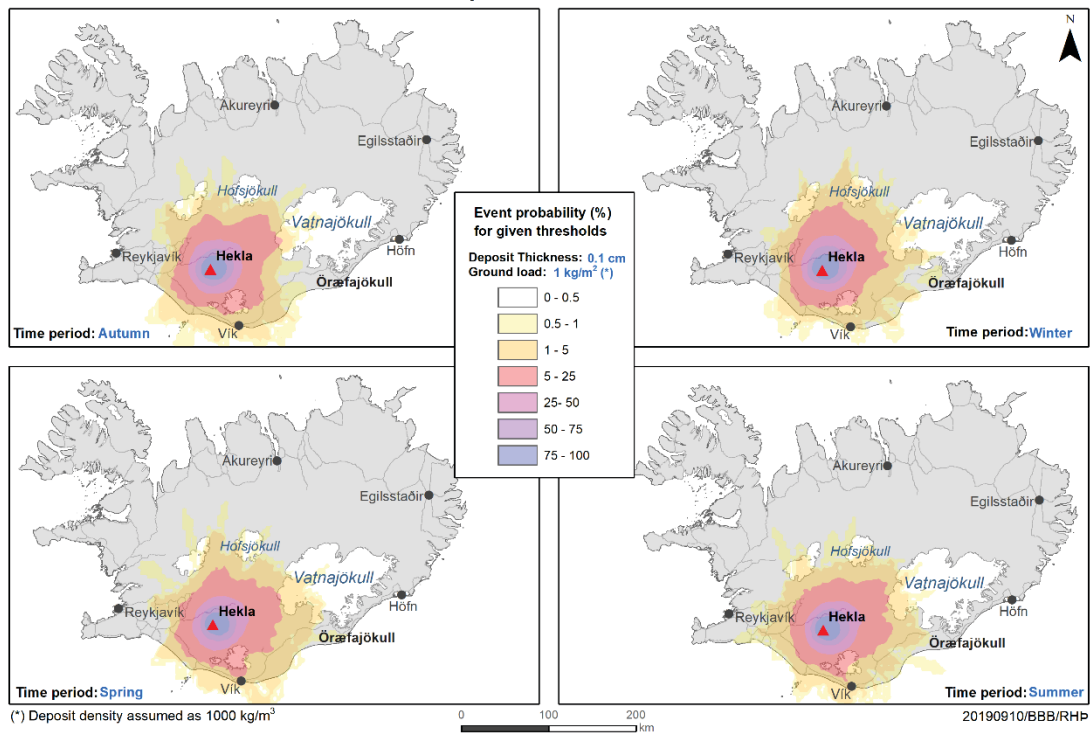


Figure 23. Seasonal analysis for tephra probability exceeding 1 kg/m² (about 1 mm of tephra deposit). Few towns are reported as reference. — *Greining á árstíðabundnum líkindum þess að gjóskuþykkt fari yfir 1 mm (≥ 1 kg/m²) í svipuðu Heklugosi og varð árið 1980 (sjá kafla 5.2.1). Haust: september, október, nóvember; Vetur: desember, janúar, febrúar; Vor: mars, apríl, maí; Sumar: júní, júlí, ágúst.*

The table in Appendix II summarizes how an eruption at Hekla might impact most of the principal towns in Iceland, by reporting the likelihood to exceed three different tephra loads of 1, 10 and 100 kg/m². The location with the highest likelihood to get a tephra deposit from Hekla higher than 1 kg/m², which correspond to thickness of about 1 mm, is Landmannalaugar (45%). The same location could experience a deposit higher than 10 kg/m² with a likelihood of 10%. All other locations have a smaller or null probability to receive tephra in these amounts.

A similar analysis can be done by seasons, to identify possible trends that are functions of the period of the year. Here we consider autumn (SON), winter (DJF), spring (MAM) and summer (JJA). Figure 22, Figure 23 and Figure 24 show the probability to exceed specific values of ground deposit for the four main seasons. No significance differences are notable between different seasons.

Hekla eruption - 1980 like scenario

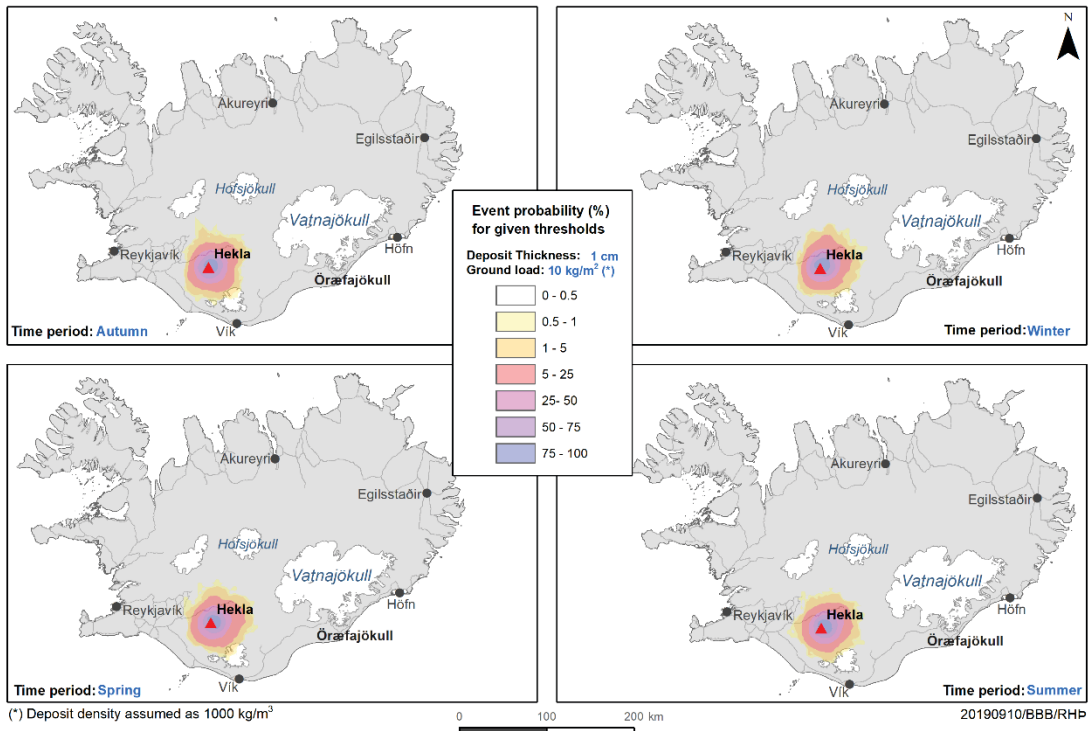


Figure 24. Seasonal analysis for tephra probability exceeding 10 kg/m² (about 1 cm of tephra deposit). Few towns are reported as reference. — *Greining á árstíðabundnum líkindum þess að gjóskuþykkt fari yfir 1 cm (≥ 10 kg/m²) í svipuðu Heklugosi og varð árið 1980 (sjá kafla 5.2.1). Haust: september, október, nóvember; Vetur: desember, janúar, febrúar; Vor: mars, apríl, maí; Sumar: júní, júlí, ágúst.*

5.2.4 Towards Impact-based maps

When adding spatial based information as roads, airports and power lines we can quantify the impact due to tephra fallout in a preliminary way. The map shown in Figure 25 has been obtained by using the results from the probabilistic hazard assessment done for a tephra load of 3 kg/m² and the distribution of road network around the volcano. Both principal routes and secondary ways have been considered. A threshold of 3 kg/m² has been used in light of what discussed in Section 3.1 and has been considered a critical amount for safe driving conditions.

The map shows that an eruption like 1980 at Hekla will cause more than 100 km of roads to be in dangerous driving conditions with a likelihood higher than 25%. Around 50 km of road network will be affected with a likelihood between 50 and 75% and 10 km of roads (those more proximal to the volcano edifice) will be impassable almost for certain.

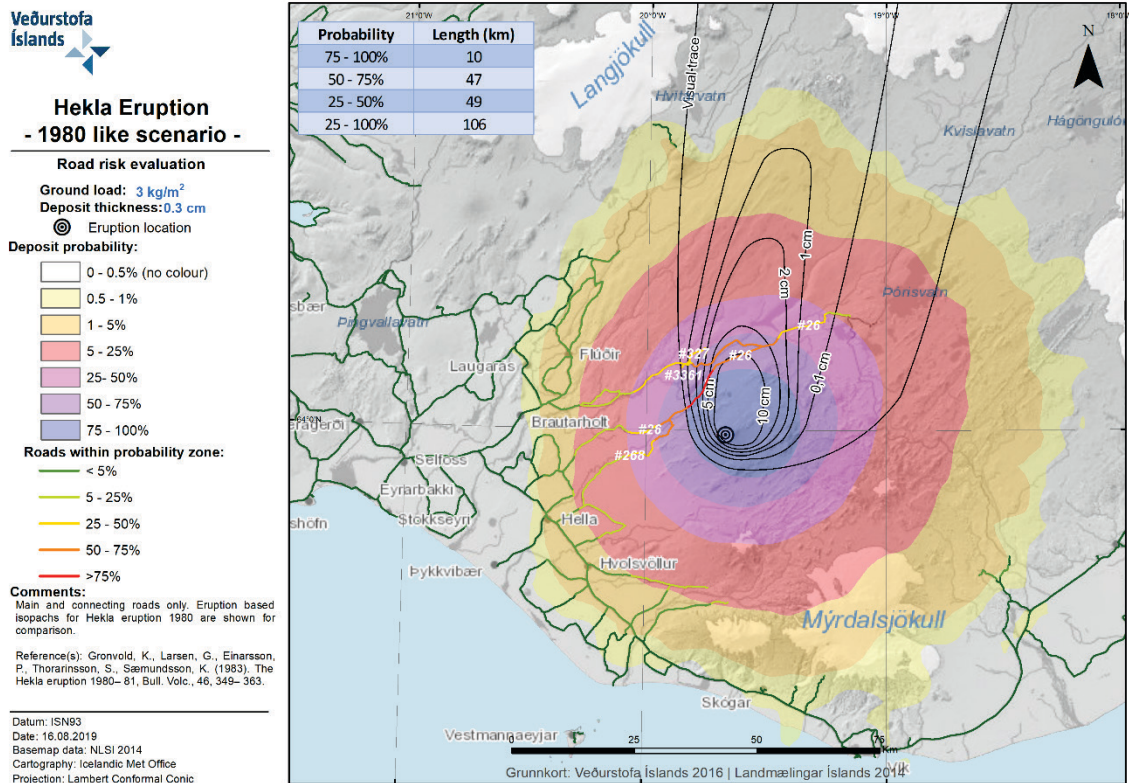


Figure 25. Impact map for road network in case of an eruption in Hekla like 1980. The main road network is overlaid on top of the contour map. The continuous black lines are isopachs as reconstructed from ground observations for the 1980 eruption. — *Áhrifakort fyrir vegi sem sýnir líkur á að ~3 mm þykkt gjóskulag ($\geq 3 \text{ kg/m}^2$) myndist af völdum goss í Heklu (sjá kafla 5.2.1) en rannsóknir benda til þess að ökuskiyrði á malbikuðum vegum skerðist við þá gjóskuþykkt. Vegakerfi svæðisins er sýnt og líkur á að vegir verði fyrir ~3 mm gjóskufalli eru gefnar með litakóða, frá grænum (<5% líkur) og upp í rauðan (>75% líkur). Svörtu línurnar eru jafnþykktarlínur teiknaðar eftir þykktarmælingum sem gerðar voru á gjóskunni úr Heklugosinu 1980 (Grönvold o.fl., 1983).*

Given the distance of Hekla volcano from the main towns, disruption to main airports is very limited. No airports are potentially affected by a tephra load of more than 1 kg/m² (about 1 mm) with a likelihood higher than 5% as shown in Figure 26. Only the airport in Heimaey could be potentially be more prone to receive ash in case of an eruption in Hekla. Airstrips in Hella and Hvolsvöllur have a likelihood between 5 and 25% to be affected and the one in Vík between 1 and 5%.

This analysis is not taking into consideration the impact of an ash rich eruption on the aviation sector in terms of the exposure of aircrafts flying in the area. Here we are only focusing on impact on the ground and the risk of having runways in dangerous conditions for landing and taking off procedures.

**Hekla Eruption
- 1980 like scenario -**

Airport risk evaluation
Ground load: 1 kg/m^2
Deposit thickness: 0.1 cm

⊙ Eruption location

■ Landing strip

Deposit probability:

□ 0 - 0.5% (no colour)

□ 0.5 - 1%

□ 1 - 5%

□ 5 - 25%

□ 25 - 50%

□ 50 - 75%

□ 75 - 100%

Airport within probability zone:

⊕ < 5%

⊕ 5 - 25%

⊕ 25 - 50%

⊕ 50 - 75%

⊕ 75 - 100%

Comments:

Eruption based isopachs for Hekla eruption 1980 are shown for comparison.

Reference(s): Grönvold, K., Larsen, G., Einarsson, P., Thorarinnsson, S., Sæmundsson, K. (1983). The Hekla eruption 1980–81, Bull. Volc., 46, 349–363.

Datum: ISN93

Date: 16.08.2019

Basemap data: NLSI 2014

Cartography: Icelandic Met Office

Projection: Lambert Conformal Conic

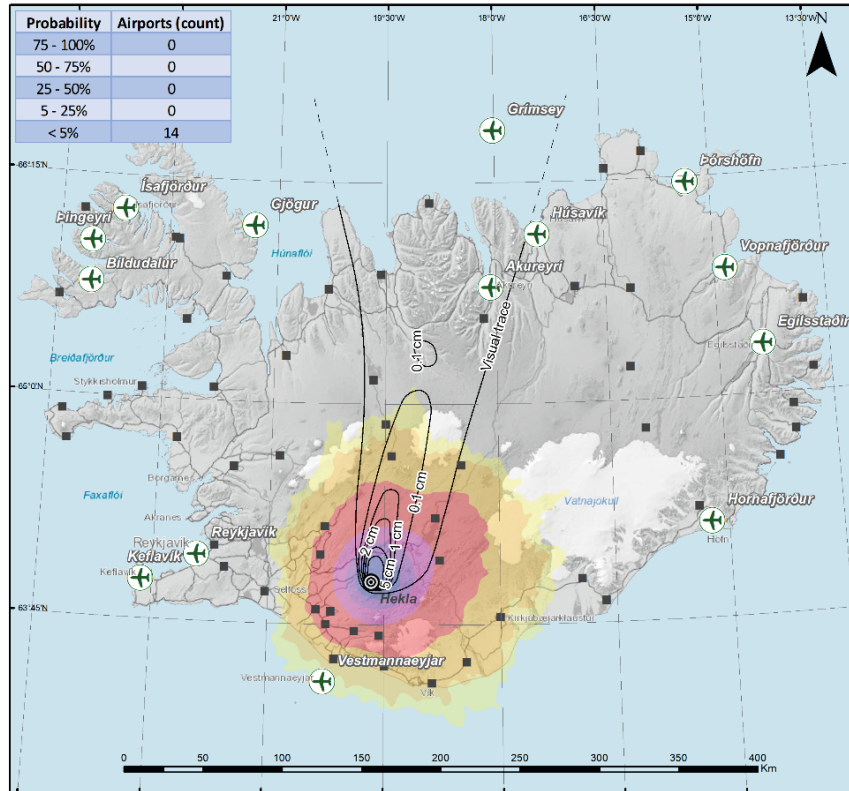


Figure 26. Impact map for airports in case of a 1980-like eruption at Hekla. Landing strips across the country are also mapped. — Áhrifakort fyrir flugvelli sem sýnir líkur á að $\sim 1 \text{ mm}$ þykkt gjóskulag ($\geq 1 \text{ kg/m}^2$) myndist af völdum Heklugoss sem svipar til gossins var 1980 (sjá kafla 5.2.1). Staðsetningar aðalflugvalla landsins eru sýndar og líkur á að þeir verði fyrir $\sim 1 \text{ mm}$ gjóskufalli eru táknaðar með litakóða frá grænum (<5% líkur) upp í rauðan (>75% líkur). Gráir ferningar sýna staðsetningar skráðra lendarstaða. Svörtu líurnar eru jafnþykkarlinur teiknaðar eftir þykktarmælingum sem gerðar voru á gjósku úr Heklugosinu 1980 (Grönvold o.fl., 1983).

As discussed in Section 3.3 power line can be affected by several levels of tephra load causing different type of disruptions (from flashover to power line damages). Here we looked into a scenario characterized by a load of 10 kg/m^2 of dry ash deposit and analyze the impact on the power line network around the volcano (Figure 27).

Up to 78 km of power line can be experiencing heavy tephra load with a likelihood larger than 25%. The nearby hydroelectrical central power located in Búrfell, at a distance of 15 km, will receive this load of ash with a likelihood higher than 5%, potentially impacting additional processes in the power generation mechanisms.

**Hekla Eruption
- 1980 like scenario -**

Powerline risk evaluation
Ground load: 10 kg/m^2
Deposit thickness: 1 cm

⊙ Eruption location

Deposit probability:

- 0 - 0.5% (no colour)
- 0.5 - 1%
- 1 - 5%
- 5 - 25%
- 25 - 50%
- 50 - 75%
- 75 - 100%

Powerlines within probability zone:

- 1 - 5%
- 5 - 25%
- 25 - 50%
- 50 - 75%
- >75%

Comments:

Eruption based isopachs for Hekla eruption 1980 are shown for comparison.

Reference(s): Grönvold, K., Larsen, G., Einarsson, P., Thorarinnsson, S., Sæmundsson, K. (1983). The Hekla eruption 1980–81. Bull. Volc., 46, 349–363.

Datum: ISN83
Date: 16.08.2019
Basemap data: NLSI 2014
Cartography: Icelandic Met Office
Projection: Lambert Conformal Conic

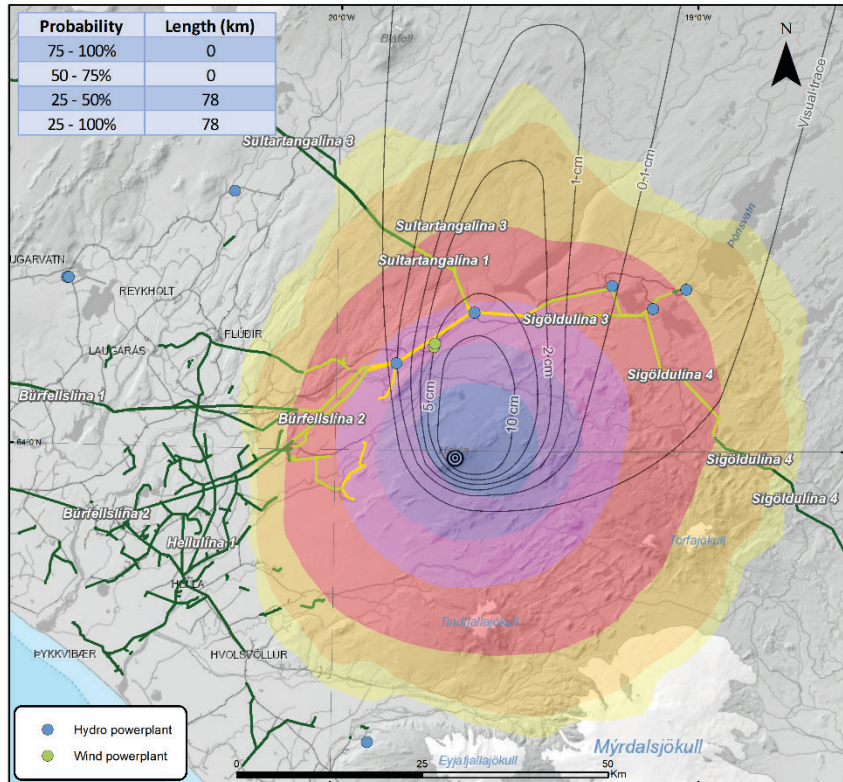


Figure 27. Impact map for power lines in case of a 1980-like eruption at Hekla. — Áhrifakort fyrir raflínur sem sýnir líkur á að $\sim 1 \text{ cm}$ þykkt gjóskulag ($\geq 10 \text{ kg/m}^2$) myndist af völdum Heklugoss sem svipar til gossins 1980 (sjá kafla 5.2.1). Raflínukerfi svæðisins er sýnt og líkur á að það verði fyrir $\sim 1 \text{ cm}$ gjóskufalli eru sýndar með litakóða, frá grænum ($< 5\%$ líkur) og upp í rauðan ($> 75\%$ líkur). Svörtu línurnar eru jafnþykkjarlínur teiknaðar eftir þykktarmælingum sem gerðar voru á gjósku úr Heklugosinu 1980 (Grönvold o.fl., 1983). Bláir punktar sýna vatnsaflsvirkjanir og grænir vindaflsvirkjanir.

5.2.5 Probability of exceedance and accumulation rate

Another way to investigate the ground impact of an eruption is by analyzing the probability of exceeding a range of tephra loads at a specific location. Figure 28 shows eleven curves for as many locations within 60 km from the volcano summit, including touristic locations and main towns in the proximity. A range of tephra load between 0.001 and $10,000 \text{ kg/m}^2$ has been investigated and for each location a curve showing the likelihood to exceed this threshold is plotted. Two locations (Landmannalaugar and Sigöldustöð) are those more prone to receive more ash and have higher likelihood compared to other places. Both can experience a tephra ground load larger than 30 kg/m^2 . Most of the locations investigated have likelihood between 10-20% to get a very light deposit (0.001 kg/m^2). For all curves the deposit is calculated after 24 hours since the eruption onset.

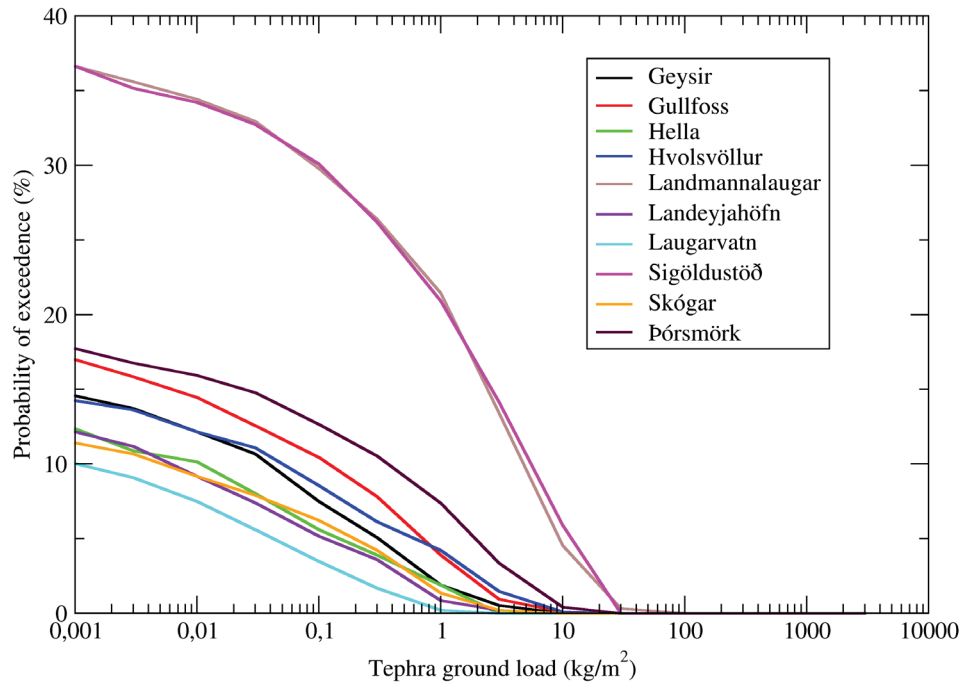


Figure 28. Probability of exceedance graph shows the likelihood of exceeding specific threshold in tephra ground load after 24 hours from the eruption onset. The different curves correspond to different localities within 60 km from the Hekla volcano summit. See Figure 8 for the locations map. — *Likur á að þyngd gjósku nái ákveðinni þyngd á flatareiningu (kg/m²) eftir 24 klst gjóskufall á mismunandi stöðum innan 60 km ræðius frá toppgíg Heklu. Sjá staðsetningar á mynd 8.*

Table 9. Worst-case scenario at several locations in Iceland given as the maximum possible load in kg/m². Highlighted in orange are localities within 60 km from the volcano summit. — *Versta mögulega sviðsmynd gjóskubýngdar á flatareiningu (kg/m²) á völdum staðsetningum eftir 24 klst gjóskufall frá Heklu. Staðir innan 60 km radius frá Heklu eru litaðir með appelsinugulu.*

Location	Maximum possible load (kg/m ²) after 24 hours from the eruption onset – worst-case scenario	Distance from Hekla volcano summit (km)
Landmannalaugar	37.3	29
Sigöldustöð	34.3	33
Þórsmörk; Básar	25.6	36
Hvolsvöllur	10.9	38
Hella	2.9	39
Gullfoss	16.7	43
Geysir	7.6	47
Skógar undir Eyjafjöllum	6.4	52
Landeyjahöfn	3.8	55
Laugarvatn	3.7	57
Vík	3.4	71
Reykjavík	1.1	110
Skaftafell	1.4	132
Akureyri	0.2	202
Egilsstaðir	0.0	289

From these data is also possible to extract the worst-case scenario to quantify the maximum possible load received at the different locations (Table 9). The four closest model grid-points have been used to infer the mass load at a specific place. The analysis has been extended to few more places located far from the volcano, but of interest for a vulnerability assessment (see Figure 8 for reference).

These results mainly reflect the distances of the different locations from the volcano. Reykjavík can experience up to 1 kg/m² as well as Skaftafell. Locations more far to the NE can be affected by a small amount of ash on the ground.

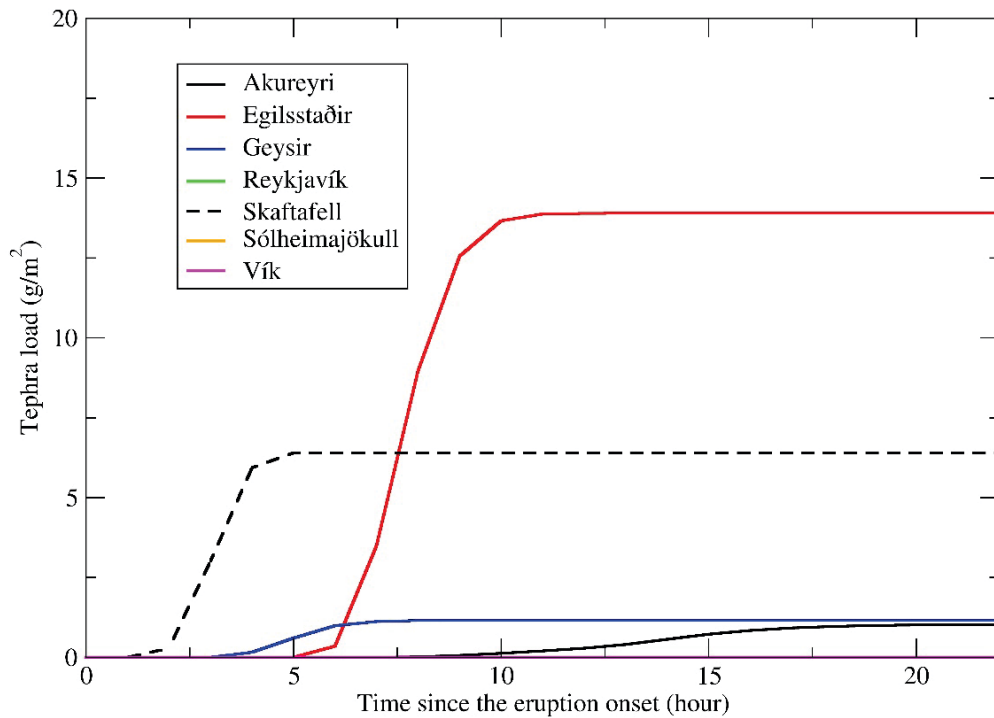


Figure 29. Tephra accumulation rate on the ground at seven locations in Iceland in case of an eruption at Hekla like 1980. The plot shows the results for an eruption occurring on the 11. June 1984. The graph shows how quickly a specific tephra load can be reached as a function of time. The index on the x-axis starts at 0 and it corresponds to the first hour from the eruption onset. See Figure 8 for the locations map. — *Gjóskuþykknunarhraði á sjö stöðum á landinu miðað við Heklugos sambærilegu því sem varð árið 1980 í veðri eins og 11. júní 1984. Grafíð sýnir þann tíma sem þarf til að ná ákveðinni gjóskuþyngd á flatareiningu. Núllpunktur á x-ási táknar upphaf goss. Staðsetningar sem skoðaðar eru má sjá á mynd 8.*

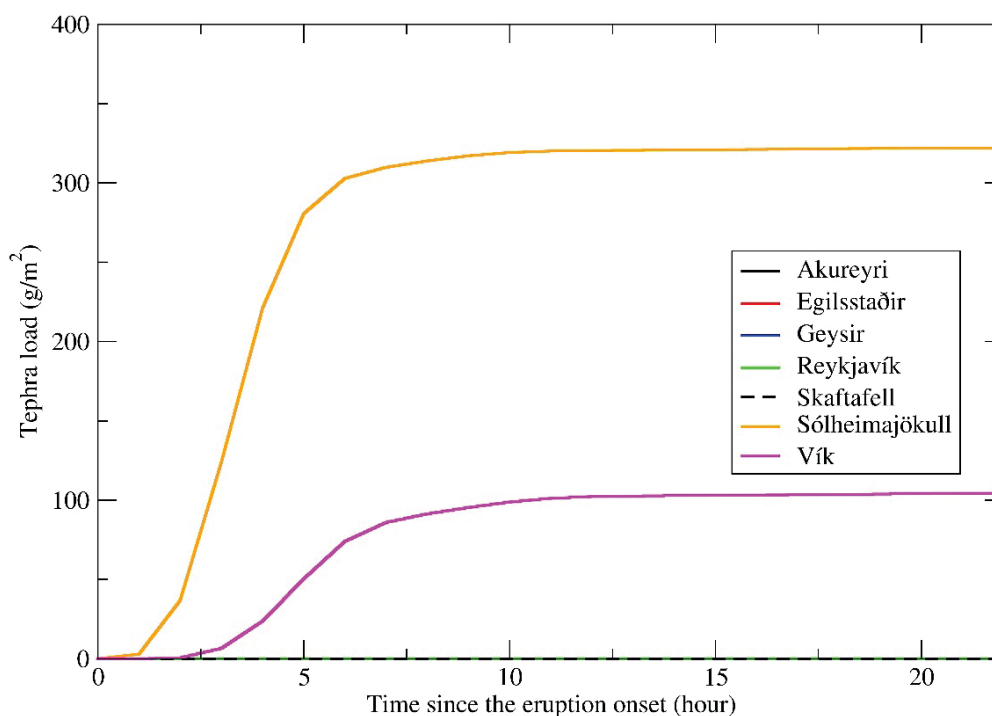


Figure 30. Tephra accumulation rate on the ground at seven locations in Iceland in case of an eruption at Hekla like 1980. The plot shows the results for a similar eruption occurring during weather conditions based upon 21 September 1983. The graph shows how quickly a specific tephra load can be reached as a function of time. The index on the x-axis starts at 0 and it corresponds to the first hour from the eruption onset. See Figure 8 for the locations map. — *Gjóskuþykknunarhraði á sjö stöðum á landinu miðað við Heklugos sambærilegu því sem varð árið 1980 í veðri eins og 21. september 1983. Grafið sýnir þann tíma sem þarf til að ná ákveðinni gjóskuþyngd á flatareiningu. Núll punktur á x-ási táknar upphaf goss. Staðsetningar sem skoðaðar eru má sjá á mynd 8.*

The tephra does not accumulate instantaneously but it is a process that occurs throughout the duration of the eruption and, occasionally, in the following hours. The accumulation rate has been calculated for some specific target locations. Here few towns and touristic places have been selected. To give some examples the hour by hour accumulation of tephra on the ground has been calculated and plotted for some selected dates (Figure 32, Figure 30, Figure 31, Figure 32). Different colored curves correspond to different locations.

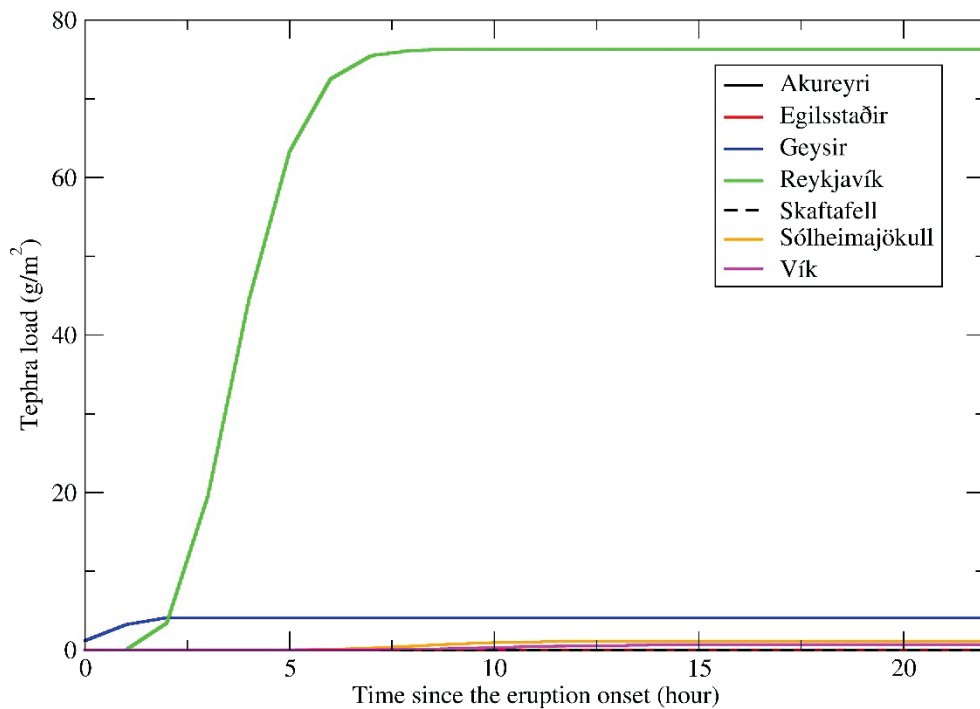


Figure 31. Tephra accumulation rate on the ground at seven locations in Iceland in case of an eruption at Hekla like 1980. The plot shows the results for a similar eruption occurring during weather conditions based upon 9 June 1986. The graph shows how quickly a specific tephra load can be reached as a function of time. The index on the x-axis starts at 0 and it corresponds to the first hour from the eruption onset. See Figure 8 for the locations map. — *Gjóskuþykknunarhraði á sjö stöðum á landinu miðað við Heklugos sambærilegu því sem varð árið 1980 í veðri eins og 9. júní 1986. Grafið sýnir þann tíma sem þarf til að ná ákveðinni gjóskuþyngd á flatareiningu. Núll punktur á x-ási táknar upphaf goss. Staðsetningar sem skoðaðar eru má sjá á mynd 8.*

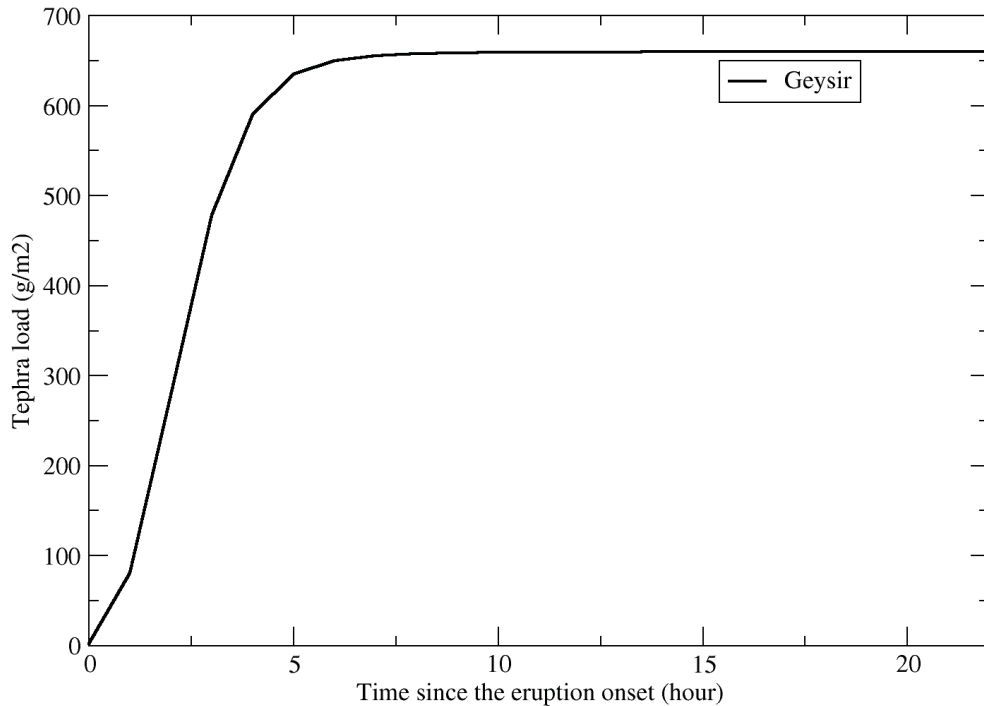


Figure 32. Tephra accumulation rate on the ground in Geysir in case of an eruption at Hekla like 1980. The plot shows the results for a similar eruption occurring during weather conditions based upon 3 October 1985. The graph shows how quickly a specific tephra load can be reached as a function of time. The index on the x-axis starts at 0 and it corresponds to the first hour from the eruption onset. See Figure 8 for the locations map. — *Gjóskuþykknunarhraði við Geysi miðað við Heklugos sambærilegu því sem varð árið 1980 í veðri eins og 3. október 1984. Grafið sýnir þann tíma sem þarf til að ná ákveðinni gjóskuþyngd á flatareiningu. Núll punktur á x-ási táknar upphaf goss. Staðsetningar sem skoðaðar eru má sjá á mynd 8.*

At a specific location, the accumulation rate varies from date to date, reflecting the sensitivity of the deposit pattern to the wind direction and the short duration of the event. The three plots reported here show three different days during which Reykjavík (green line — Figure 31), Egilsstaðir (red line — Figure 29) and Sólheimajökull (orange line — Figure 30) have been the locations receiving more tephra, respectively. In all cases the tephra starts to accumulate after few hours since the beginning of the eruption: 2 hours for Reykjavík and Sólheimajökull and 6 hours for Egilsstaðir. The last graph in Figure 32 shows the accumulation in Geysir. Due to its vicinity to the volcano the rate of accumulation is higher here than anywhere else and it starts 1 hour after the beginning of the eruption.

5.3 Katla

5.3.1 Input parameters and synthetic scenario

The structure of the ET designed for Katla volcano is quite complex as the volcanic system can produce vent openings in different places (i.e. main caldera or on fissures on the outer flanks or outside the central volcano — Figure 33).

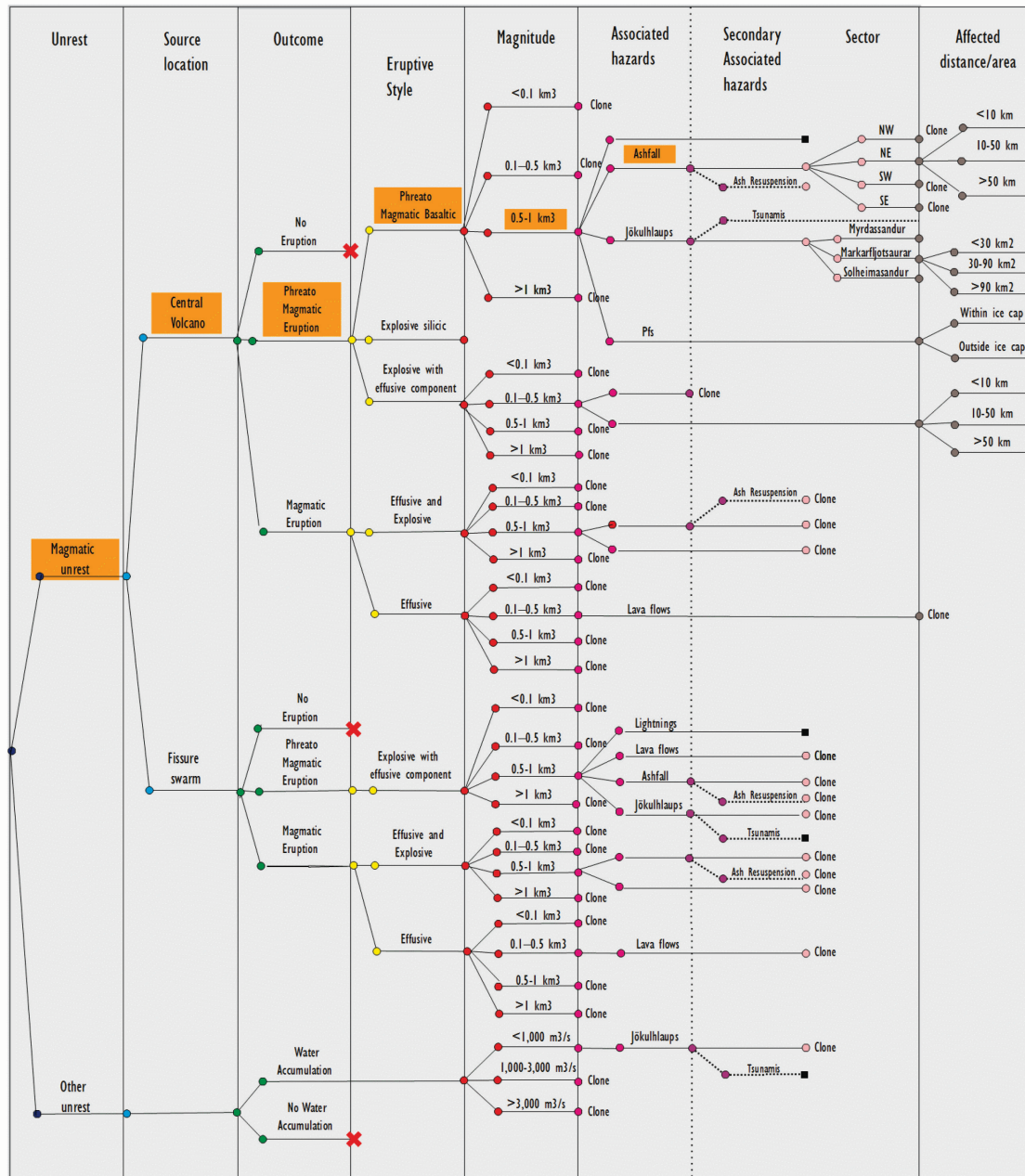


Figure 33. Event Tree for Katla volcano. The orange highlighted part refers to the scenario chosen for this report. PFs stands for Pyroclastic Flows. — *Atburðagreining fyrir eldstöðvakerfi Kötlu. Hér er unnið með þá sviðsmynd sem sýnd er með appelsínugulri yfirstríkun.*

In addition, it can produce different types of magmas that could originate different eruptive styles. The presence of thick ice covering the whole caldera plays also a role in the type of hazards that can potentially occur in case of an eruption at Katla (with jökulhlaup the most frequent and dangerous phenomenon associated with it). Each branch developing at each node have happened in the past (i.e. constrained on previous historical activity) or cannot be excluded from happening in the future (i.e. occurred at analogous volcanoes).

In orange is highlighted the scenario that was chosen for this report to assess the hazard due to tephra fallout. The scenario corresponds to the one listed in Table 4.

In order to numerically reproduce this scenario, the following input parameters have been used to initialize the dispersal runs:

- Vent velocity: 250 m/s
- Vent radius: 35 m
- Total Grain Size Distribution (TGSD) see Figure 16
- Mass flow rate: 4.8×10^6 kg/s (this estimates value applies to the subaerial eruption only and not to the initial hours of the eruption when ice melting most likely took up a large part of the energy of the eruption)

With these conditions the following quantities have been obtained:

- Plume height: 12.2 ± 2 km asl¹
- Total mass: 4.1×10^{11} kg

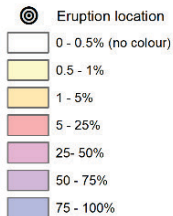
These numbers are in reasonable agreement with those presented in Table 4 to characterize the volcanological scenario.

¹ Recent studies revealed that plume originated during the Katla eruption in 1918 reached even higher heights (Höskuldsson, Þórðarson, et al., 2018). In this perspective the simulated event adopted for this hazard assessment at Katla volcano should be seen as a low end-member scenario.

**Katla Eruption
- 1918 like scenario -
(Preliminary)**

Event probability for given thresholds

Deposit thickness: 0.01 cm
Ground load: 0.1 kg/m²



Comments:

Deposit density assumed as 1000 kg/m³.
Eruption based isopachs for Katla eruption 1918 are shown.

Reference(s): Jónsdóttir T. (2015). Grain size distribution and characteristics of the tephra from the Vatnaöldur AD 871±2 and Katla 1918 eruptions, Iceland. Ms thesis

Datum: ISN93
Date: 24.01.2018
Basemap data: NLSI 2014
Cartography: Icelandic Met Office
Projection: Lambert Conformal Conic

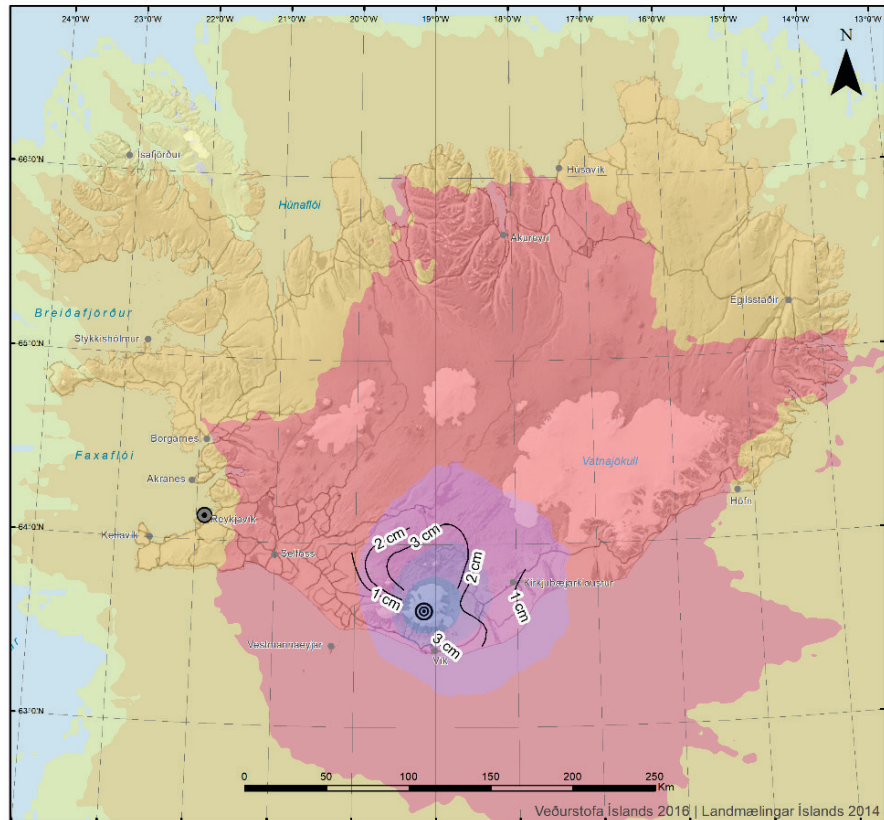


Figure 34. Probabilistic hazard map for a tephra load $\geq 0.1 \text{ kg/m}^2$. The black lines refer to the isopachs reconstructed for the 1918 eruption (Jónsdóttir, 2015). — *Hættumatskort sem sýnir líkur á að gjóskuþykkt nái 0,1 mm í Kötlugosi sambærilegu því sem var 1918 (sjá kafla 5.3.1). Svörtu línurnar eru jafnþykktarlínur gjóskunnar úr Kötlugosinu 1918 (Jónsdóttir, 2015).*

5.3.2 Probabilistic hazard maps

The results have been produced for four thresholds: 0.1, 1, 10 and 100 kg/m². The contours are quite isotropic and do not show a prevailing direction except for a minor trend to the East. Figure 34 shows the extension of the area potentially affected by loads higher than 0.1 kg/m². A wider area, if compared with the similar map for Hekla volcano, can be affected by this load with a likelihood higher than 5%. The likelihood that the entire country will experience such a load is $>1\%$. Vík, Skógar and Kirkjubæjarklaustur are all within an area with likelihood higher than 25%. Whereas towns like Hella, Hvolsvöllur, Selfoss and Vestmannaeyjar have likelihood higher than 5% to be affected by such a tephra deposit. Looking at higher load (Figure 35) the city of Reykjavík has a very low likelihood of about 0.1% (see table in Appendix III) to receive 1 mm of ash. Vík and Skógar have a likelihood higher than 5% also to receive a tephra deposit of more than 10 kg/m². All the area covered by the glacier might experience such a load with a likelihood higher than 50%. If Vestmannaeyjar seems to have very low likelihood to get such a load, Kirkjubæjarklaustur still falls within the 5% contour (Figure 36). Higher loads will affect a smaller area, showing all the Mýrdalsjökull ice cap potentially affected by a deposit thicker than 10 cm with likelihood higher than 25%.

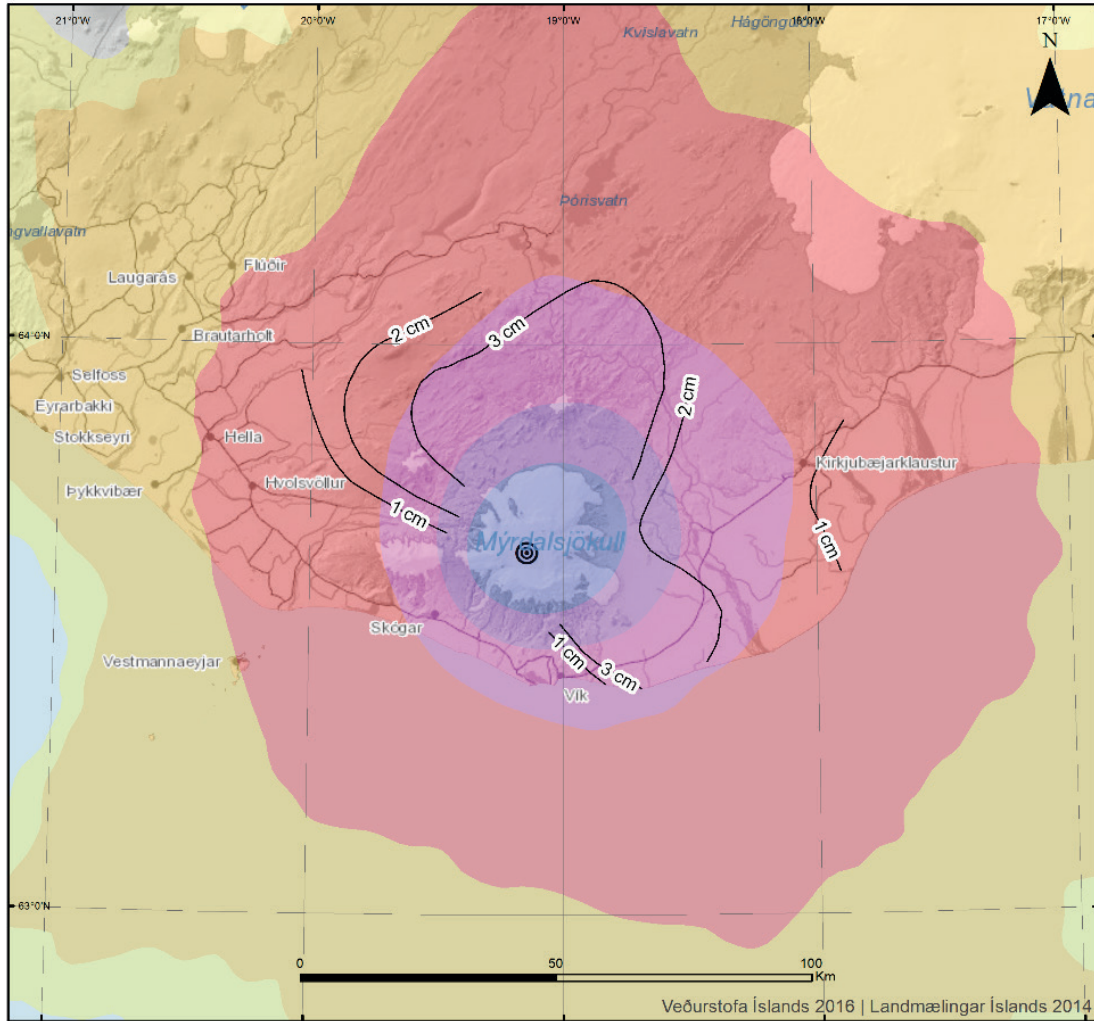


Figure 35. Probabilistic hazard map for a tephra load $\geq 1 \text{ kg/m}^2$ ($\sim 1 \text{ mm}$). The black lines refer to the isopachs reconstructed for the 1918 eruption. The color scales refer to the legend as reported in Figure 34. — *Hættumatskort sem sýnir líkur á að gjóskuþykkt nái $\sim 1 \text{ mm}$ ($\geq 1 \text{ kg/m}^2$) í Kötlugosi sambærilegu gosinu 1918 (sjá kafla 5.3.1). Svörtu línurnar eru jafnþykktarlínur gjóskunnar úr Kötlugosinu 1918 (teiknað eftir Jónsdóttir, 2015). Litanotkun er sú sama og á mynd 34.*

The table in Appendix III summarizes how an eruption at Katla might impact most of the principal towns in Iceland, by reporting the likelihood to exceed three different tephra loads of 1, 10 and 100 kg/m^2 .

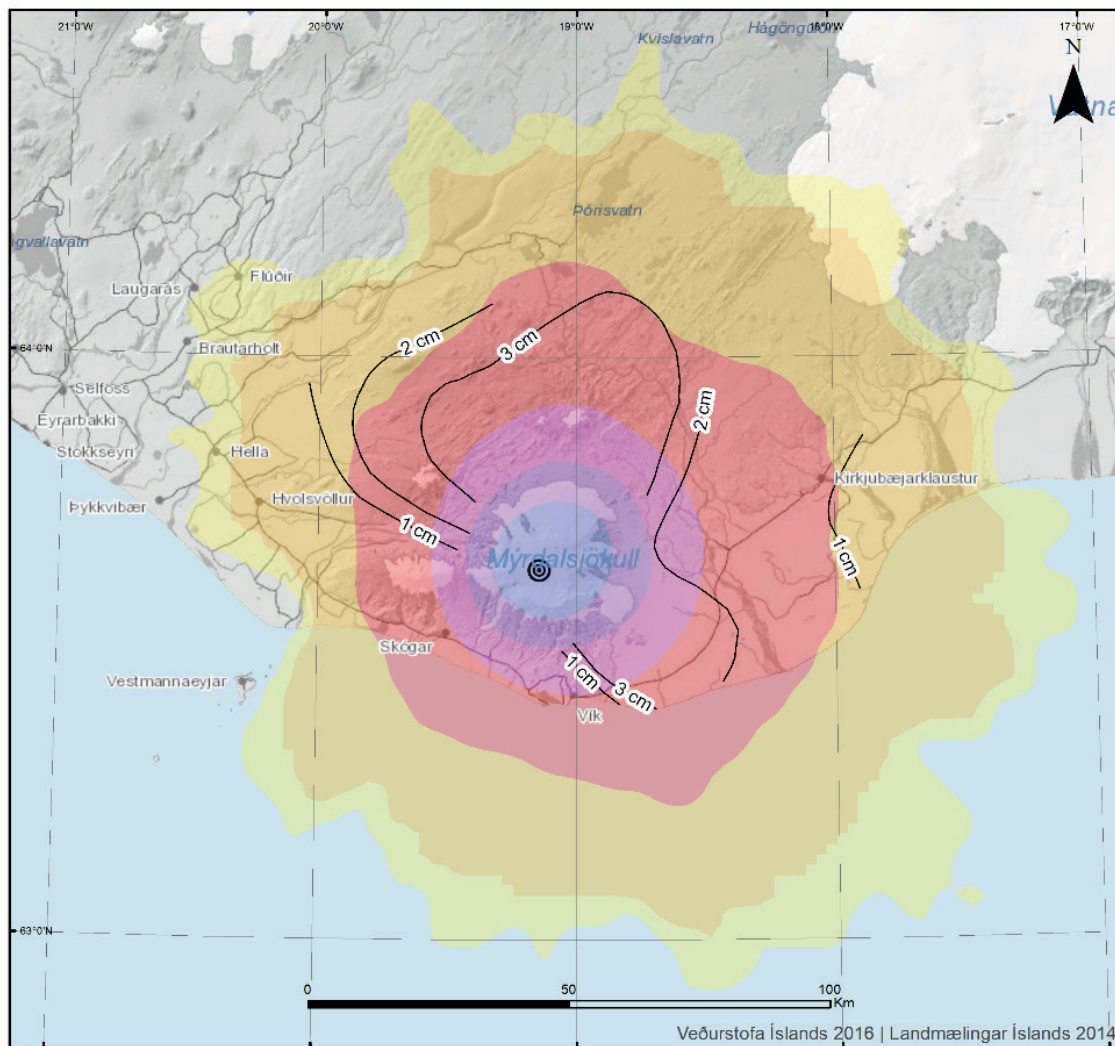


Figure 36. Probabilistic hazard maps for a tephra load $\geq 10 \text{ kg/m}^2$ ($\sim 1 \text{ cm}$). The black lines refer to the isopachs reconstructed for the 1918 eruption. The color scales refer to the legend as reported in Figure 34. — *Hættumatskort sem sýnir líkur á að gjóskuþykkt nái $\sim 1 \text{ cm}$ ($\geq 10 \text{ kg/m}^2$) í Kötlugosi sambærilegu gosinu 1918 (sjá kafla 5.3.1). Svörtu linurnar eru jafnþykktarlínur gjóskunnar úr Kötlugosinu 1918 (teiknað eftir Jónsdóttir, 2015). Litanotkun er sú sama og á mynd 34.*

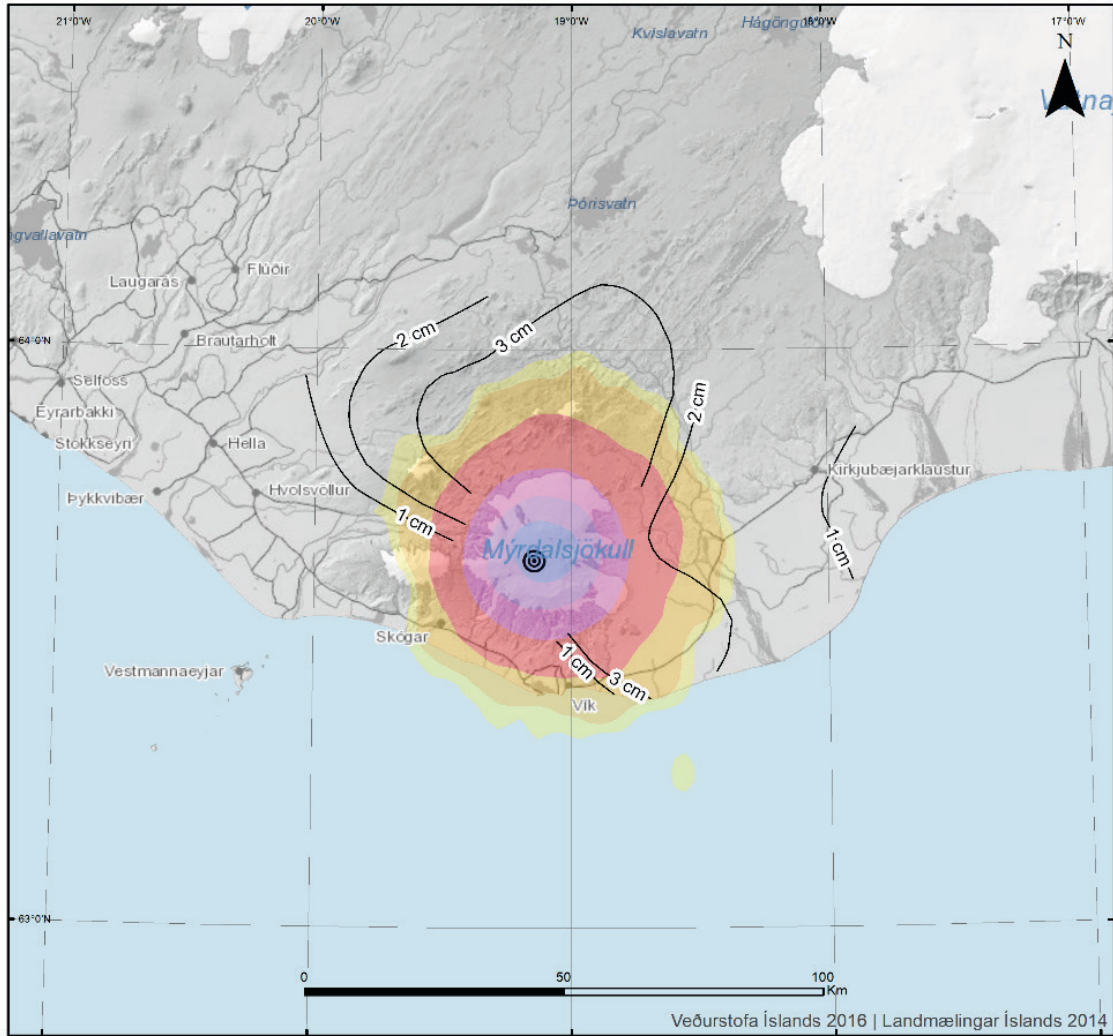


Figure 37. Probabilistic hazard maps for a tephra load $\geq 100 \text{ kg/m}^2$ ($\sim 10 \text{ cm}$). The black lines refer to the isopachs reconstructed for the 1918 eruption. The color scales refer to the legend as reported in Figure 34. — *Hættumatskort sem sýnir líkur á að gjóskuþykkt nái $\sim 10 \text{ cm}$ ($\geq 100 \text{ kg/m}^2$) í Kötlugosi sambærilegu gosinu 1918 (sjá kafla 5.3.1). Svörtu línurnar eru jafnþykktarlínur gjóskunnar úr Kötlugosinu 1918 (teiknað eftir Jónsdóttir, 2015). Litanotkun er sú sama og á mynd 34.*

Katla eruption - 1918 like scenario (Preliminary)

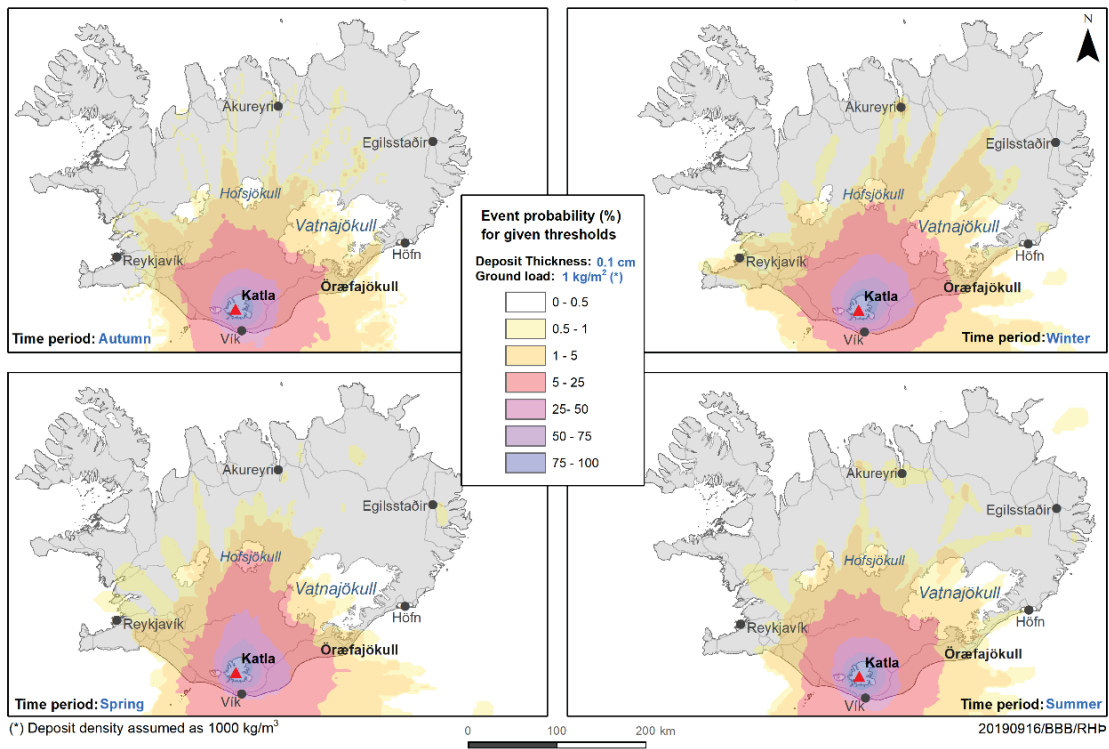


Figure 38. Seasonal analysis for tephra probability exceeding 1 kg/m² (~1 mm). Few towns are reported as reference. — *Árstíðabundin hættumatskort sem sýna líkindi þess að gjóskupykkt fari yfir 1 mm ($\geq 1 \text{ kg/m}^2$) í svipuðu Kötlugosi og varð árið 1918 (sjá kafla 5.3.1). Haust: september, október, nóvember; Vetur: desember, janúar, febrúar; Vor: mars, apríl, maí; Sumar: júní, júlí, ágúst.*

Katla eruption - 1918 like scenario (Preliminary)

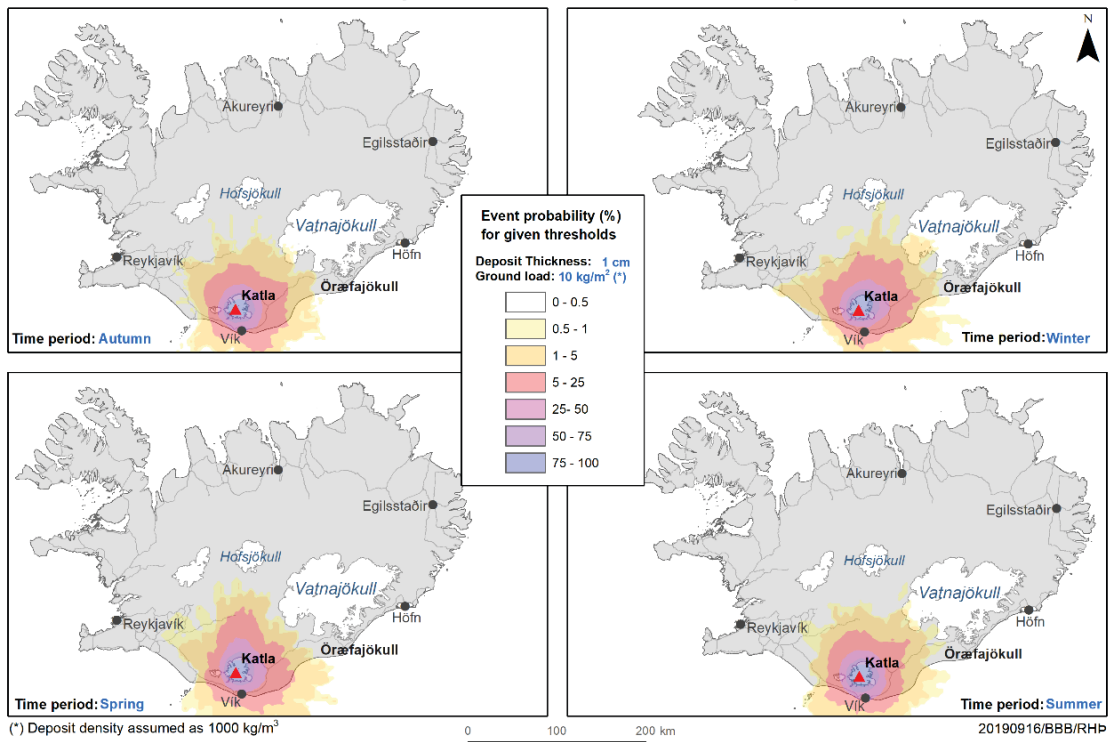


Figure 39. Seasonal analysis for tephra probability exceeding 10 kg/m^2 ($\sim 1 \text{ cm}$). Few towns are reported as reference. — *Árstíðabundin hættumatskort sem sýna líkindi þess að gjóskupykkt fari yfir 1 cm ($\geq 10 \text{ kg/m}^2$) í svipuðu Kötlugosi og varð árið 1918 (sjá kafla 5.3.1). Haust: september, október, nóvember; Vetur: desember, janúar, febrúar; Vor: mars, apríl, maí; Sumar: júní, júlí, ágúst.*

The seasonal analysis has also been done and shown in Figure 38, Figure 39 and Figure 40. Here the summer refers to JJA, the autumn to SON, the winter to DJF and the spring to MAM.

Katla eruption - 1918 like scenario (Preliminary)

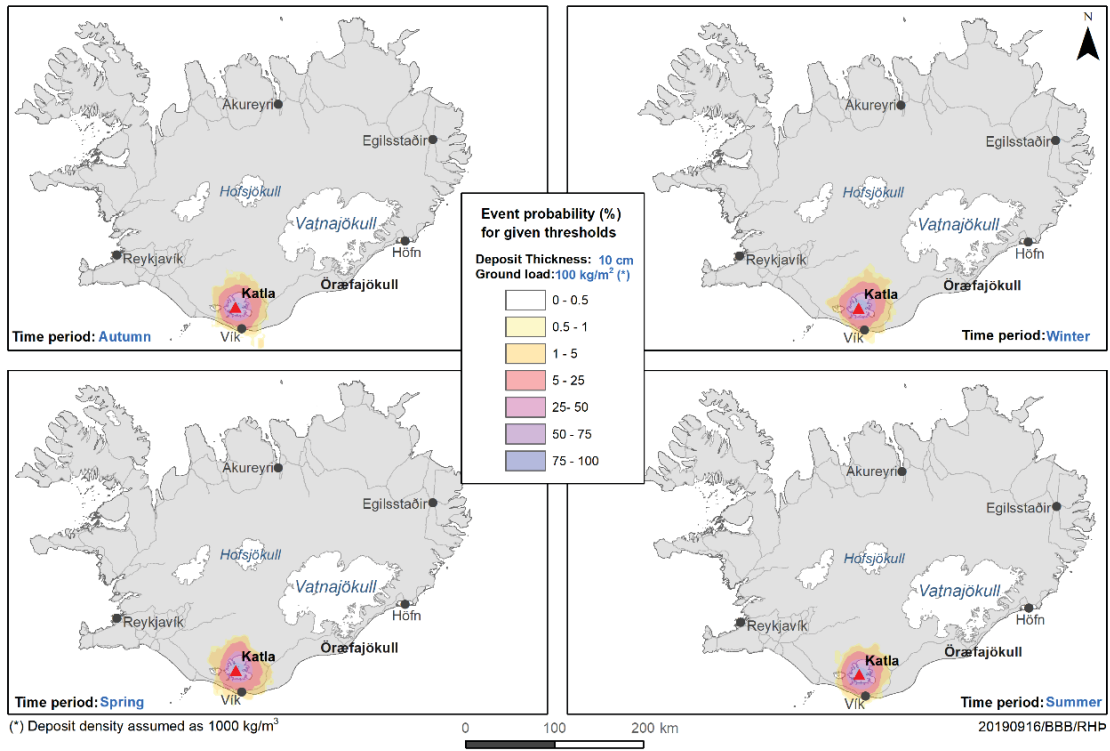


Figure 40. Seasonal analysis for tephra probability exceeding 100 kg/m² (~10 cm). Few towns are reported as reference. — *Árstíðabundin hættumatskort sem sýna líkindi þess að gjóskuþykkt fari yfir 10 cm (≥ 100 kg/m²) í svipuðu Kötlugosi og varð árið 1918 (sjá kafla 5.3.1). Haust: september, október, nóvember; Vetur: desember, janúar, febrúar; Vor: mars, apríl, maí; Sumar: júní, júlí, ágúst.*

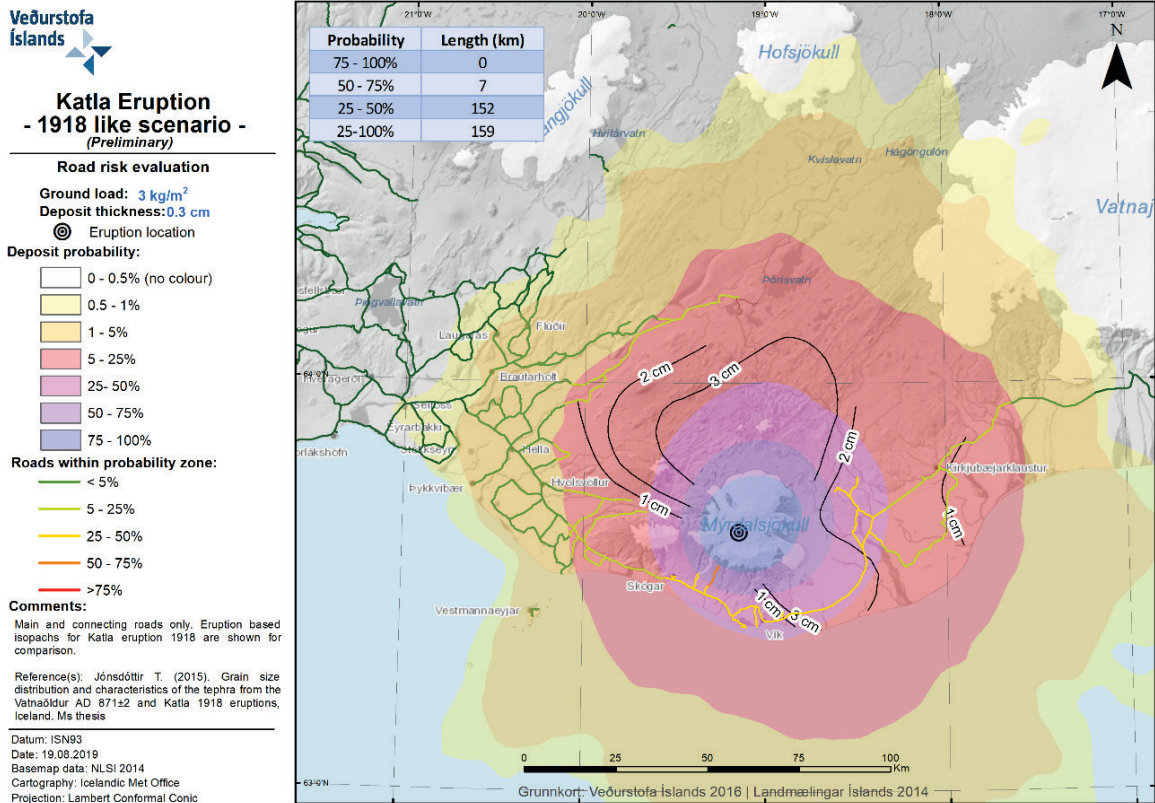


Figure 41. Impact map for road network in case of an eruption like 1918 at Katla. — *Áhrifakort fyrir vegi sem sýnir líkur á að ~3 mm þykkt gjóskulag ($\geq 3 \text{ kg/m}^2$) myndist af völdum goss í Kötlu en rannsóknir benda til að ökuskilyrði á malbikuðum vegum skerðist við þá gjóskubýkkt. Vegakerfi svæðisins er sýnt og líkur á að vegir verði fyrir ~3 mm gjóskufalli eru gefnar með litakóða, frá grænum (<5% líkur) og upp í rauðan (>75% líkur). Svörtu línurnar eru jafnþykktarlínur teiknaðar eftir þykktarmælingum sem gerðar voru á gjóskunni úr Kötlugosinu 1918 (Jónsdóttir, 2015).*

5.3.3 Towards Impact-based maps

When we look to a potential impact to infrastructure, we see that an eruption like 1918 at Katla could create difficult driving conditions up to 159 km of the road network with a likelihood higher than 25%. Seven km of the N222 road (the part accessing the Mýrdalsjökull from the South) would be affected with 75% of probability (Figure 41). The sector of the ring road departing from Vík town, both toward the East and to the West, could also be problematic with a probability more than 25% to be covered by 3 mm of ash. This would possibly make even more difficult an evacuation of this area in case of an ongoing eruption, even though most likely the road sector south of the volcano (roughly between Hvolsvöllur and Hrífunes) will be closed ahead due to jökulhlaup hazard. Tephra along the road would cause difficult driving conditions for those approaching the area in the aftermath of the eruption.

Katla Eruption - 1918 like scenario - (Preliminary)

Airport risk evaluation

Ground load: 1 kg/m²

Deposit thickness: 0.1 cm

⊙ Eruption location

■ Landing strip

Deposit probability:

- 0 - 0.5% (no colour)
- 0.5 - 1%
- 1 - 5%
- 5 - 25%
- 25 - 50%
- 50 - 75%
- 75 - 100%

Airport within probability zone:

- < 5%
- 5 - 25%
- 25 - 50%
- 50 - 75%
- 75 - 100%

Comments:

Eruption based isopachs for Katla eruption 1918 are shown for comparison.

Reference(s): Jónsdóttir T. (2015). Grain size distribution and characteristics of the tephra from the Vatnaöldur AD 871±2 and Katla 1918 eruptions, Iceland. Ms thesis

Datum: ISN93

Date: 19.08.2018

Basemap data: NLSI 2014

Cartography: Icelandic Met Office

Projection: Lambert Conformal Conic

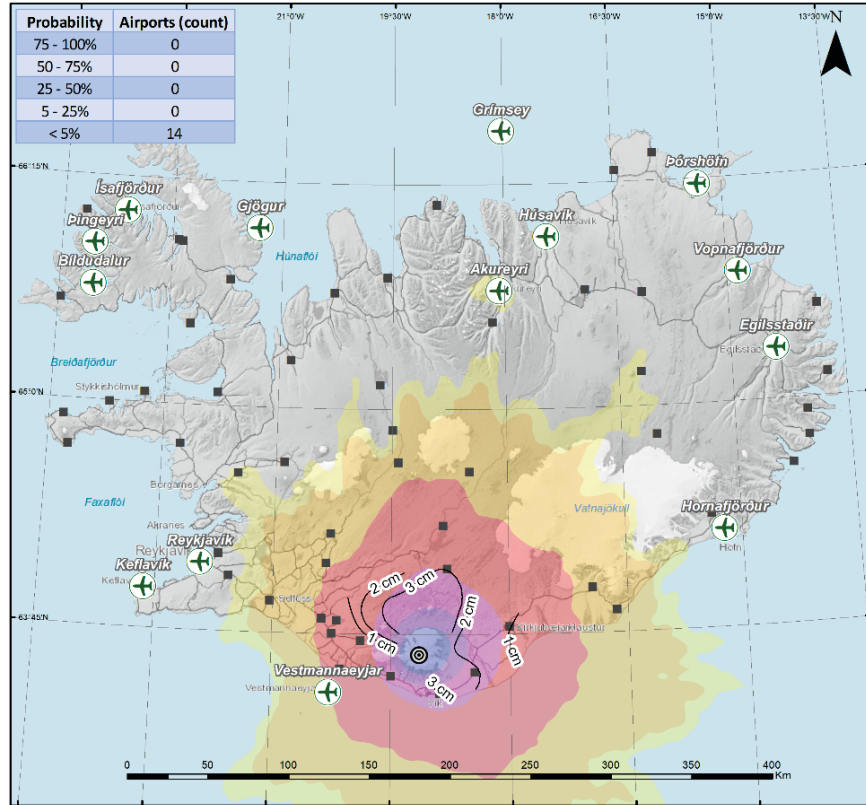


Figure 42. Impact map for airports in the country in case of an eruption like 1918 at Katla. Landing strips across the country are also mapped. — Áhrifakort sem sýnir líkur á að ~1 mm þykkt gjóskulag ($\geq 1 \text{ kg/m}^2$) myndist af völdum Kötlugoss sem svipar til gossins 1918 (kafla 5.3.1). Staðsetningar aðalflugvalla landsins eru sýndar og líkur á að þeir verði fyrir ~1 mm gjóskufalli eru táknadað með litakóða frá grænum (<5% líkur) upp í rauðan (>75% líkur). Gráir ferningar sýna staðsetningar skráðra lendingarstaða. Svörtu línurnar eru jafnþykktarlínur teiknaðar eftir þykktarmælingum sem gerðar voru á gjóskunni úr Kötlugosinu 1918 (Jónsdóttir, 2015).

No airports have a likelihood higher than 5% to receive ash in such an amount to disrupt operations. The airport closest to the volcano is the one in Heimaey island and it can be potentially affected by such ash deposit with a likelihood between 1 and 5% (Figure 42).

**Katla Eruption
- 1918 like scenario -
(Preliminary)**

Powerline risk evaluation

Ground load: 10 kg/m²

Deposit thickness: 1 cm

⊙ Eruption location

Deposit probability:

- 0 - 0.5% (no colour)
- 0.5 - 1%
- 1 - 5%
- 5 - 25%
- 25 - 50%
- 50 - 75%
- 75 - 100%

Powerlines within probability zone:

- 1 - 5%
- 5 - 25%
- 25 - 50%
- 50 - 75%
- >75%

Comments:

Eruption based isopachs for Katla eruption 1918 are shown for comparison.

Reference(s): Jónsdóttir T. (2015). Grain size distribution and characteristics of the tephra from the Vatnaöldur AD 871±2 and Katla 1918 eruptions, Iceland. Ms thesis

Datum: ISN93

Date: 10.09.2019

Basemap data: NLSI 2014

Cartography: Icelandic Met Office

Projection: Lambert Conformal Conic

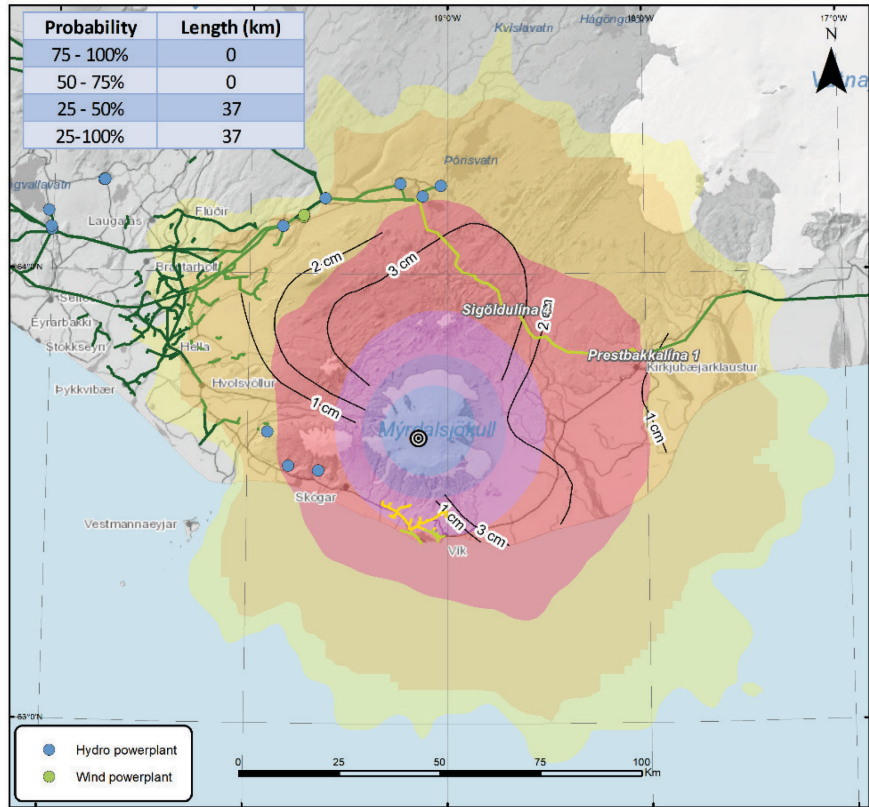


Figure 43. Impact map for power line in case of an eruption like 1918 at Katla. — Áhrifakort sem sýnir líkur á að ~1 cm þykk gjóskulag ($\geq 10 \text{ kg/m}^2$) myndist af völdum Kötlugoss sem svipar til gossins 1918. Raflínukerfi svæðisins er sýnt og líkur þess á það verði fyrir ~1 cm gjóskufalli eru sýndar með litakóða, frá grænum (<5% líkur) og upp í rauðan (>75% líkur). Svörtu línurnar eru jafnþykktarlinur teiknaðar eftir þykktarmælingum sem gerðar voru á gjóskunni úr Kötlugosinu 1918 (Jónsdóttir, 2015). Blái punktar sýna vatnsaflsvirknanir og grænir vindaflsvirkjanir.

Thirty-seven km of power line will be exposed to a tephra load higher than 10 kg/m² with a likelihood between 25–50%. This mainly covers the network around the town of Vík that might experience some disruption in the energy supply (Figure 43).

5.4 Öräfajökull

5.4.1 Input parameters and synthetic scenario

Paucity of field data and direct observations of the 1362 eruption makes complex to establish well constrained scenario for this event. However, the available publications (Jónsson, 2007; Sharma et al., 2008; Thorarinsson, 1958) provide the general framework for obtaining the eruption source parameters relevant for running the dispersal simulations. Calculating the total mass emitted during the Plinian phase of the eruption is challenging because a lot of tephra fell into the sea (see Figure 1). Using the information in Thorarinsson (1958) the total mass is assessed to be 4.8×10^{12} kg (Table 4).

A GIS referenced reconstruction of the original map by Thorarinsson (1958) is used to recalculate the erupted tephra mass by 1) assuming a constant thickness between the different isopachs and 2) by interpolating between two successive isopachs assuming a linear trend. These two estimates give an erupted tephra mass of 4.3×10^{12} kg and 6.9×10^{12} kg, where the latter is about factor of 1.5 larger than that obtained from Thorarinsson's (1958) data (see Table 10).

In order to run a dispersal model various input parameters need to be defined. In an attempt to reproduce the scenario reported in Table 4 and to match the isopachs as depicted in Thorarinsson (1958), the VOL-CALPUFF dispersal model was run multiple times using a vent radius from 150 to 300 m; a gas mass fraction from 1 to 5 % and three different TGSDs (one peaked at 125 microns, one peaked at one millimeter and a bi-modal distribution with two peaks at 125 microns and 4 millimeters, respectively). By a comparison of the model results and the original isopach map and by constraining the top plume height between 24–34 km, we got the best fit by using the following input parameters:

- Vertical velocity: 300 m/s
- Vent radius: 300 m
- Gas mass fraction: 3%
- Total Grain Size Distribution (TGSD) as shown in Figure 44
- Mass flow rate: 4.2×10^8 kg/s
- Duration of the emission: 18 hours

Running the plume model with these input parameters gives the following values for plume height and tephra emitted mass (to compare with values reported in Table 4):

- Plume height: 23.5-37 km asl
- Total erupted tephra mass: 2.7×10^{13} kg

This synthetic scenario is in a reasonable agreement with anticipated duration of the Plinian phase and plume height. However, there is a larger discrepancy in terms of mass. The new numerical simulation results suggest that in order to match the original isopachs, the Dense Rock Equivalent (DRE) volume is 5.5 km^3 . This volume is 2.75 times larger than that provided by Thorarinsson, and 1.9 times larger than the value calculated with the GIS interpolation (Table 10). Considering the huge uncertainty affecting the meteorological conditions during the eruption, the real extension of the deposit and the few observational data available, we considered valuable in this study to use those input parameters obtained through the matching procedure to perform the probabilistic assessment.

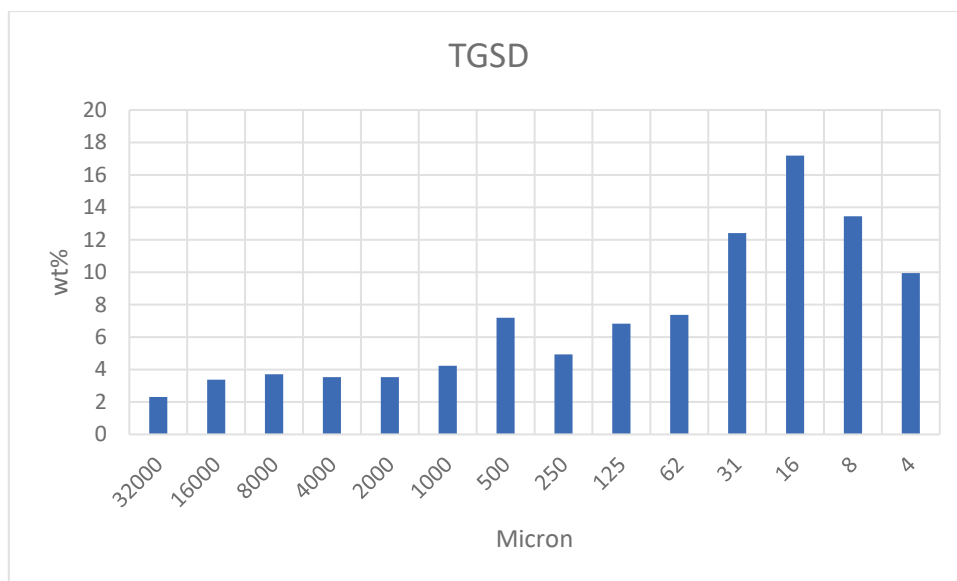


Figure 44. Reconstructed Total Grain Size Distribution (TGSD) for a typical rhyolitic Plinian fall deposit (adapted from Stevenson et al., 2015) used for the synthetic scenario. Important to note that no accretionary lapilli have been identified in the 1362 CE fall deposit (Thorvaldur Thordarson pers. com. 2018). — *Dæmigerð heildarkornastærðardreifing úr kísilríku (súru) gosi (byggt á gögnum úr Stevenson o.fl., 2015). Þessi tilbúna kornastærðardreifing var notuð við líkanútreikninga á sviðsmynd goss úr Öräfajökli, svipuðu því sem varð árið 1362. Engar öskubaunir (accretionary lapilli) hafa fundist í gjósku frá Ö-1362 (Þorvaldur Þórðarson, munnleg heimild, 2018).*

5.4.2 Validating model results with real deposit map

The synthetic scenario has been finalized by running the model and comparing qualitatively the results with the isopachs reconstructed for the real event. Figure 45 shows this comparison. The brown lines are the model results whereas the continuous black lines are the deposit isopachs as reconstructed by Thorarinsson 1958. A westerly wind has been selected to run the dispersal and match the general feature of the deposit pattern. For the same simulation the model predicted a super-buoyant plume with height of 30.6 km above the vent (Figure 46).

Table 10. Total mass and volume calculations summary. — *Yfirlit yfir mismunandi mat á heildarþunga og rúmmál gjósku úr Öräfajökulsgosinu 1362.*

	Total Mass	Total Volume
Thorarinsson (1958)	4.8×10^{12} kg	2 km ³ DRE
Thorarinsson GIS Simple	4.3×10^{12} kg	1.8 km ³ DRE
Thorarinsson GIS Interpolation	6.9×10^{12} kg	2.9 km ³ DRE
Model	2.7×10^{13} kg	5.5 km ³ DRE

**Öræfajökull Eruption
- 1362 like scenario -**

Comparison between model results
and Thorarinsson results (1958)

- ⊙ Eruption location
- Deposit thickness (modelled):
- 0.1 cm
- 1 cm
- 2 cm
- 5 cm
- 10 cm
- 20 cm
- 50 cm

Comments:

Eruption based isopachs for Öræfajökull eruption 1362 are shown for comparison.

Reference(s): Thorarinsson, S. (1958). The Öræfajökull eruption of 1362. Acta Naturalia Islandica II(2), 99 pp.

Datum: ISN93
Date: 16.09.2019
Basemap data: NLSI 2014
Cartography: Icelandic Met Office
Projection: Lambert Conformal Conic

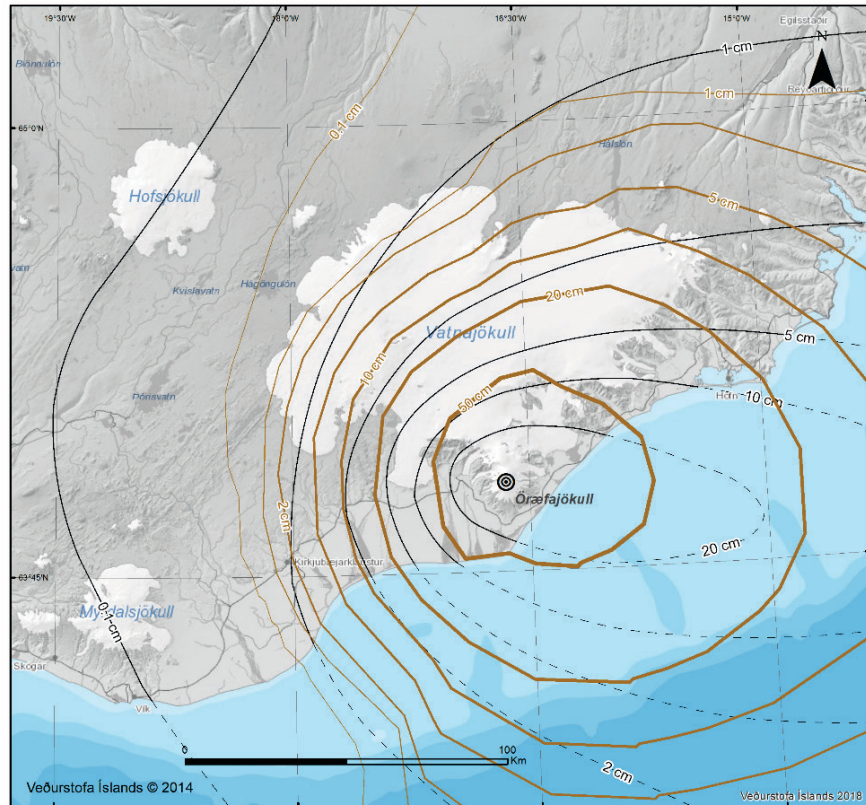


Figure 45. Model results are over-laid with the deposit isopach for the 1362 eruption. The simulation has been run by using a wind field characterized by a westerly wind to match the prevailing direction of the deposit. — *Niðurstöður hermunar gjóskufalls úr kisilríku gosi sambærilegu því sem átti sér stað í Öræfajökli árið 1362 (brúnar jafnþykktarlinur), einungis vestlægir vindar voru notaðir í gjóskufallshermun til að líkja eftir ríkjandi vindátt þegar gjóskan féll. Svörtu linurnar eru jafnþykktarlinur teiknaðar eftir þykktarmælingum sem gerðar voru á gjóskunni úr Öræfajökulsgosinu 1362 (Thorarinsson, 1958).*

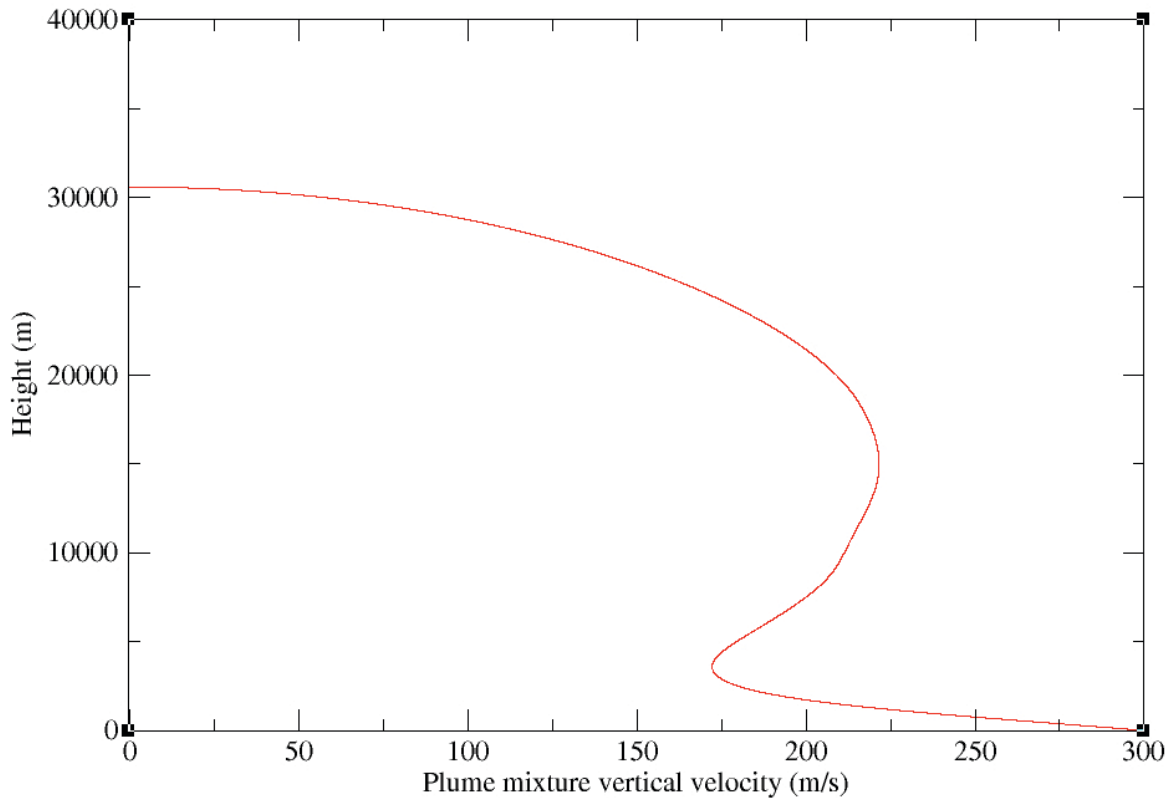


Figure 46. Vertical velocity profile of the eruptive mixture as a function of the height above the vent. Effective mixing of the volcanic mixture with the ambient air during the ascent phase (gas-thrust region) which allows the mixture to become less dense than the surrounding air and consequently becoming super-buoyant. — *Lóðrétt snið í gegnum gosmökk sem sýnir breytilegan hraða gosefna með hæð yfir gosupptökum. Þegar gosefnin draga inn í sig loft úr andrúmslofti hitnar það og þenst út vegna snertingar við heit gosefnin, gosmökkurinn verður því eðlisléttari en andrúmsloftið og stígur vegna uppdrifskrafts.*

The model result contours match the general trend of the reconstructed isopachs mapped by Thorarinnsson, but they generally overestimate the deposit thickness. Considering the larger volume used to reproduce a 30-km height plume this is not surprising. In addition, up to a factor of 3 increase in thickness of the Plinian fall in the most proximal sites compared to that given by Thorarinnsson (1958) has been identified by a recent survey (Thorvaldur Thordarson, unpublished data 2020). In light of this, we consider that the modelled scenario covers the most possible extreme case and it is worth to consider it.

**Öræfajökull Eruption
- 1362 like scenario -**

Event probability for given thresholds

Ground load: **1.0 kg/m²**
Deposit thickness: **0.1 cm**

- ⊙ Eruption location
- 0 - 0.5% (no colour)
- 0.5 - 1%
- 1 - 5%
- 5 - 25%
- 25 - 50%
- 50 - 75%
- 75 - 100%

Comments:

Eruption based isopachs for Öræfajökull eruption 1362 are shown for comparison.

Reference(s): Thorarinsson, S. (1958). The Öræfajökull eruption of 1362. Acta Naturalia Islandica II(2), 99 pp.

Datum: ISN93
Date: 05.09.2019
Basemap data: NLSI 2014
Cartography: Icelandic Met Office
Projection: Lambert Conformal Conic

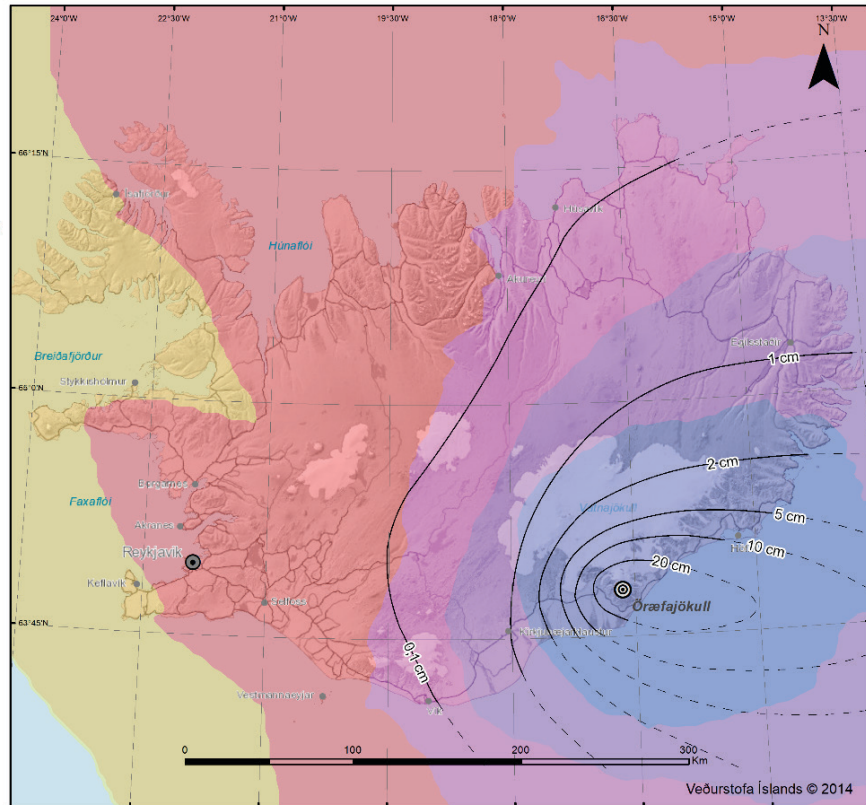


Figure 47. Probabilistic hazard map of tephra loading threshold of 1.0 kg/m² (~1 mm) for the eruption scenario at Öræfajökull. — *Hættumatskort sem sýnir líkur á að ~1 mm þykkt gjóskulag ($\geq 1.0 \text{ kg/m}^2$) myndist af völdum Öræfajökulsgoss sem svipar til gossins 1362 (sjá kafla 5.4.1). Svörtu línurnar eru jafnþykkjarlínur teiknaðar eftir þykktarmælingum sem gerðar voru á gjóskunni úr Öræfajökulsgosinu 1362 (Thorarinsson, 1958).*

5.4.3 Probabilistic hazard maps

We performed numerical simulations of volcanic ash dispersal by using VOL-CALPUFF code (Barsotti et al., 2018). The simulations yielded tephra thicknesses and concentrations data points over Iceland. We then generated probabilistic hazard maps for tephra loading at given thresholds for the eruption scenario at Öræfajökull, by adopting a Monte-Carlo approach. This was achieved by performing about 500 numerical simulations and conducting a thorough post processing of the data. In this report, we present three probabilistic hazard maps (see Figure 47, Figure 48 and Figure 49) for the tephra loading thresholds of 1.0 kg/m² (equivalent to 0.1 cm), 100 kg/m² (equivalent to 10 cm) and 1000 kg/m² (equivalent to 1 m).

In Figure 47 the 0.1 cm isoline produced by Thorarinsson falls entirely within the 25–50% probability of reaching this deposit thickness. All of Iceland, apart from some areas of the north-west fjords, has at least a 5% probability of exceeding a load threshold of 1 kg/m² equivalent to 1 mm of tephra deposit.

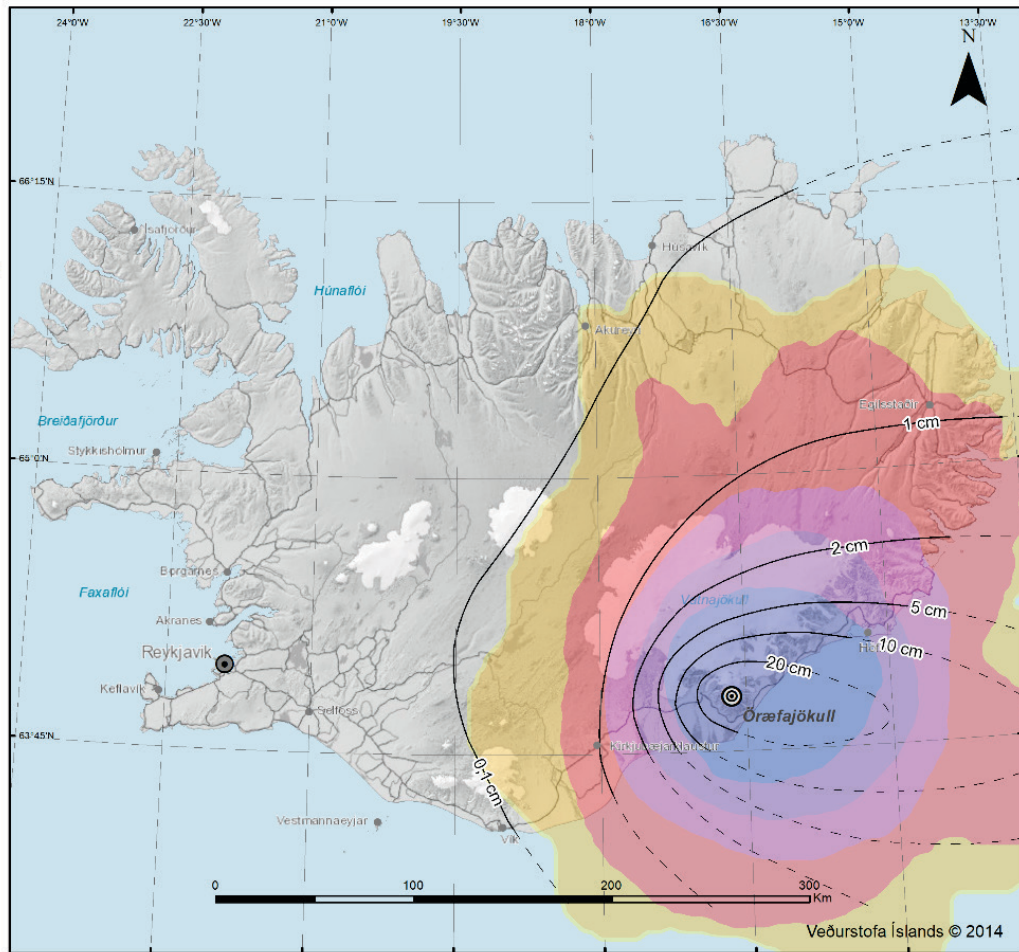


Figure 48. Probabilistic hazard map of tephra loading threshold of 100 kg/m^2 ($\sim 10 \text{ cm}$) for the eruption scenario at Örfajökull. The color scale refers to the legend in Figure 47. — *Hættumatskort sem sýnir líkur á að $\sim 10 \text{ cm}$ þykkt gjóskulag ($\geq 100 \text{ kg/m}^2$) myndist af völdum Örfajökulsgoss sem svipar til gossins 1362 (sjá kafla 5.4.1). Svörtu linurnar eru jafnþykktarlínur teiknaðar eftir þykktarmælingum sem gerðar voru á gjóskunni úr Örfajökulsgosinu 1362 (Thorarinsson, 1958). Litaskali er sá sami og á mynd 47.*

In Figure 48 the isoline of 10 cm produced by Thorarinsson falls entirely within the 75–100% probability of reaching this deposit thickness. The part of Iceland enclosed within the smallest isoline of 0.1 cm has at least a probability of 1% of exceeding a load of 100 kg/m^2 . This area includes eastern and south-eastern Iceland, most of the highlands and parts of the north-east.

In Figure 49 the likelihood of exceeding a threshold of 1000 kg/m^2 is limited to a small area closest to the volcanic vent. Part of the proximal area enclosed within the 20 cm isoline falls within the 5–25% probability of reaching a deposit thickness of 1 m.

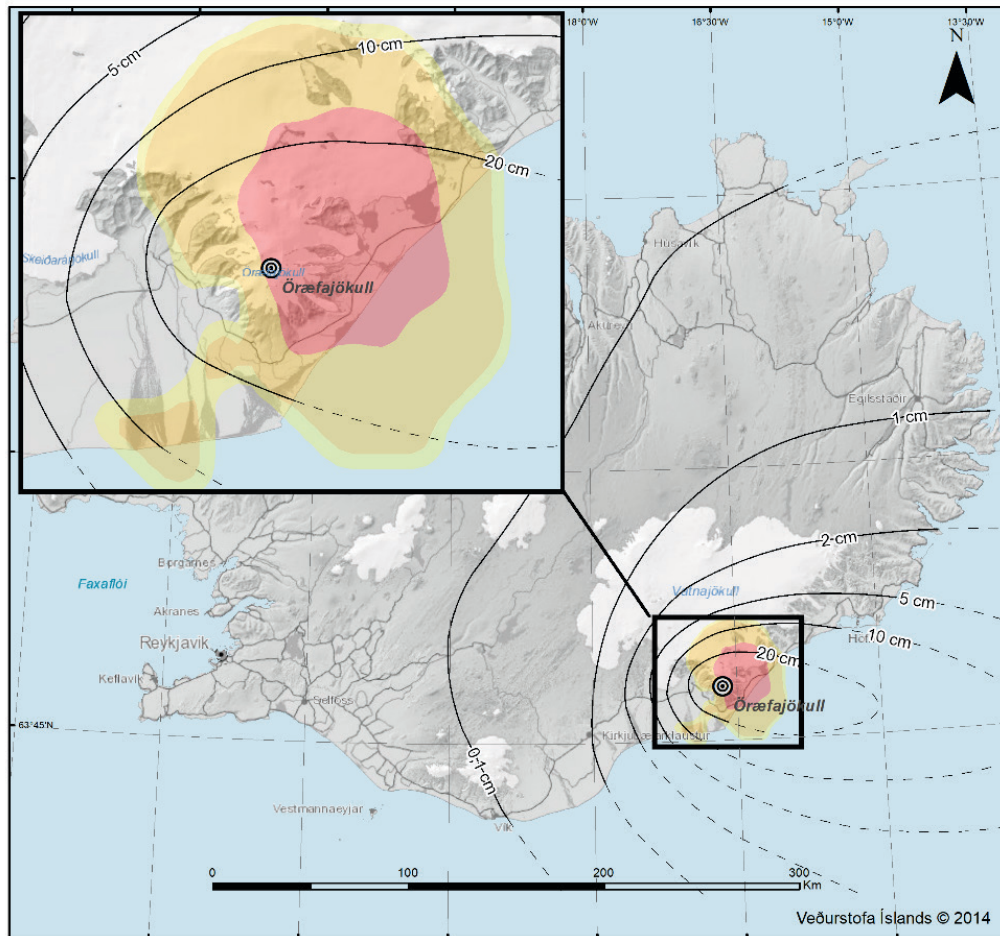


Figure 49. Probabilistic hazard map of tephra loading threshold of 1000 kg/m^2 ($\sim 100 \text{ cm}$) for the eruption scenario at Öræfajökull. The color scale refers to the legend in Figure 47. — Hættumatskort sem sýnir líkur á að $\sim 100 \text{ cm}$ þykkt gjóskulag ($\geq 1000 \text{ kg/m}^2$) myndist af völdum Öræfajökulsgoss sem svipar til gossins 1362 (sjá kafla 5.4.1). Svörtu línurnar eru jafnþykktarlínur teiknaðar eftir þykktarmælingum sem gerðar voru á gjóskunni úr Öræfajökulsgosinu 1362 (Thorarinsson, 1958). Litaskali er sá sami og á mynd 47.

The table in Appendix IV summarizes how an eruption at Öræfajökull might impact most of the principal towns in Iceland, by reporting the likelihood to exceed three different tephra loads of 1, 10 and 100 kg/m^2 . Fagurhólsmýri (100%) and Höfn (97.8%) are those with the highest likelihood to get ash exceeding 1 mm deposit. They are the most exposed ones due to their vicinity to the volcano and the prevailing wind directions. They are both heavily exposed to even higher loads (100 kg/m^2) with a likelihood of about 97% and 73%, respectively. Reykjavík is less exposed due to the distance to the volcano and mainly because it is located upwind the dominant wind. Akureyri, despite its distance, is showing intermediate values.

Öræfajökull eruption - 1362 like scenario

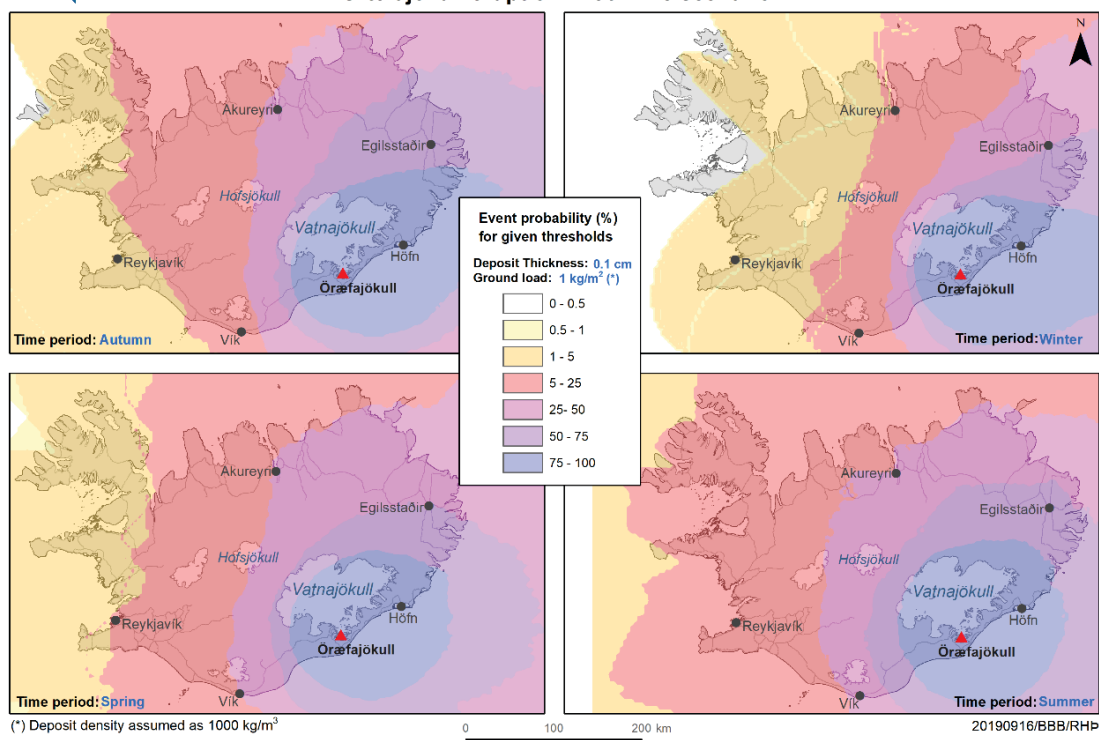


Figure 50. Seasonal analysis for 1 kg/m^2 ($\sim 1 \text{ mm}$) tephra ground load. Few towns are reported as reference. — *Árstíðabundin hættumatskort sem sýna líkindi þess að gjóskuþykkt fari yfir 1 mm ($\geq 1 \text{ kg/m}^2$) í svipuðu Öræfajökulsgosi og varð árið 1362 (sjá kafla 5.4.1). Haust: september, október, nóvember; Vetur: desember, janúar, febrúar; Vor: mars, apríl, maí; Sumar: júní, júlí, ágúst.*

A seasonal analysis has been done to identify some specific trend due to major shift in wind direction and intensity. The analysis has been performed investigating the four thresholds of 0.1 , 1 , 10 and 100 kg/m^2 . The results for 1 and 10 kg/m^2 are showed in Figure 50 and Figure 51. Here we consider autumn (SON), winter (DJF), spring (MAM) and summer (JJA).

As already seen a load equal or larger than 1 kg/m^2 equivalent to 1 mm of tephra deposit can be expected almost everywhere in Iceland, with the West Fjords showing the lowest probability (Figure 47). The seasonal analysis reveals that the intermediate seasons (autumn and spring) have almost the same pattern of deposition. More evident differences characterize the results obtained for winter and summer. In the winter period the deposit is much more oriented toward the East and very low likelihoods are expected over the western part of the country. The area with the highest likelihood to exceed 1 kg/m^2 is oriented toward the East and extends well into the sea. The summer scenario is significantly different with the entire country potentially affected with a likelihood higher than 5% . The eastern half of the country shows a likelihood higher than 25% . Probabilities higher than 75% include all Vatnajökull and a large sector of the south-east sector of the country.

Öræfajökull eruption - 1362 like scenario

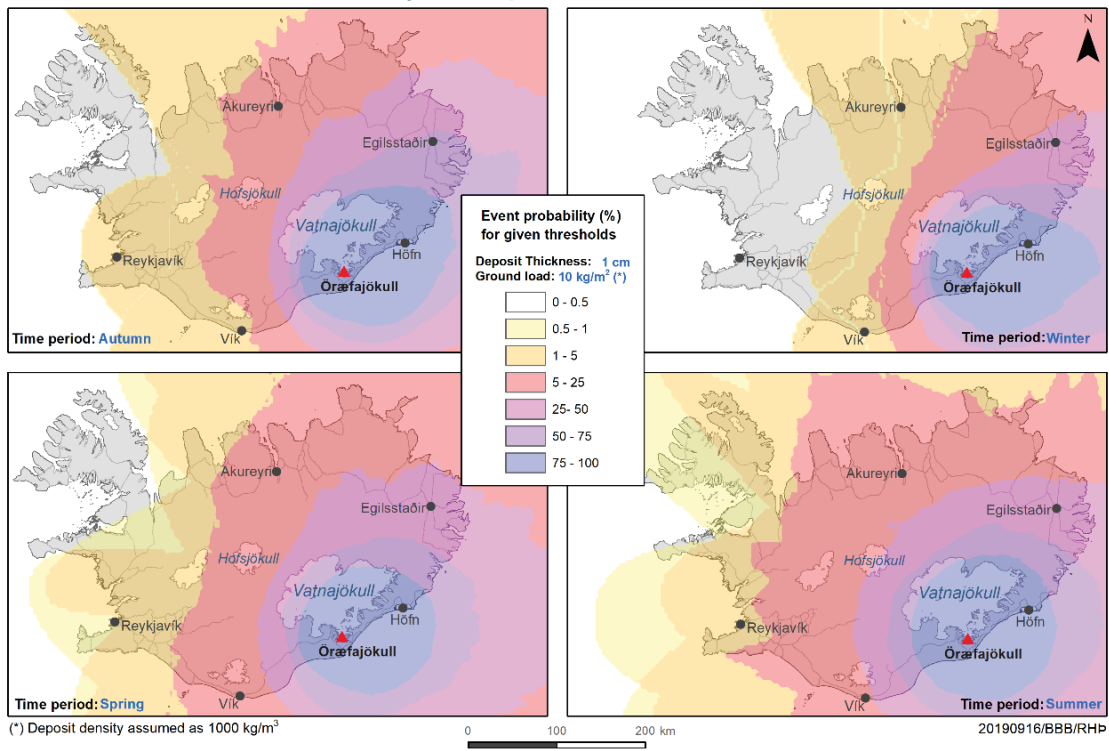


Figure 51. Seasonal analysis for 10 kg/m² (~1 cm) tephra ground load. Few towns are reported as reference. — *Árstíðabundin hættumatskort sem sýna líkindi þess að gjóskubýkkt fari yfir 1 cm (≥ 10 kg/m²) í svipuðu Öræfajökulsgosi og varð árið 1362 (sjá kafla 5.4.1). Hausti: september, október, nóvember; Vetur: desember, janúar, febrúar; Vor: mars, apríl, maí; Sumar: júní, júlí, ágúst.*

A similar trend is generally valid also for the results obtained for the 10 kg/m² threshold. Autumn and spring have similar results even though the autumn results identify a NE trend of the iso-contours. During the winter time the deposit is mainly oriented toward East with likelihood to have the Western part of the country affected by this tephra load below 0.5%. During the summer the whole country could expect some tephra deposit higher than 10 kg/m² with likelihood larger than 0.5%.

All those results are consistent with the general trend of the wind field that sees a prevailing westerly wind during the winter months at the high altitudes, and an easterly direction during the summer months (Lacasse, 2001). At the same time stronger winds are on averaged observed during the winter time and weaker wind are usually characterizing the summer time (Lacasse, 2001).

Öræfajökull Eruption - 1362 like scenario -

Road risk evaluation
 Ground load: 3 kg/m²
 Deposit thickness: 0.3 cm

⊙ Eruption location

Deposit probability:

- 0 - 0.5% (no colour)
- 0.5 - 1%
- 1 - 5%
- 5 - 25%
- 25 - 50%
- 50 - 75%
- 75 - 100%

Roads within probability zone:

- < 5%
- 5 - 25%
- 25 - 50%
- 50 - 75%
- >75%

Comments:
 Main and connecting roads only. Eruption based isopachs for Öræfajökull eruption 1362 are shown for comparison.

Reference(s): Thorarinsson, S. (1958). The Öræfajökull eruption of 1362. Acta Naturalia Islandica II(2), 99 pp.

Datum: ISN83
 Date: 23.11.2016
 Basemap data: NLSI 2014
 Cartography: Icelandic Met Office
 Projection: Lambert Conformal Conic

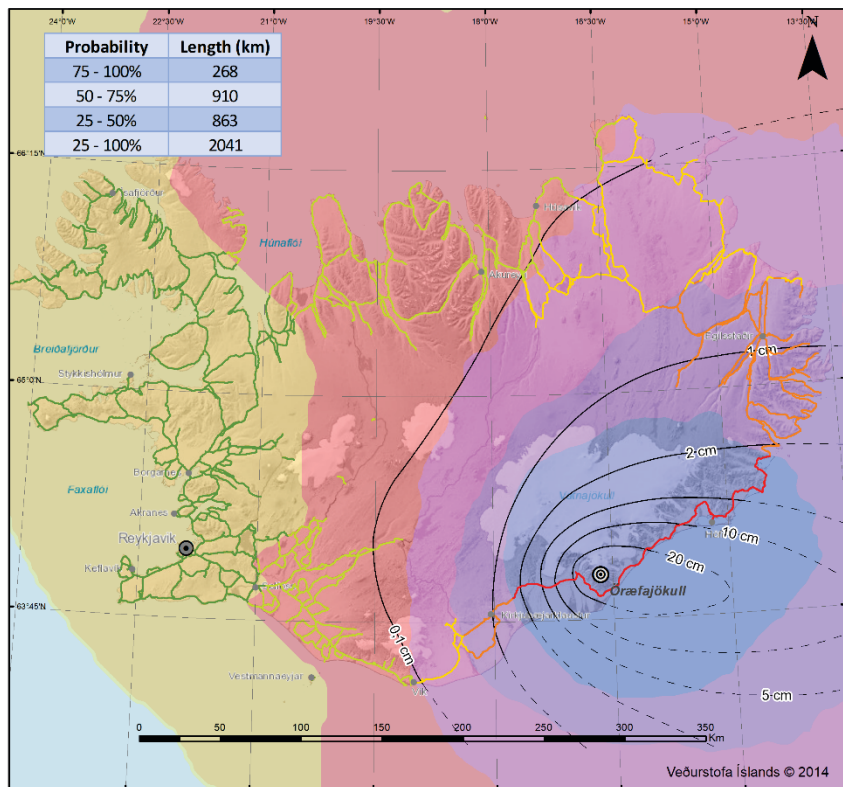


Figure 52. Impact map for roads in case of a 1362-like eruption at Öræfajökull. — *Ahrifakort sem sýnir líkur á að ~3 mm þykkt gjóskulag ($\geq 3 \text{ kg/m}^2$) myndist af völdum goss í Öræfajökli sambærilegt því sem varð árið 1362 (sjá kafla 5.4.1) en rannsóknir benda til að öskukilyrði á malbikuðum vegum skerðist við þá gjóskubýkkt. Vegakerfi svæðisins er sýnt og líkur á að vegir verði fyrir ~3 mm gjóskufalli eru gefnar með litakóða, frá grænum (<5% líkur) og upp í rauðan (>75% líkur). Svörtu línurnar eru jafnþykktarlínur teiknaðar eftir þykktarmælingum sem gerðar voru á gjóskunni úr Öræfajökulsgosinu 1362 (Thorarinsson, 1958).*

5.4.4 Towards Impact-based maps

A similar analysis as performed for Hekla and Katla volcanoes has been done for a potential eruption at Öræfajökull. The results are shown in Figure 52, Figure 53 and Figure 54. When looking to the possible disturbance to road traffic we can see that up to 268 km of the main road system will be affected with a likelihood between 75 and 100% (red road sector in Figure 52). Some localities in the East part of the country will not be reachable by driving through the Southern Coast ring road section due to roads cuts by jökulhlaups (Pagneux et al., 2015). Even a longer part of the road network can be affected by dangerous driving conditions with a likelihood higher than 25%; this affects more than 2000 km of the network, extending from Vík, in the South, to Húsavík, in the North. To re-establish safe driving conditions would need actions to clean the roads as soon as the visibility conditions will allow. This might take up to one full day since the beginning of the operations. If we consider that also the airports in Höfn and Egilsstaðir can be disrupted with a likelihood higher than 50% (Figure 53), then it results in that the connection with the Eastern part of the country will be very difficult and dangerous during and shortly (days-weeks) after the eruption.

**Öræfajökull Eruption
- 1362 like scenario -**

Airport risk evaluation
Ground load: 1 kg/m^2
Deposit thickness: 0.1 cm

⊙ Eruption location
■ Landing strip

Deposit probability:

- 0 - 0.5% (no colour)
- 0.5 - 1%
- 1 - 5%
- 5 - 25%
- 25 - 50%
- 50 - 75%
- 75 - 100%

Airport within probability zone:

- ⊕ 1 - 5%
- ⊕ 5 - 25%
- ⊕ 25 - 50%
- ⊕ 50 - 75%
- ⊕ 75 - 100%

Comments:

Eruption based isopachs for Öræfajökull eruption 1362 are shown for comparison.

Reference(s): Thorarinsson, S. (1958). The Öræfajökull eruption of 1362. Acta Naturalia Islandica II(2), 99 pp.

Datum: ISN93
Date: 09.09.2019
Basemap data: NLSI 2014
Cartography: Icelandic Met Office
Projection: Lambert Conformal Conic

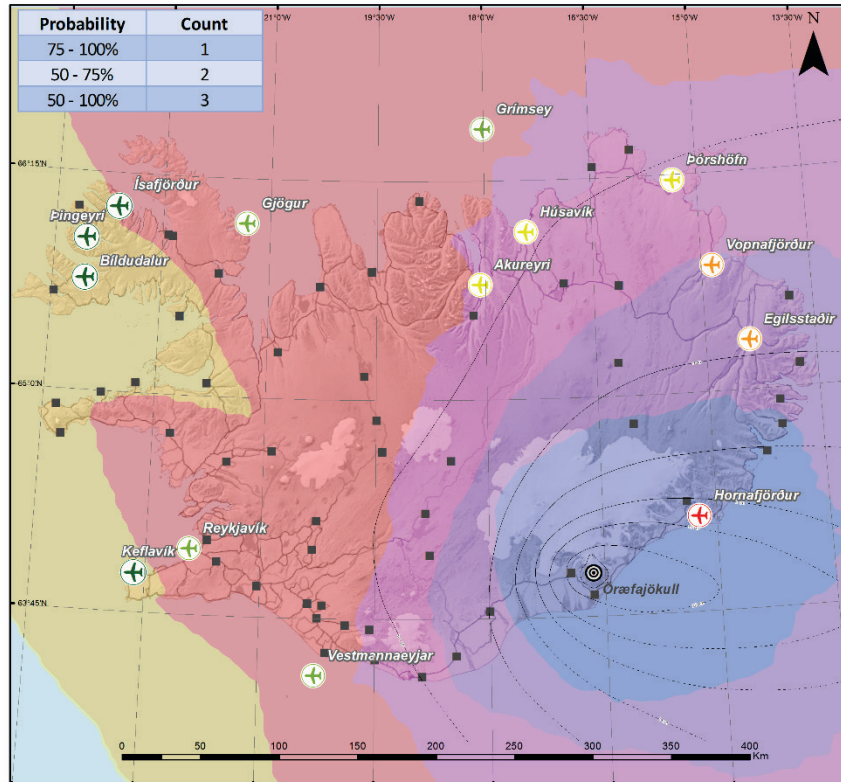


Figure 53. Impact map for airports in case of a 1362-like eruption at Öræfajökull. Landing strips across the country are also mapped. — Áhrifakort sem sýnir líkur á að $\sim 1 \text{ mm}$ þykkt gjóskulag ($\geq 1 \text{ kg/m}^2$) myndist af völdum Öræfajökulsgoss svipuðu því sem varð 1362 (sjá kafla 5.4.1). Staðsetningar aðalflugvalla landsins eru sýndar og líkur á að þeir verði fyrir $\sim 1 \text{ mm}$ gjóskufalli eru táknaðar með litakóða frá grænum ($< 5\%$ líkur) upp í rauðan ($> 75\%$ líkur). Gráir ferningar sýna staðsetningar skráðra lendingarstaða. Svörtu línurnar eru jafnþykktarlínur teiknaðar eftir þykktarmælingum sem gerðar voru á gjóskunni úr Öræfajökulsgosinu 1362 (Thorarinsson, 1958).

An eruption like 1362 will most likely reduce the capability to connect to the East part of the country by impacting severely the air traffic and road traffic infrastructures.

An eruption of this size has a potential to create disruption to all the main airports in the country, with the domestic airport in Reykjavík showing a likelihood above 5% to receive 1 mm of ash and Keflavík International Airport 1%.

Figure 54 shows a zoomed domain around Öræfajökull, as the main impact on the power line network is assessed to be quite proximal to the volcano. For this investigation a threshold of 100 mm of ash has been adopted, as reported in Table 3 and 4. We assume this condition, corresponding to a load of about 100 kg/m^2 , to be representative of critical conditions for power line damage. The results show that up to 115 km of power line network will be exposed to such a load with likelihood between 75 and 100%. This is the part of the power line passing nearby the volcano at a minimum distance of about 9.5 km (red line sector). About 45 km in addition, are exposed to such load with a likelihood between 50 and 75%, so that more than 160 km of the power line network can be damaged due to an eruption at Öræfajökull with a likelihood higher than 50%. Almost the entire power line network feeding the Örfæfi district is highly exposed to serious damage due to tephra fallout.

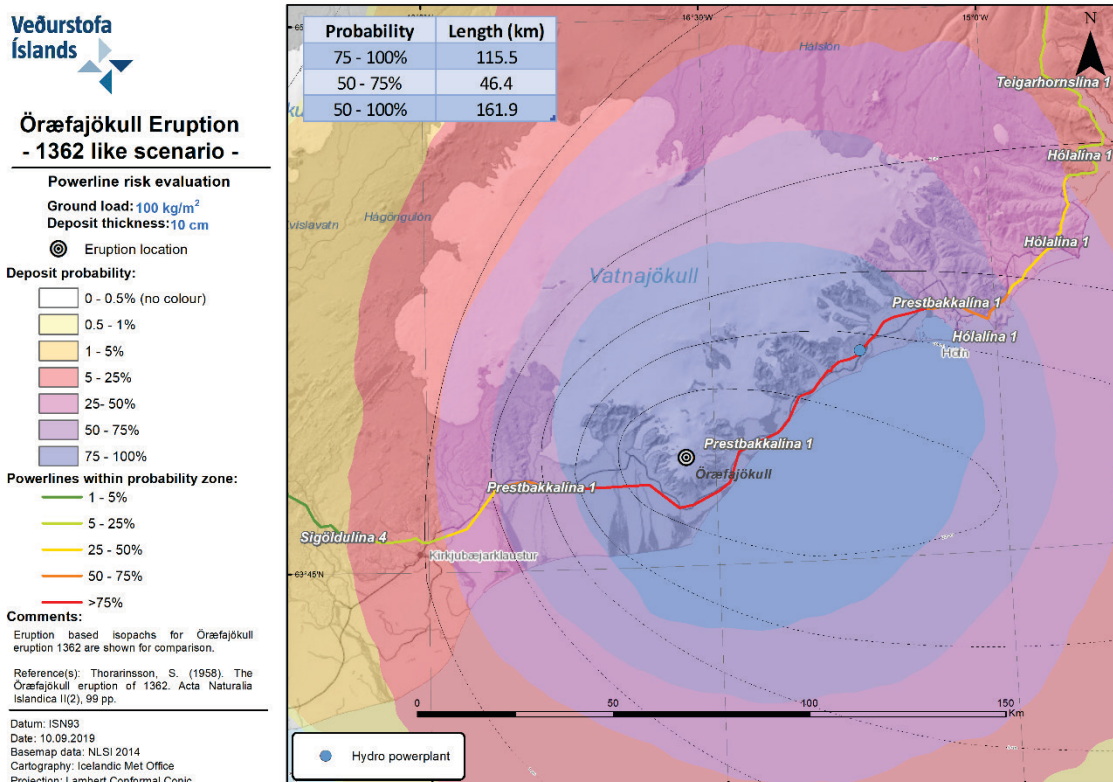


Figure 54. Impact map for power lines in case of a 1362-like eruption at Öraefajökull. — Áhrifakort sem sýnir líkur á að ~10 cm þykk gjóskulag ($\geq 100 \text{ kg/m}^2$) myndist af völdum Öraefajökulsgoss svipuðu því sem varð 1362. Raflínakerfi svæðisins er sýnt og líkur á að það verði fyrir ~10 cm gjóskufalli eru sýndar með litakóða, frá grænum (<5% líkur) og upp í rauðan (>75% líkur). Svörtu líurnar eru jafnþykkarlinur teiknaðar eftir þykktarmælingum sem gerðar voru á gjóskunni úr Kötlugosinu 1918 (Jónsdóttir, 2015). Blái punktar sýna vatnsaflsvirknanir og grænir vindafllsvirkjanir.

Few more special maps have been produced to estimate the potential impact of such an eruption on human health. Figures 55, 56 and 57 show the temporal evolution of the area potentially affected by critical concentration of PM₁₀ (as introduced in Section 3.2) with likelihood larger than 5, 25 and 50%, respectively. Each map shows for a specific probability of occurrence, the extension of the area affected by concentration higher than 300 and 3000 $\mu\text{g/m}^3$ as function of time (i.e. after 1, 3, 6, 12, and 24 hours since the onset of the eruption). It results that after the first hour a large part of the country (including around 6200 inhabitants) will be experiencing unhealthy conditions (hourly PM₁₀ concentration higher than 3000 $\mu\text{g/m}^3$) with a probability higher than 5% (Figure 55). After 12 hours since the beginning of the eruption the entire country, except for the Reykjanes tip and the West Fjords) will be affected by such low air-quality conditions. One day into the eruption all country has a likelihood higher than 5% to reach such unhealthy condition (Figure 55).

A smaller area (with around 2000 inhabitants) will be affected by high level of volcanic PM₁₀ after the first hour with a likelihood of 50%. After one day since the beginning of the eruption only the Eastern sector of the country will be exposed to unhealthy conditions (Figure 57).

**Öræfajökull Eruption
- 1362 like scenario -**

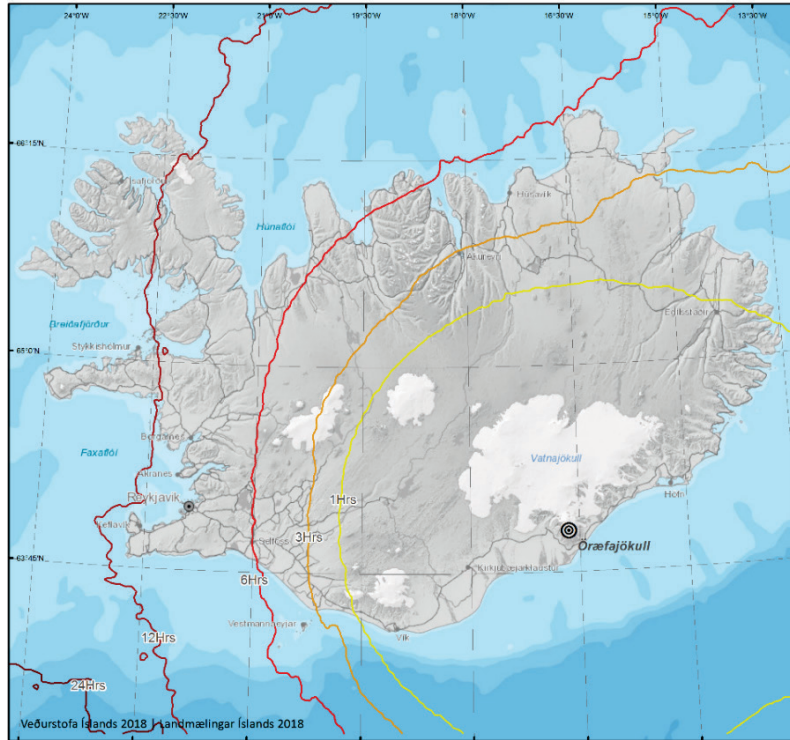
Probability of PM₁₀ threshold exceedance

Threshold: 300 µg/m³
Probability: 5%



Comments:
Concentrations are calculated at ground level.

Datum: ISN93
Date: 05.12.2018
Basemap data: NLSI 2014
Cartography: Icelandic Met Office
Projection: Lambert Conformal Conic



**Öræfajökull Eruption
- 1362 like scenario -**

Probability of PM₁₀ threshold exceedance

Threshold: 3000 µg/m³
Probability: 5%



Comments:
Concentrations are calculated at ground level.

Datum: ISN93
Date: 05.12.2018
Basemap data: NLSI 2014
Cartography: Icelandic Met Office
Projection: Lambert Conformal Conic

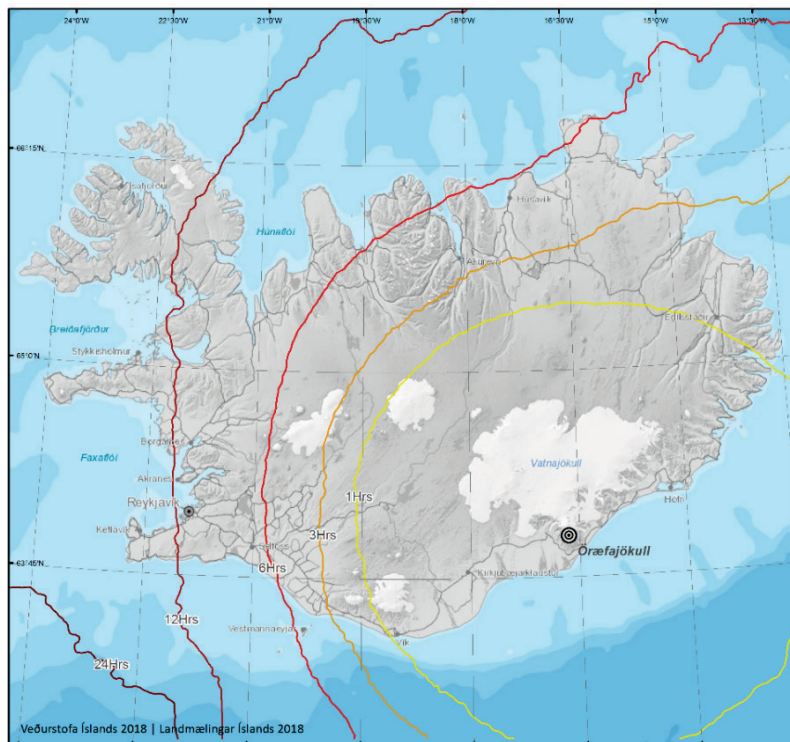


Figure 55. PM₁₀ probability map for the modelled Öræfajökull eruption. The map shows the probability that a PM₁₀ concentration of 300 (up) and 3000 (bottom) µg/m³ will be exceeded after 1, 3, 6, 12, and 24 hours since the beginning of the eruption with a likelihood of 5%. PM₁₀ concentration is calculated at ground level. — *Hættumatskort sem sýna 5% líkur á að styrkur gjóskukorna (minni en 10 míkrometrar; PM₁₀) í andrúmslofti við jörðu fari yfir 300 µg/m³ (efri mynd) og yfir 3000 µg/m³ (neðri mynd) eftir 1, 3, 6, 12 og 24 klst frá upphafi goss í Öræfajökli.*

**Öræfajökull Eruption
- 1362 like scenario -**

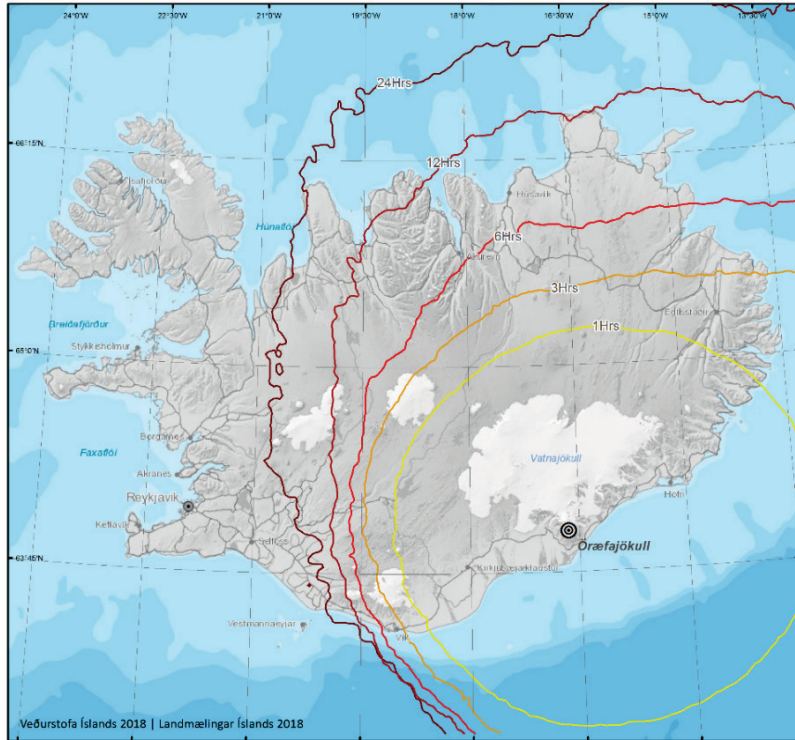
Probability of PM₁₀ threshold exceedance

Threshold: 300 µg/m³
Probability: 25%



Comments:
Concentrations are calculated at ground level.

Datum: ISN93
Date: 05.12.2018
Basemap data: NLSI 2014
Cartography: Icelandic Met Office
Projection: Lambert Conformal Conic



**Öræfajökull Eruption
- 1362 like scenario -**

Probability of PM₁₀ threshold exceedance

Threshold: 3000 µg/m³
Probability: 25%



Comments:
Concentrations are calculated at ground level.

Datum: ISN93
Date: 05.12.2018
Basemap data: NLSI 2014
Cartography: Icelandic Met Office
Projection: Lambert Conformal Conic

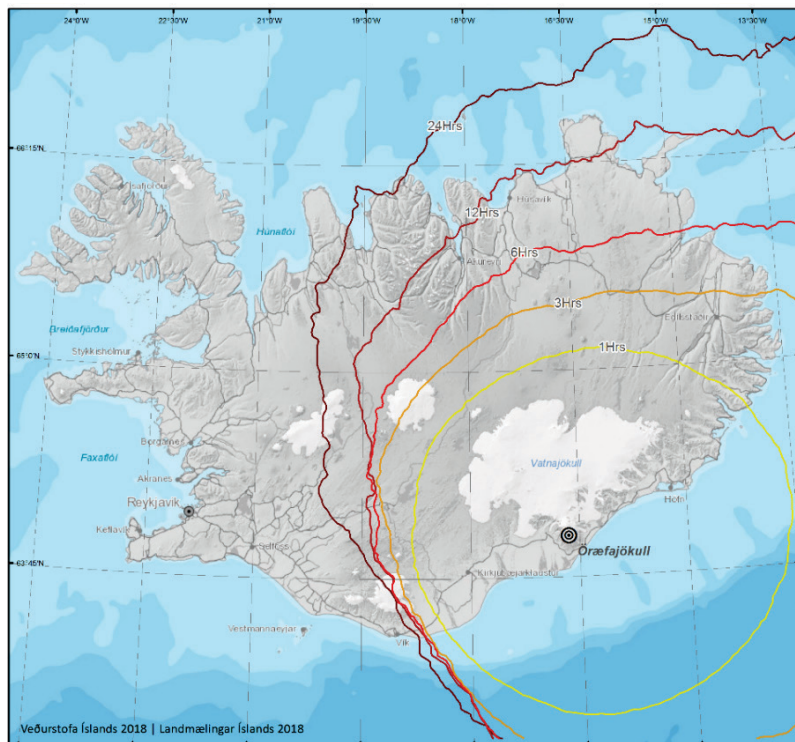


Figure 56. PM₁₀ probability map for the modelled Öræfajökull eruption. The map shows the probability that a PM₁₀ concentration of 300 (top) and 3000 (bottom) µg/m³ will be exceeded after 1, 3, 6, 12, and 24 hours since the beginning of the eruption with a likelihood of 25%. PM₁₀ concentration is calculated at ground level. — *Hættumatskort sem sýna 25% líkur á að styrkur gjóskukorna (minni en 10 mikrometrar; PM₁₀) í andrúmslofti við jörðu fari yfir 300 µg/m³ (efri mynd) og yfir 3000 µg/m³ (neðri mynd) eftir 1, 3, 6, 12 og 24 klst frá upphafi goss í Öræfajökli.*

Öræfajökull Eruption - 1362 like scenario -

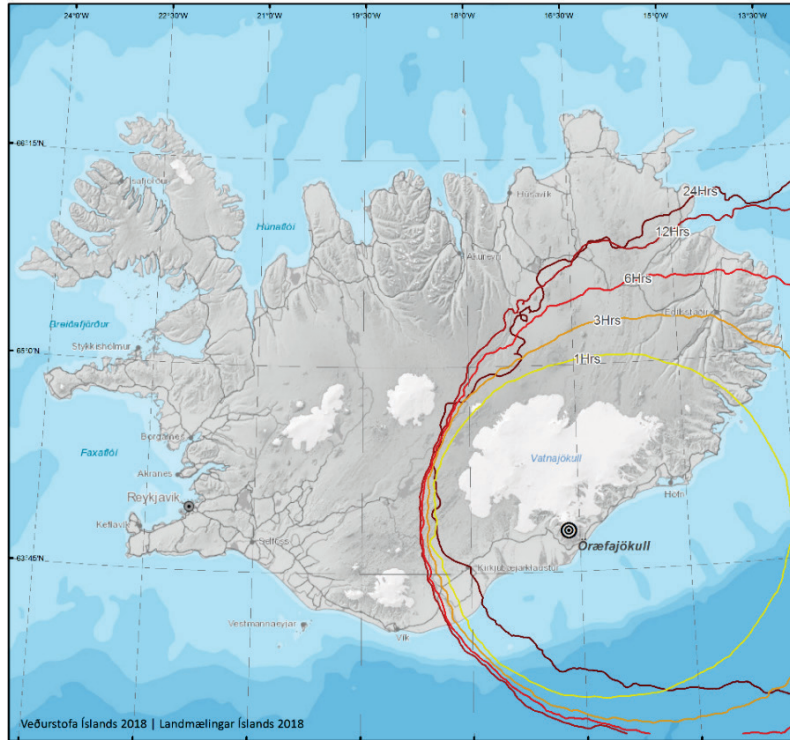
Probability of PM₁₀ threshold exceedance

Threshold: 300 µg/m³
Probability: 50%



Comments:
Concentrations are calculated at ground level.

Datum: ISN93
Date: 05.12.2018
Basemap data: NLSI 2014
Cartography: Icelandic Met Office
Projection: Lambert Conformal Conic



Öræfajökull Eruption - 1362 like scenario -

Probability of PM₁₀ threshold exceedance

Threshold: 3000 µg/m³
Probability: 50%



Comments:
Concentrations are calculated at ground level.

Datum: ISN93
Date: 05.12.2018
Basemap data: NLSI 2014
Cartography: Icelandic Met Office
Projection: Lambert Conformal Conic

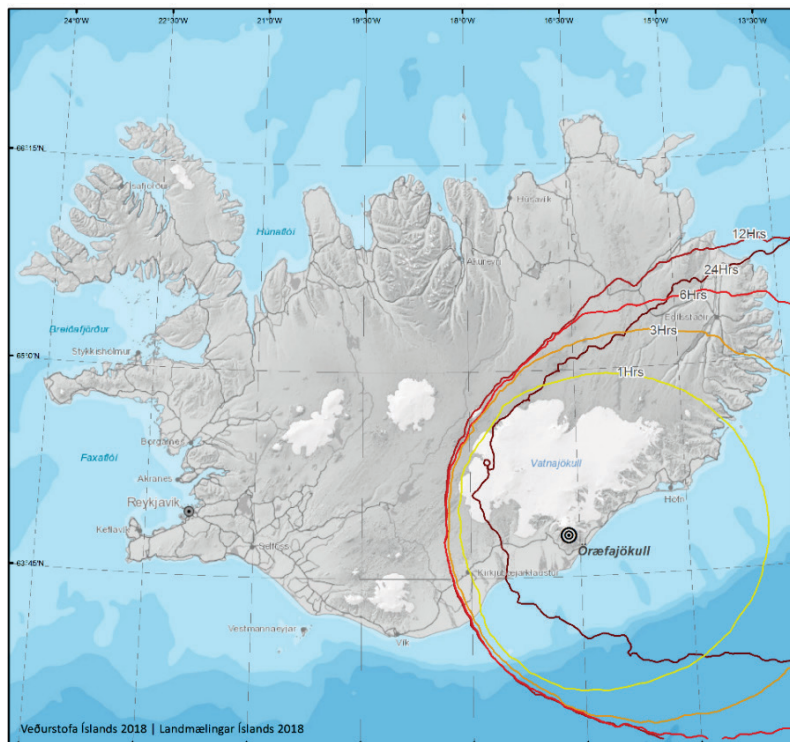


Figure 57. PM₁₀ probability map for the modelled Öræfajökull eruption. The map shows the probability that a PM₁₀ concentration of 300 (top) and 3000 (bottom) µg/m³ will be exceeded after 1, 3, 6, 12, and 24 hours since the beginning of the eruption with a likelihood of 50%. PM₁₀ concentration is calculated at ground level. — *Hættumatskort sem sýna 50% líkur á að styrkur gjóskukorna (minni en 10 míkrometrar; PM₁₀) í andrúmslofti við jörðu fari yfir 300 µg/m³ (efri mynd) og yfir 3000 µg/m³ (neðri mynd) eftir 1, 3, 6, 12 og 24 klst frá upphafi goss í Öræfajökli.*

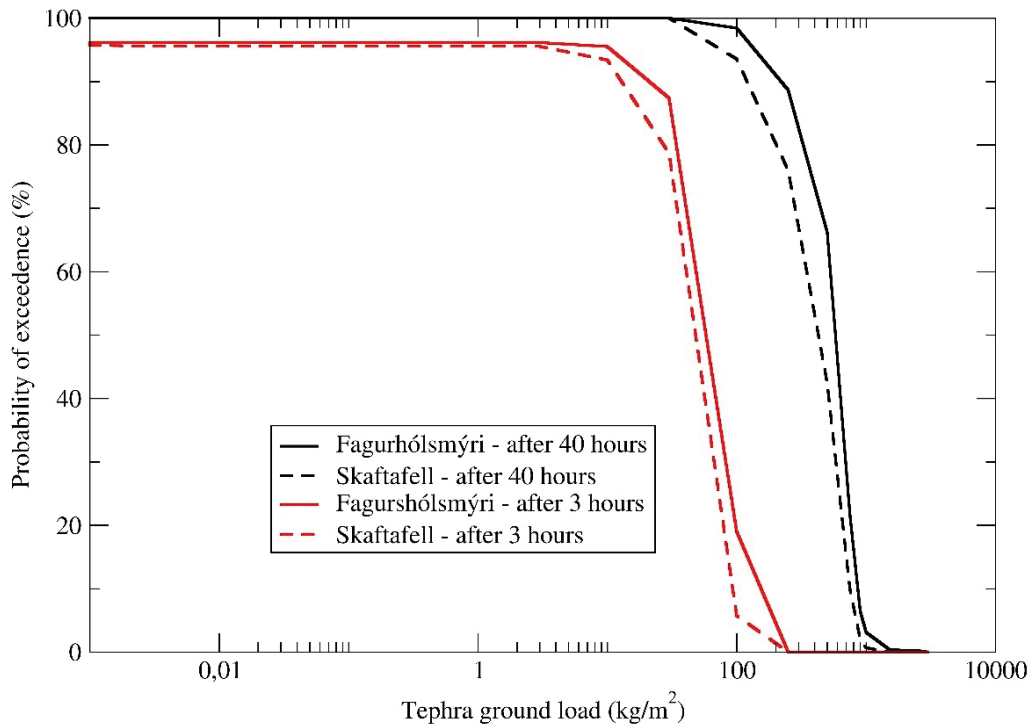


Figure 58. The probability of exceedance curve shows the likelihood to exceed a specific tephra load on the ground after 40 hours (black lines) and 3 hours (red lines) since the eruption onset. The two curves correspond to two locations: Skaftafell (dashed) and Fagurhólmseyri (continuous). — *Líkur á að ákveðnu gjóskumagni á flatareiningu í Öræfajökulsgosi verði náð eftir 3 klst (rautt) og 40 klst (svart) á Fagurhólmseyri (óbrotin lína) og í Skaftafelli (brotin lína).*

5.4.5 Probability of exceedance and accumulation rate

The two closest inhabited locations, i.e. Skaftafell and Fagurhólmseyri, have been investigated to estimate the probability of exceedance of a range of tephra ground deposits (Figure 58). The results show that after three hours since the beginning of the eruption these two locations have a probability of 50% to get a tephra load of about 100 kg/m². After 40 hours this load will be reached with a likelihood of 100%. At the same time, a load of about 600 kg/m² (~60 cm) will be reached with a likelihood of about 50%. In addition, the specific cases shown here reveal that the arrival time varies from location to location with a delay of several hours depending on the wind direction and relative distances from the volcano (Figure 59 to Figure 62). In most locations (see Figure 9 for reference), the accumulation is almost linear with time and reaches a peak a bit later the end of the emission phase (i.e. 20 hours). Locations not directly downwind and bit further away (e.g. Reykjavík- green curve) can get a maximum in the load after 20–30 hours since the beginning of the eruption. Skaftafell, due to its vicinity to the volcano, will receive constant fallout since the initial phase of the eruption and will get up to several hundreds of kg/m² of tephra at the end of the event. After the first hour of an eruption Skaftafell already is loaded by 50 kg/m² of tephra.

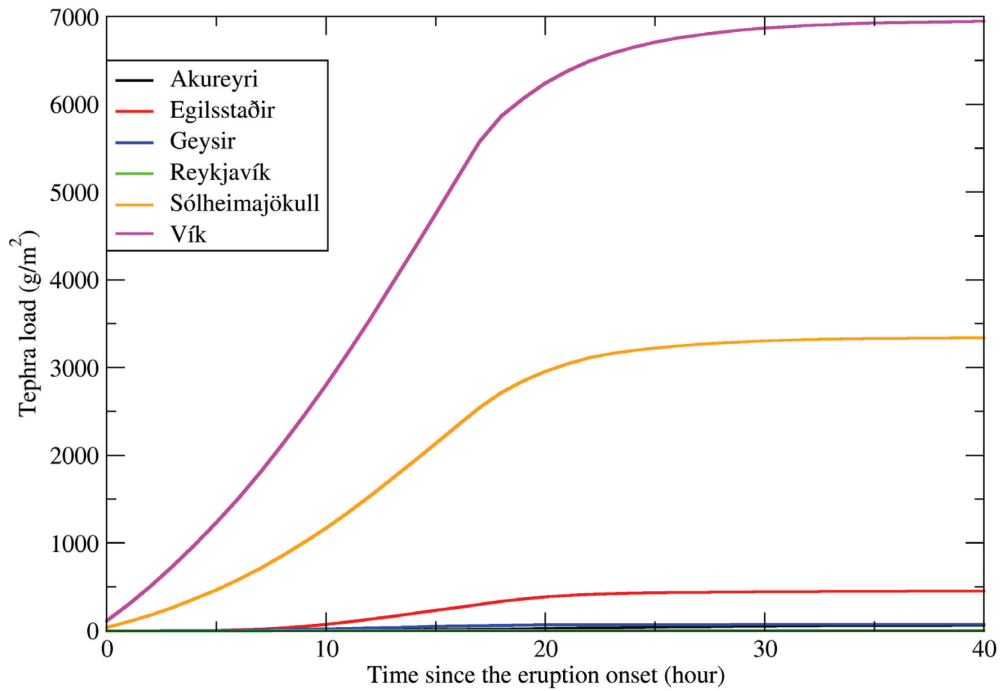


Figure 59. Tephra accumulation rate on the ground at six locations in Iceland in case of an eruption at Örfajökull like 1362. The plot shows the results for an similar eruption occurring during weather conditions based upon 7 May 1982. The graph shows how quickly a specific tephra load can be reached as a function of time. The index on the x-axis starts at 0 and it corresponds to the first hour from the eruption onset. See Figure 9 for the locations map. — *Gjóskuþykkunarhraði á sex stöðum á Íslandi í Örfajökulsgosi sambærilegu því sem varð árið 1362 m.v. veður frá 7. maí 1982. Grafið sýnir hver hatt gjóskuþyngd á flatareiningu breytist en núllpunktur táknar fyrstu klukkustund frá upphafi goss. Sjá staðsetningar á mynd 9.*

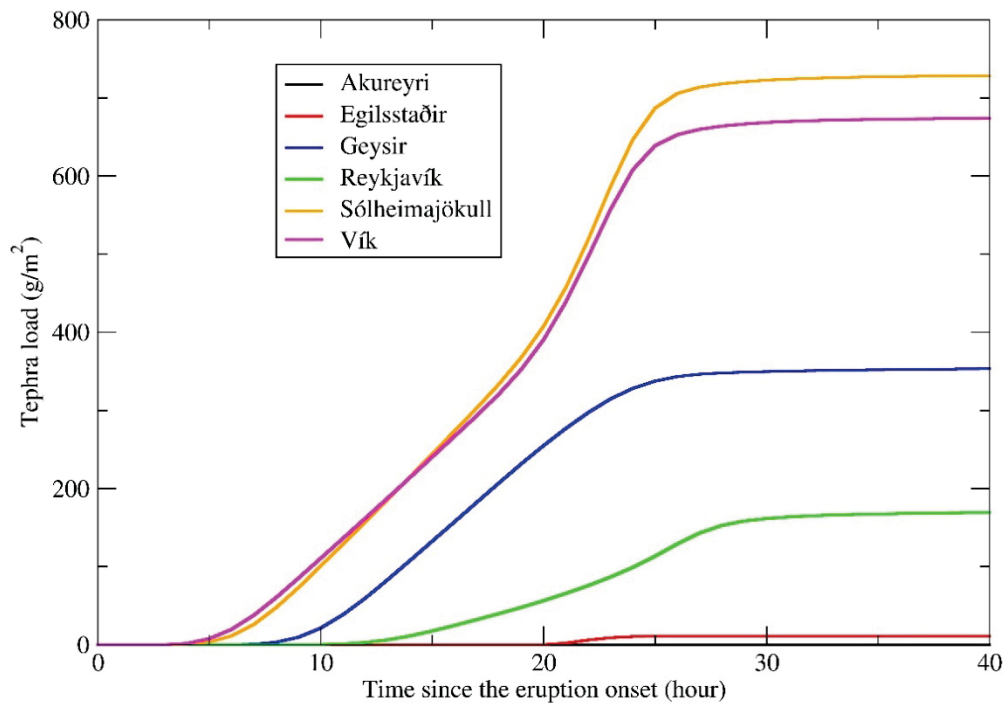


Figure 60. Tephra accumulation rate on the ground at six locations in Iceland in case of an eruption at Örfajökull like 1362. The plot shows the results for an similar eruption occurring during weather conditions based upon 5 May 1981. The graph shows how quickly a specific tephra load can be reached as a function of time. The index on the x-axis starts at 0 and it corresponds to the first hour from the eruption onset. See Figure 9 for the locations map. — *Gjóskuþykunarhraði á sex stöðum á Íslandi í Örfajökulsgosi sambærilegu því sem varð árið 1362 m.v. veður frá 5. maí 1981. Grafið sýnir hve hratt gjóskuþyngd á flatareiningu breytist en núllpunktur táknar fyrstu klukkustund frá upphafi goss. Sjá staðsetningar á mynd 9.*

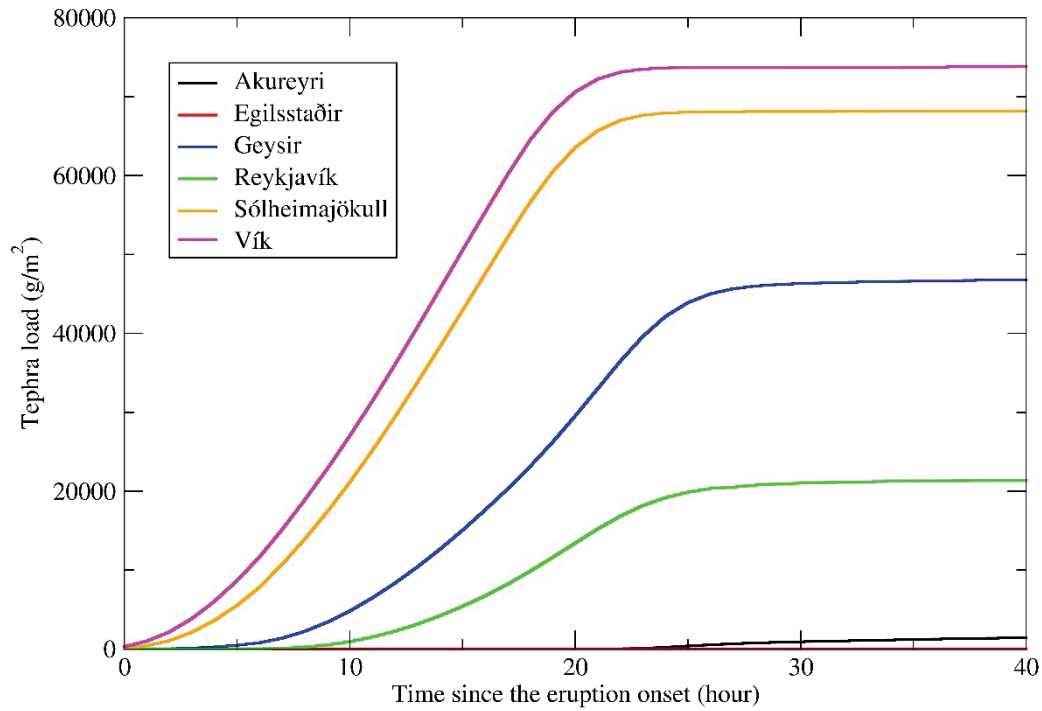


Figure 61. Tephra accumulation rate on the ground at six locations in Iceland in case of an eruption at Örfajökull like 1362. The plot shows the results for an similar eruption occurring during weather conditions based upon 8 October 1982. The graph shows how quickly a specific tephra load can be reached as a function of time. The index on the x-axis starts at 0 and it corresponds to the first hour from the eruption onset. See Figure 9 for the locations map. — *Gjóskuþykkunarhraði á sex stöðum á Íslandi í Örfajökulsgosi sambærilegu því sem varð árið 1362 m.v. veður frá 8. október 1982. Grafið sýnir hve hratt gjóskuþyngd á flatareiningu breytist en núllpunktur táknar fyrstu klukkustund frá upphafi goss. Sjá staðsetningar á mynd 9.*

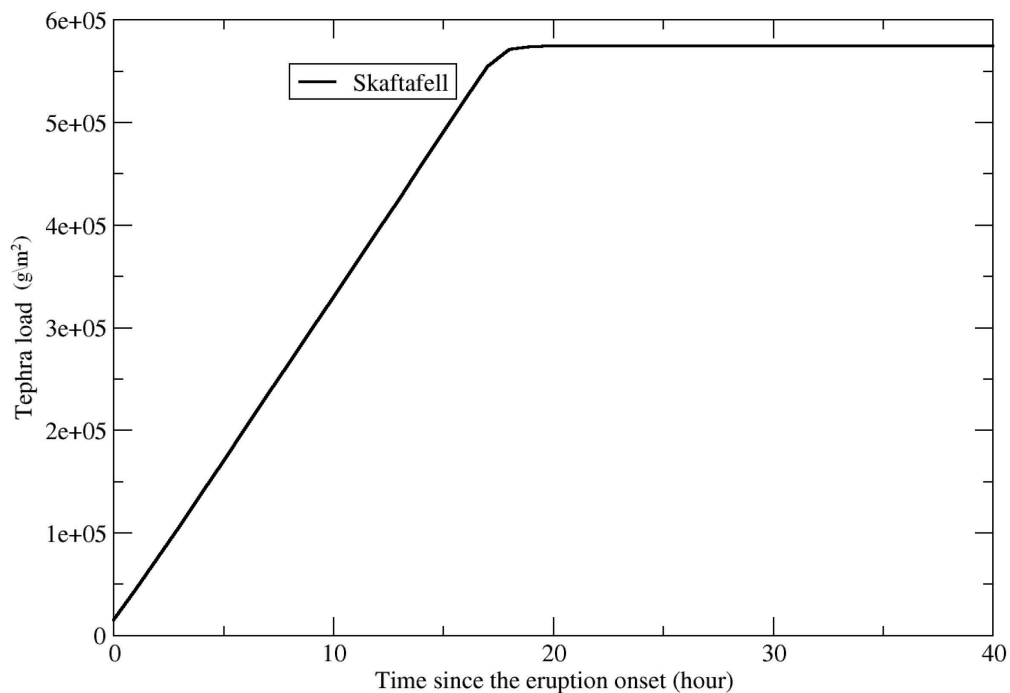


Figure 62. Tephra accumulation rate on the ground in Skaftafell in case of an eruption at Öraefajökull like 1362. The plot shows the results for an similar eruption occurring during weather conditions based upon 5 May 1981. The graph shows how quickly a specific tephra load can be reached as a function of time. The index on the x-axis starts at 0 and it corresponds to the first hour from the eruption onset. See Figure 9 for the locations map. — *Gjóskupykkunarhraði í Skaftafelli í Öraefajökulsgosi sambærilegu því sem varð árið 1362 m.v. veður frá 5. maí 1981. Grafið sýnir hve hratt gjóskupyngd á flatareiningu breytist en núllpunktur táknar fyrstu klukkustund frá upphafi goss. Sjá staðsetningar á mynd 9.*

Table 11. Worst-case scenario of tephra load after 40 hours from the eruption onset for twelve locations in Iceland. Highlighted in orange are those localities within 60 km from the volcano summit. — *Versta mögulega sviðsmynd gjóskuþyngdar á flatareiningu eftir 40 klst gjóskufall á 12 stöðum á landinu. Þeir staðir sem eru innan 60 km radíuss frá gosupptökum í Öræfajökli eru litaðir appelsínugulir.*

Towns/Locations	Maximum possible load (kg/m ²) after 40 hours from the eruption onset – worst-case scenario (~deposit thickness in cm)	Distance from Öræfajökull volcano summit (km)
Fagurhólsmýri	2690 (~269 cm)	13
Skaftafell	1037 (~103 cm)	15
Kirkjubæjarklaustur	360 (~36 cm)	72
Höfn	484 (~48 cm)	76
Vík	128 (~13 cm)	133
Egilsstaðir	214 (~21 cm)	177
Hvolsvöllur	85 (~8.5 cm)	178
Geysir	71 (~7 cm)	181
Hella	80 (~8 cm)	184
Akureyri	102 (~10 cm)	200
Selfoss	70 (~7 cm)	214
Reykjavík	52 (~5.2 cm)	257

The worst-case scenario has been also investigated (Table 11). The table shows that Skaftafell is the most exposed one with a maximum load larger than 1,000 kg/m². Reykjavík can receive up to 165 kg/m² and all the other main towns can get more than 100 kg/m² with Egilsstaðir up to 214 kg/m². Kirkjubæjarklaustur and Höfn are the two closest towns where the current evacuation plan designed by Almannavarnir (Civil Protection) is indicating the population to move. Both locations can receive more than 350 kg/m² that in terms of deposit thickness corresponds roughly to 35 cm. In light of this, whenever an eruption will be imminent, it is important to review the evacuation plan and destinations areas considering the current weather forecast and the forecasted dispersal of tephra. The identification of selected destination locations should be considered a dynamic element in the emergency plan. These results might also suggest to the Civil Protection the importance of an additional evacuation plan to be put in practice whenever the eruption will occur in the worst meteorological conditions (easterly wind).

At locations exposed to a load higher than 350 kg/m², timely tephra removal from the roofs would be recommended to avoid enhancing the risk of building collapse and/or damages.

Preliminary Intersectional Map

The map shows the area prone to receive tephra from any of the three considered volcanological scenarios:

- Hekla 1980
- Katla 1918
- Öraefajökull 1362

- ⊙ Eruption locations for the selected volcanological scenarios
- ⊘ Intersection area

Comments:

The area is obtained by finding the intersection of the three scenario specific contours for the 10 kg/m² load. This map should not be seen as a probability map, since the absolute occurrence probabilities of the three volcanological scenarios have not been taken into account.

Datum: ISN83
 Date: 16.09.2019
 Basemap data: NLSI 2014
 Cartography: Icelandic Met Office
 Projection: Lambert Conformal Conic

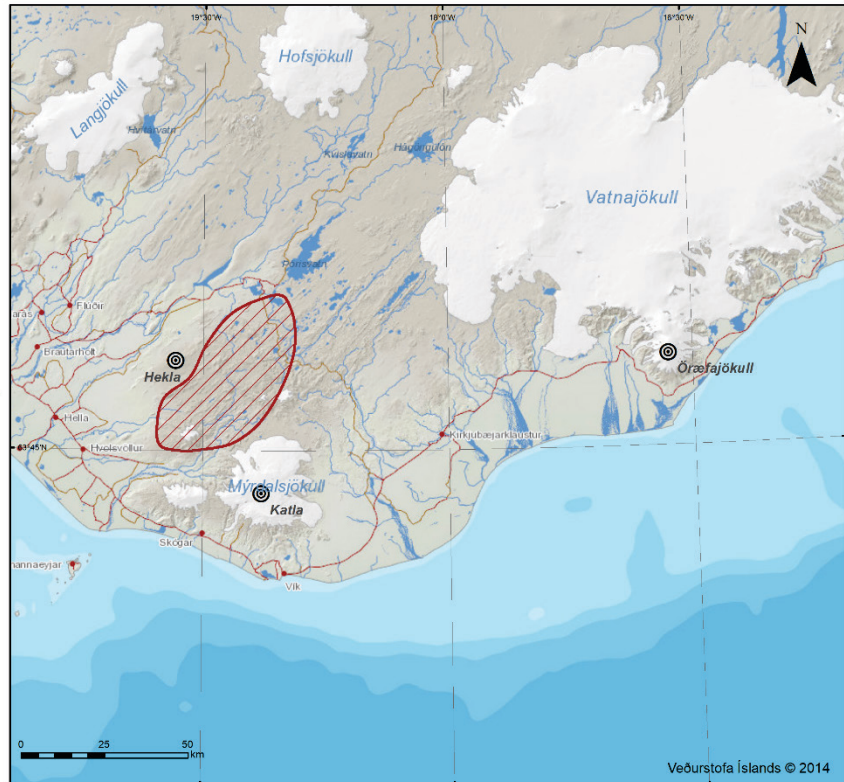


Figure 63. Preliminary intersectional map showing the area prone to receive tephra from any of the three volcanological scenarios considered; i.e. Hekla 1980, Katla 1918 and Öraefajökull 1362. — *Svæði sem varð fyrir gjóskufalli í öllum þremur sviðsmyndum þ.e. úr gosum sem eiga upptök í Heklu (sambærilegt gosinu 1980), Kötlu (1918) og Öraefajökli (1362).*

5.5 Towards an integration of the three explosive eruptive scenarios

The probabilistic hazards maps produced for the three reference eruptions at Hekla, Katla and Öraefajökull can be used to identify areas prone to receive tephra from any of these three eruptive scenarios. Figure 63 shows an area that, given an eruption at any of these three volcanoes, might get tephra fallout up to 1 cm as it sits within the intersection between all three scenario-specific extents.

The map does not show the probability that this area will get tephra during the next eruption at any of these volcanoes. To quantify this information the absolute probability of each specific volcanic scenario needs to be calculated whereas here we have been considering the probability conditional to the occurrence of an eruption.

6 Main conclusions and next steps

From the several maps and the results presented in this report we can summarize the following points:

6.1 Tephra fallout impact during an eruption at Hekla, like 1980

General extent of the tephra deposit:

An eruption like the 1980 event at Hekla would have a quite local impact on the ground due to its short duration (~2 hours). Heavy tephra fallout is expected within few kms from the summit. Landmannalaugar and Sigöldustöð are the two most exposed locations considered in this study. Both can be affected by a deposit thicker than 1 cm with a likelihood higher than 10%. Towns like Hella, Hvolsvöllur and Vík might receive ~1 mm of ash (very minor impact) with probabilities of 6%, 9% and 2%, respectively. The worst-case scenario for touristic areas around Hekla (Landmannalaugar, Þórsmörk and Gullfoss) is of deposit exceeding 10 kg/m² (~1 cm), i.e. 37, 25 and 17 cm, respectively.

Impact on the infrastructure considered:

The results show that up to 10 km of road would be affected by critical conditions with high (>75%) probability. More than 100 km of road will be in critical conditions with a likelihood higher than 25%. No airports would be directly affected by ash falling on the ground with a likelihood higher than 5%. More than 95 km of power line network could suffer by heavy load and potential flashover with a probability lower than 25%.

Additional remarks and shortcomings:

It is very important to clarify here that this report is not intended to investigate the hazard posed to the aircrafts flying in the area neither on the long nor short-term window. It is known that Hekla might erupt with very short precursors and the hazard for the aviation is high. This sensitive issue has been tackled in separate instances together with Icelandic Transport Authority, Isavia and ICAO (International Civil Aviation Organization) (Barsotti et al., 2019). The short precursors at the volcano also might lead to a very short warning time for those hiking the mountain at the time of the eruption. The National Civil Protection (NCIP-DCPEM) is responsible for issuing warning to the people in the area and the warning will be triggered by the real-time monitoring data used by Icelandic Meteorological Office for the 24-hours monitoring of the country.

6.2 Tephra fallout impact during an eruption at Katla, like 1918

General extent of the tephra deposit:

An eruption like 1918 at Katla would have an intermediate impact on the ground with few inhabited or touristic areas possibly affected by a deposit higher than 100 kg/m² (~10 cm). Þórsmörk, Vík, Landmannalaugar Skógar are the locations potentially affected by such a deposit. These locations in addition to Kirkjubæjarklaustur would be impacted by tephra fallout from Katla with the highest frequencies of occurrence. Þórsmörk has a likelihood higher than 50% to receive tephra of 1 mm thickness during an eruption.

Impact on the infrastructure considered:

No road has high probability (> 75%) to be in critical driving conditions, but more than 150 km can be dangerous with likelihood higher than 25%. Part of this sector road includes the main ring road from Skógar to Eystri Ásar. No airports would be directly affected by ash falling on the ground with a likelihood higher than 5%. Up to 37 km of power line can be damaged by tephra fallout with a likelihood <25%. Based on that we could expect that an eruption in Katla might cause disruption to the commutation in the southern part of the country. Possibly over long period, if the eruption would be prolonged in time. It should be added that most of the disruption in case of an explosive eruption originating within the caldera of Katla volcano, will be due to the jökulhlaup caused by the melting of the ice. In this sense the impact due to tephra fallout on the road as well as on the power line will be secondary as, in this scenario, a jökulhlaup is expected to occur prior the generation of tephra.

Additional remarks and shortcomings:

It is important to note that the model results refer to the most intense phase of the eruption that we have assessed to last 24 hours. From historical eruption it is known that the explosive phase would possibly continue for weeks. We can argue that a longer eruption will emit more airborne material exacerbating the effects already described in this report.

6.3 Tephra fallout impact during an eruption at Öräfajökull, like 1362

General extent of the tephra deposit:

This analysis raises two main issues: firstly there are no places in the country completely safe from receiving tephra generated from an eruption like 1362 at Öräfajökull; second the tephra fallout can have a very severe impact in the proximity of the volcano with up to 1000 kg/m² of tephra equivalent to thickness of 100 cm expected up to a distance of only 25 km from the vent. Most of the main towns in Iceland have likelihood higher than 1% to receive an amount of ash of more than 10 kg/m². The worst-case scenario analyses show that Fagurhólsmýri and Skaftafell have the potential to get up to 2600 and 1000 kg/m², respectively which corresponds approximately to thickness of 260 and 100 cm. They have a likelihood of about 100% to receive more than 100 kg/m² (~10 cm). The timeline shows that in Fagurhólsmýri such a load will be reached after 3 hours with a likelihood higher than 90%.

Impact on health:

The PM₁₀ analysis shows that almost the whole country would be exposed to unhealthy air-quality conditions after 12 hours since the beginning of the eruption with a likelihood higher than 5%. After the first hour almost half of the country will be experiencing such conditions. The first hour after the eruption will cause the SE of the country to experience high hourly concentration of volcanic PM₁₀ (> 3000 µg/m³) with a likelihood higher than 50%.

Impact on the infrastructure considered:

The impact analysis performed for three different types of infrastructures (roads, airports and power lines) reveals the vulnerability of the country in case of such an eruption. Figure 52 shows the kilometers of road network potentially affected by critical driving conditions. The results indicate that, except for the sector of road exposed directly to jökulhlaup, the driving condition in large part of the country might be as such to call for clearing operations using similar methods as used in winter. The main town of Egilsstaðir and the very popular localities of Höfn, Skaftafell and Jökulsarlón will be cut off the main viable connections, with important

implications for either inhabitants and tourists potentially trapped in the area due to very low visibility conditions and unsafe driving conditions of paved roads.

Considering also that the airports in Hornafjörður (next to Höfn) and Egilsstaðir can be disrupted with a likelihood higher than 50%, then it results that any connection with the Eastern part of the country will be very difficult and dangerous during and shortly after the eruption (days, weeks). An eruption like 1362 will most likely reduce the capability to connect the capital area to the East part of the country by impacting either the domestic air traffic and road traffic infrastructures. This result calls for definition of contingency plans and measures to minimize the effect of tephra on transport infrastructure (including maritime traffic).

Failure of the electricity provision can be expected due to damages to power lines during and shortly after the eruption. These data need to be seriously evaluated when planning for mitigation actions and evacuation plans. The impact of a similar scenario would be even more dramatic if an eruption will take place during the winter time when the daylight time is very short and the need for electricity to illuminate is higher and essential for the daily activities of the society and its economy.

Inhabited regions exposed to large amount of tephra should be recommended to be ready for regular roof cleaning to avoid accumulation of critical load potentially causing collapse and damages to house and buildings.

Additional remarks and shortcomings:

It is worth to remind that the considered scenario is the worst-case scenario expected at Öraefajökull and not necessarily the future one. The choice of a scenario of reference is often matter of debate, but it should be addressed and identified by the end-users. For this volcano, the National Civil Protection identified a VEI=6 eruption to be the reference scenario for the evacuation plan and the analysis reported in this study is functional to this choice.

6.4 Recommendations and next steps

- *Calculating probabilities weighted with likelihood of eruption occurrence:* this is an important step toward a full PVHA (probabilistic volcanic hazard assessment) which includes all the possible scenarios that a volcano could experience (based on historical activity). An outcome of the PVHA would be the identification of the most likely scenario, identifying in this way which scenario to investigate next. In addition, a full hazard assessment study should include a wider range of phenomena or processes associated with volcanic eruption in Iceland. The integration of the different scenarios to identify the most exposed areas and locations and the likelihood of the impact will be feasible (see Section 5.6).
- *A proper multi-hazard assessment:* integrating hazard assessment for different phenomena (both in terms of temporal evolution and in cumulative effects) will give the chance to compare the risk and design appropriate mitigation measures. This analysis should include an extensive investigation of all the possible impact on different aspects of the society and economy as listed in Section 3.1 that have been not treated in this study. For example, impact on the environment including agriculture, eco-system, water contamination.
- *Worst-case scenarios:* Each municipality should receive the worst-case scenario in order to provide the basic elements to design local plans to manage an emergency (e.g. highest amount of ash on their roof during unfavorable constant wind, probability of

lahars, infiltration capabilities of soil, probability of damaging effects on ecosystems (soil and vegetation)).

- *Other hazards*: a wider range of hazard might occur during an eruption. For example, ballistic and pyroclastic density currents are often produced during explosive eruptions. The most recent eruption at Holuhraun (2014–2015) raised the importance of a long-term assessment for volcanic gas pollution. The extent and potential impact of these hazards need to be quantified and compared.
- *Long-term effects*: a specific study should look into quantifying the long-term effects that could potentially follow an eruption, i.e. associated to airborne material event of resuspension of ash and the possibility of low air-quality conditions, extent of damage to ecosystems, but also more general disruption to the society. Ideally, a study should investigate the time needed to clean areas affected by heavy tephra fallout and estimate after how much time people could access them again. An estimate of the “back to normal condition” time frame would also be important for the designing of mitigation actions in case of explosive eruptions.
- *Vulnerability studies*: A dedicated study should investigate the vulnerability and the effect on lives of those communities affected by tephra fallout (on both short- and long-term). This should include an evaluation on the capability of generation and distribution of electricity from power plants affected by the eruption, the impact on food production chain, the recovery time given a large disruption of the main services in the affected communities, magnitude of expense to repair the systems/services, and so on. To do this vulnerability study for such infrastructure is needed and is recommended to be done in collaboration with those institutions/companies in charge of operating these services. Studies on possible mitigation actions prior to events would be less costly to society than expensive repairs after events have occurred.
- *Cost-estimates*: effects on society, disruptions and malfunctioning of vital services could be prolonged in time. The cost associated to such malfunctions should be assessed and possibly considered within a cost-benefit analysis for the designing of mitigation measures.

Note on maps and graphical tools

The maps in this report were created using multiple sources of information to construct both the background topographic map (basemap) and in some cases the information overlaid on top of those maps. In all instances where a background map is present, the main cartographic elements are based on data from The National Land Survey of Iceland (NLSI for short or Landmælingar Íslands) and styled and composed by The Icelandic Met Office. Depending on when the figure was created, the year referenced can vary. This stems from the fact that the background map is a dynamic product that is used throughout the Icelandic Met Office and is periodically updated as new data becomes available. In some cases, where newer data is overlaid on top of the background map, two different dates are used even if the data is from the same agency.

Acknowledgements

The Authors gratefully acknowledge the experts who reviewed the report and provided valuable feedback, improving it significantly: Prof. Magnús T. Guðmundsson, Institute of Earth Sciences, University of Iceland; Dr. Þórður Arason, Icelandic Met Office; and Dr. Chiara Cardaci of the Italian Civil Protection Department. We are also thankful to Ragnar Heiðar Þrastarson, Icelandic Met Office, for exceptional graphical and technical support.

Appendix 0. Volcano Hazard Index

In Loughlin et al. (2015), Auken et al. (2015) describes how to calculate the hazard score for a volcano. There is a conceptual structure that considers elements like eruption frequency, extreme and frequent characteristics of volcano's eruptions. The formula for scoring hazard for a specific volcano is expressed as (Auken et al., 2015):

$$[\text{frequency status score} \times (\text{modal VEI} + \text{PF score} + \text{mudflow score} + \text{lava score})] + \text{maximum recorded VEI}$$

Total scores in the range 0–8 correspond to VHI Level I, total scores in the range 8–16 correspond to VHI Level II and scores higher than 16 are VHI Level III.

As reported in the cited paper the full method relies on the following scoring system:

Table 12. Scoring system developed by Auken et al. (2015) to quantify the Volcanic Hazard Index for a volcano.

Indicator	Class	Criteria	Scoring
<i>Eruption frequency</i>	Fully dormant	No time in eruption recorded since AD1900 and No recorded unrest since AD1900	1
	Semi-dormant	No Holocene eruptions but unrest recorded since AD 1900 Or - Holocene (pre-AD 1500) eruptions but no recorded unrest since AD 1900	1.5
	Semi-active	Holocene (pre-AD 1500) eruptions and unrest since 1900 Or - Historical (AD 1500-1900) eruptions with or without unrest since AD 1900	2
	Active	One or more years with eruptions recorded since AD 1900	$2 + \left(\frac{N}{113}\right)$ where N is the number of years in which the volcano is recorded as erupting since AD 1900

Continued

<i>Pyroclastic flow occurrence</i>	Pyroclastic flows are a significant hazard	Pyroclastic flows are recorded in 10% or more of eruptions occurring partially or fully within the volcano's counting period	4
	Pyroclastic flows are not a significant hazard	Pyroclastic flows are recorded in fewer than 10% of eruptions occurring partially or fully within the volcano's counting period	0
<i>Mudflow occurrence (here considered to be jökulhlaup)</i>	Mudflows (jökulhlaups) are a significant hazard	Mudflows (jökulhlaups) are recorded in 10% or more of eruptions occurring partially or fully within the volcano's counting period	2
	Mudflows (jökulhlaups) are not a significant hazard	Mudflows (jökulhlaup) are recorded in fewer than 10% of eruptions occurring partially or fully within the volcano's counting period	0
<i>Lava flow occurrence</i>	Lava flows are a significant hazard	Lava flows are recorded in 10% or more of eruptions occurring partially or fully within the volcano's counting period	0.1
	Lava flows are not a significant hazard	Lava flows are recorded in fewer than 10% of eruptions occurring partially or fully within the volcano's counting period	0
<i>Modal VEI</i>	N/A	The modal VEI of eruptions recorded with a known VEI within the volcano's counting period is X. A minimum of four such eruptions are required. Where there is no mode, the mean is used	X
<i>Maximum recorded VEI</i>	N/A	The greatest VEI of any eruption recorded within the volcano's Holocene eruptive history is Y	Y

The scores have been calculated for the three volcanoes considered in this project, i.e. Hekla, Katla and Öräfajökull. In order to adapt the general scheme to the Icelandic types of eruptions some considerations have been done regarding sizes of jökulhlaups and PFs maximum distances.

In particular, for what concerns jökulhlaup, the scores have been assigned following the rule:

2= likely to have a flood larger than 10,000 m³

1=likely to have a flood larger than 1,000 m³

0= very low likelihood to have any flood

For pyroclastic flows the rule for scoring is:

4= likely to have pyroclastic flows reaching farer than 5 km

2= likely to have PFs reaching farer than 1 km

0= very low likelihood to have any PFs

The results obtained for the three volcanoes here considered are summarized in Table 13 and the VHI/PEI is shown in Figure 1.

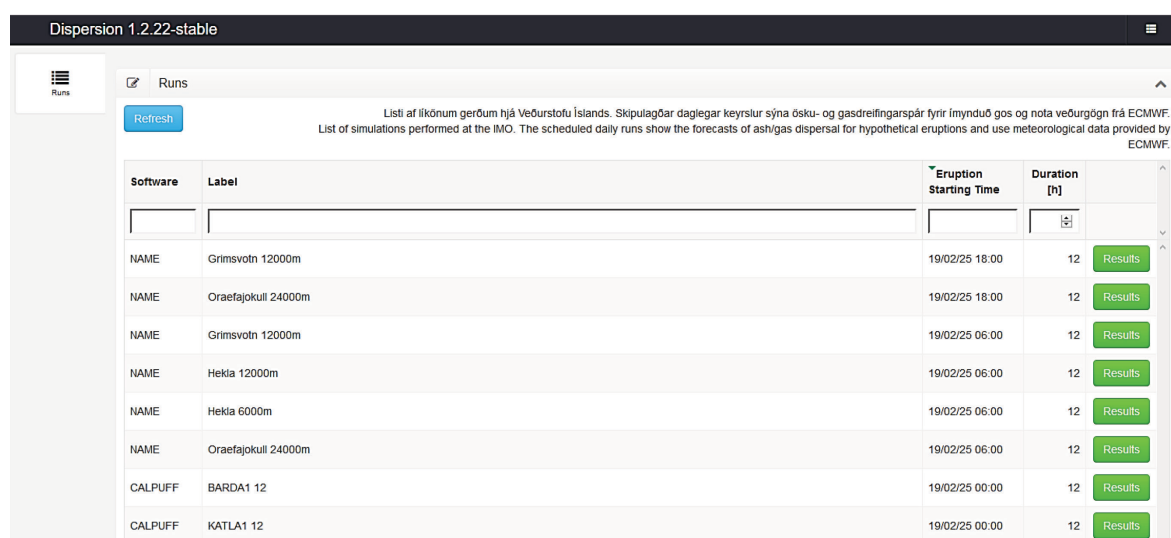
Table 13. Volcano Hazard Index calculated for Hekla, Katla and Öräfajökull volcanoes.

Volcano name	Eruption Frequency (1: Fully Dormant; 1,5: Semi-dormant; 2: Semi-active; >2: Active)	Number of Years (N) the Active Volcano is recorded as Erupting since 1900	Pyroclastic Flow Occurrence*	Mudflow Occurrence**	Lava Flow Occurrence	Modal VEI	Maximum Recorded VEI in Holocene	Total score	VHI
Öräfajökull	2.00	-	4	2	0	4	5	25 to 27	III
Hekla	2.06	7	2	1	0.1	3	6	19	III
Katla	2.01	1	0	2	0.1	4	5	17	III

Appendix I. Daily tephra dispersal simulation

Since November 2018 a public website has been created to allow the access to the daily forecast of tephra dispersal over Iceland. The results are available at the following link: dispersion.vedur.is.

Through the main page (Figure 64) the user can have access to several simulations created each day that show the extension of the area (both in the atmosphere and on the ground) potentially affected by tephra contamination each hour. The Label indicate the name of the volcano modelled and the plume height is reported after the name. So for example “Grímsvötn 12000 m” will show the results for an eruption started at Grímsvötn with a plume height of 12000 m above the sea level. The eruption starting time and the duration is reported along the same line. By clicking on the green button, the user can visualize the results of the simulations.



Dispersion 1.2.22-stable

Runs

Refresh

Listi af líkönum gerðum hjá Veðurstofu Íslands. Skipulagðar daglegar keyrstur sjna ösku- og gasdreifingarspár fyrir ímynduð gos og nota veðurgögn frá ECMWF. List of simulations performed at the IMO. The scheduled daily runs show the forecasts of ash/gas dispersal for hypothetical eruptions and use meteorological data provided by ECMWF.

Software	Label	Eruption Starting Time	Duration [h]	
NAME	Grímsvotn 12000m	19/02/25 18:00	12	Results
NAME	Öraefajökull 24000m	19/02/25 18:00	12	Results
NAME	Grímsvotn 12000m	19/02/25 06:00	12	Results
NAME	Hekla 12000m	19/02/25 06:00	12	Results
NAME	Hekla 6000m	19/02/25 06:00	12	Results
NAME	Öraefajökull 24000m	19/02/25 06:00	12	Results
CALPUFF	BARDA1 12	19/02/25 00:00	12	Results
CALPUFF	KATLA1 12	19/02/25 00:00	12	Results

Figure 64. Initial user-interface to visualize the daily simulation of tephra dispersal over Iceland (see dispersion.vedur.is).

Once the simulation of interested is selected and the green button is clicked a new page will open. The map shows the extension of the area investigated and the image contains the details about the simulation selected (in Figure 65 it refers to a simulated eruption at Öraefajökull volcano characterized by a plume height of 24000 m asl).

By clicking on the play button, the animation starts, showing the temporal evolution of tephra concentration in the atmosphere (colored contours) and the cumulative ground loading (grey contours). The up-right symbol of layers allows to visualize a single level of information at a time (Figure 66).



Figure 65. Example of visualization of a selected scenario (map extent, legend, timeline).

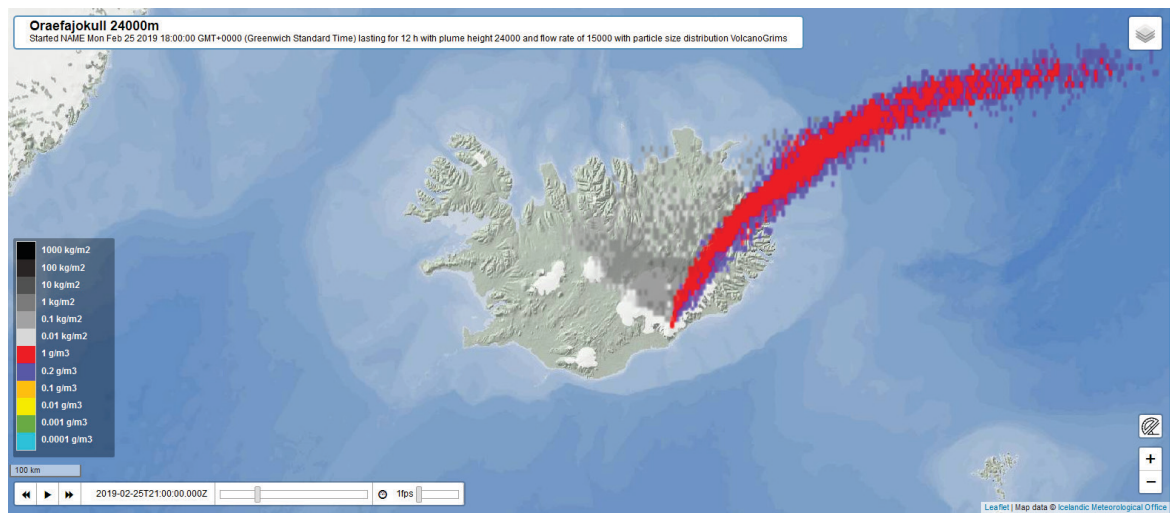


Figure 66. Example of visualization of ground loading in kg/m^2 (grey contours) and tephra concentration in g/m^3 at a specific altitude (colored contours).

In the time controller the date and time is reported in the following format: YYYY-mm-ddThh.mm.ssZ. To control the speed of the animation the frame-per-second (fps) parameter can be changed.

The information contained in the simulation results is either qualitative (area affected by the presence of ash in the atmosphere and on the ground as function of time) and also quantitative (concentration at different heights and the load on the ground). In order to make use of the information it might be useful to know that on average we can assume $1 \text{ kg}/\text{m}^2$ to correspond to roughly 1 mm of tephra on the ground (a thin layer). $10 \text{ kg}/\text{m}^2$ would then be 1 cm and $100 \text{ kg}/\text{m}^2$ would roughly correspond to 10 cm of deposit thickness.

Appendix II. Hekla 1980 – the likelihood of receiving tephra at different locations

Likelihood of receiving different amount of tephra calculated for different towns and locations in the country.

<i>Locality name</i>	Probability to exceed 1 kg/m ² (~1 mm) expressed as %	Probability to exceed 10 kg/m ² (~1 cm) expressed as %	Probability to exceed 100 kg/m ² (~10 cm) expressed as %
<i>Akranes</i>	0	0	0
<i>Akureyri</i>	0	0	0
<i>Arnarstapi</i>	0	0	0
<i>Ásbyrgi</i>	0	0	0
<i>Bakkafjörður</i>	0	0	0
<i>Bakkagerði</i>	0	0	0
<i>Bildudalur</i>	0	0	0
<i>Bjarkalundur</i>	0	0	0
<i>Blönduós</i>	0	0	0
<i>Bolungarvík</i>	0	0	0
<i>Borgarnes</i>	0	0	0
<i>Breiðdalsvík</i>	0	0	0
<i>Búðardalur</i>	0	0	0
<i>Dalvík</i>	0	0	0
<i>Djúpivogur</i>	0	0	0
<i>Egilsstaðir</i>	0	0	0
<i>Eiðar</i>	0	0	0
<i>Eskifjörður</i>	0	0	0
<i>Eyrbakki</i>	0.1	0	0
<i>Fagurhólsmýri</i>	0.1	0	0
<i>Fáskrúðsfjörður</i>	0	0	0
<i>Flateyri</i>	0	0	0
<i>Flókalundur</i>	0	0	0
<i>Geysir</i>	4.5	0	0
<i>Grenivík</i>	0	0	0
<i>Grindavík</i>	0	0	0
<i>Grundarfjörður</i>	0	0	0
<i>Gullfoss</i>	8.3	0.1	0
<i>Hallormsstaður</i>	0	0	0
<i>Hella</i>	6.4	0	0
<i>Hellissandur</i>	0	0	0
<i>Herðubreiðarlindir</i>	0	0	0
<i>Hofsós</i>	0	0	0
<i>Hólmavík</i>	0	0	0

<i>Húsafell</i>	0	0	0
<i>Húsavík</i>	0	0	0
<i>Hvammstangi</i>	0	0	0
<i>Hveragerði</i>	0.3	0	0
<i>Hveravellir</i>	0.7	0	0
<i>Hvolsvöllur</i>	8.7	0.1	0
<i>Höfn í Hornafirði</i>	0	0	0
<i>Ísafjörður</i>	0	0	0
<i>Keflavík</i>	0	0	0
<i>Kirkjubæjarklaustur</i>	1.6	0	0
<i>Kópasker</i>	0	0	0
<i>Króksfjarðarnes</i>	0	0	0
<i>Landeyjahöfn</i>	1.8	0	0
<i>Landmannalaugar</i>	45.4	10.0	0
<i>Laugarvatn</i>	1.0	0	0
<i>Mýri í Bárðardal</i>	0	0	0
<i>Neskaupstaður</i>	0	0	0
<i>Norðurfjörður á Ströndum</i>	0	0	0
<i>Nýidalur</i>	0.3	0	0
<i>Ólafsfjörður</i>	0	0	0
<i>Ólafsvík</i>	0	0	0
<i>Patreksfjörður</i>	0	0	0
<i>Raufarhöfn</i>	0	0	0
<i>Reyðarfjörður</i>	0	0	0
<i>Reykholt í Borgarfirði</i>	0.0	0	0
<i>Reykjahlíð við Mývatn</i>	0	0	0
<i>Reykjavík</i>	0	0	0
<i>Sandgerði</i>	0	0	0
<i>Sauðárkrókur</i>	0	0	0
<i>Selfoss</i>	0.3	0	0
<i>Seyðisfjörður</i>	0	0	0
<i>Siglufjörður</i>	0	0	0
<i>Sigöldustöð</i>	39.3	10.3	0
<i>Skaftafell</i>	0.15	0	0
<i>Skagaströnd</i>	0	0	0
<i>Skógar undir Eyjafjöllum</i>	2.9	0.0	0
<i>Staðarskáli</i>	0	0	0
<i>Stykkishólmur</i>	0	0	0
<i>Stöðvarfjörður</i>	0	0	0
<i>Suðureyri í Súgandafirði</i>	0	0	0
<i>Tálknafjörður</i>	0	0	0
<i>Unaðsdalskirkja</i>	0	0	0

<i>Varmahlíð</i>	0	0	0
<i>Vestmannaeyjar</i>	0.8	0	0
<i>Vík í Mýrdal</i>	2.5	0	0
<i>Vopnafjörður</i>	0	0	0
<i>Þingeyri</i>	0	0	0
<i>Þingvellir; þjónustumiðstöð</i>	0.4	0	0
<i>Þorlákshöfn</i>	0.1	0	0
<i>Þórshöfn</i>	0	0	0
<i>Þórsmörk; Básar</i>	14.7	1.1	0

Appendix III. Katla 1918 – the likelihood of receiving tephra at different locations

Likelihood of receiving different amount of tephra is calculated for different towns and locations in the country.

<i>Locality name</i>	Probability to exceed 1 kg/m ² (~1 mm) expressed as %	Probability to exceed 10 kg/m ² (~1 cm) expressed as %	Probability to exceed 100 kg/m ² (~10 cm) expressed as %
<i>Akranes</i>	0.2	0	0
<i>Akureyri</i>	0.7	0	0
<i>Arnarstapi</i>	0	0	0
<i>Ásbyrgi</i>	0	0	0
<i>Bakkafjörður</i>	0	0	0
<i>Bakkagerði</i>	0	0	0
<i>Bildudalur</i>	0	0	0
<i>Bjarkalundur</i>	0	0	0
<i>Blönduós</i>	0.1	0	0
<i>Bolungarvík</i>	0	0	0
<i>Borgarnes</i>	0.3	0	0
<i>Breiðdalsvík</i>	0	0	0
<i>Búðardalur</i>	0	0	0
<i>Dalvík</i>	0	0	0
<i>Djúpivogur</i>	0	0	0
<i>Egilsstaðir</i>	0.0	0	0
<i>Eiðar</i>	0	0	0
<i>Eskifjörður</i>	0.02	0	0
<i>Eyrarbakki</i>	1.5	0	0
<i>Fagurhólsmýri</i>	1.7	0	0
<i>Fáskrúðsfjörður</i>	0.1	0	0
<i>Flateyri</i>	0	0	0
<i>Flókalundur</i>	0	0	0
<i>Geysir</i>	2.7	0	0
<i>Grenivík</i>	0	0	0
<i>Grindavík</i>	0	0	0
<i>Grundarfjörður</i>	0	0	0
<i>Gullfoss</i>	2.2	0	0
<i>Hallormsstaður</i>	0	0	0
<i>Hella</i>	5.9	0.9	0
<i>Hellissandur</i>	0	0	0
<i>Herðubreiðarlindir</i>	0.6	0	0
<i>Hofsós</i>	0	0	0
<i>Hólmavík</i>	0	0	0
<i>Húsafell</i>	0.1	0	0

<i>Húsavík</i>	0	0	0
<i>Hvammstangi</i>	0	0	0
<i>Hveragerði</i>	0.8	0	0
<i>Hveravellir</i>	0.4	0	0
<i>Hvolsvöllur</i>	7.9	1.4	0
<i>Höfn í Hornafirði</i>	0.0	0	0
<i>Ísafjörður</i>	0	0	0
<i>Keflavík</i>	0.19	0	0
<i>Kirkjubæjarklaustur</i>	24.4	6.2	0
<i>Kópasker</i>	0	0	0
<i>Króksfjarðarnes</i>	0	0	0
<i>Landeyjahöfn</i>	9.8	0.1	0
<i>Landmannalaugar</i>	35.5	15.8	0.4
<i>Laugarvatn</i>	2.0	0	0
<i>Mýri í Bárðardal</i>	0.3	0	0
<i>Neskaupstaður</i>	0	0	0
<i>Norðurfjörður á Ströndum</i>	0	0	0
<i>Nýidalur</i>	1.7	0	0
<i>Ólafsfjörður</i>	0	0	0
<i>Ólafsvík</i>	0	0	0
<i>Patreksfjörður</i>	0	0	0
<i>Raufarhöfn</i>	0	0	0
<i>Reyðarfjörður</i>	0.1	0	0
<i>Reykholt í Borgarfirði</i>	0.4	0	0
<i>Reykjahlið við Mývatn</i>	0.03	0	0
<i>Reykjavík</i>	0.2	0	0
<i>Sandgerði</i>	0.2	0	0
<i>Sauðárkrókur</i>	0	0	0
<i>Selfoss</i>	1.5	0	0
<i>Seyðisfjörður</i>	0	0	0
<i>Siglufjörður</i>	0	0	0
<i>Sigöldustöð</i>	21.4	4.6	0
<i>Skaftafell</i>	3.2	0	0
<i>Skagatrönd</i>	0	0	0
<i>Skógar undir Eyjafjöllum</i>	37.0	22.8	3.7
<i>Staðarskáli</i>	0	0	0
<i>Stykkishólmur</i>	0	0	0
<i>Stöðvarfjörður</i>	0	0	0
<i>Suðureyri í Súgandafirði</i>	0	0	0
<i>Tálknafjörður</i>	0	0	0
<i>Unaðsdalskirkja</i>	0	0	0
<i>Varmahlíð</i>	0.08	0	0
<i>Vík í Mýrdal</i>	37.2	24.2	3.2
<i>Vestmannaeyjar</i>	4.9	0	0

<i>Vopnaffjörður</i>	0	0	0
<i>Þingeyri</i>	0	0	0
<i>Þingvellir; þjónustumiðstöð</i>	1.06	0	0
<i>Þorlákshöfn</i>	0.69	0	0
<i>Þórshöfn</i>	0	0	0
<i>Þórsmörk; Básar</i>	51.5	36.2	10

Appendix IV. Öræfajökull 1362 – the likelihood of receiving tephra at different locations

Likelihood of receiving different amount of tephra is calculated for different towns and locations in the country.

<i>Locality name</i>	Probability to exceed 1 kg/m ² (~1mm) expressed as %	Probability to exceed 10 kg/m ² (~1 cm) expressed as %	Probability to exceed 100 kg/m ² (~10cm) expressed as %
<i>Akranes</i>	5.7	1.4	0
<i>Akureyri</i>	25.4	10.2	1.2
<i>Arnarstapi</i>	4.3	0	0
<i>Ásbyrgi</i>	38.5	19.0	0
<i>Bakkafjörður</i>	42.8	22.6	0
<i>Bakkagerði</i>	57.1	37.0	1.4
<i>Bildudalur</i>	3.1	1.4	0
<i>Bjarkalundur</i>	4.3	1.4	0
<i>Blönduós</i>	16.0	4.7	0
<i>Bolungarvík</i>	6.2	1.4	0
<i>Borgarnes</i>	5.7	1.4	0
<i>Breiðdalsvík</i>	75.6	56.8	12.4
<i>Búðardalur</i>	4.3	1.4	0
<i>Dalvík</i>	23.9	9.6	0
<i>Djúpivogur</i>	77.0	64.6	19.2
<i>Egilsstaðir</i>	61.4	49.2	7.0
<i>Eiðar</i>	61.4	46.6	4.3
<i>Eskifjörður</i>	65.0	51.3	8.6
<i>Eyrarbakki</i>	7.2	1.4	0
<i>Fagurhólsmýri</i>	100	100	97.1
<i>Fáskrúðsfjörður</i>	72.8	51.5	10.4
<i>Flateyri</i>	2.8	1.4	0
<i>Flókalundur</i>	4.3	1.4	0
<i>Geysir</i>	11.0	2.9	0
<i>Grenivík</i>	25.8	11.2	0
<i>Grindavík</i>	4.3	1.3	0
<i>Grundarfjörður</i>	5.4	1.4	0
<i>Gullfoss</i>	15.2	2.8	0
<i>Hallormsstaður</i>	68.0	56.7	12.3
<i>Hella</i>	12.8	1.4	0
<i>Hellissandur</i>	2.9	0	0
<i>Herðubreiðarlindir</i>	65.3	43.3	10
<i>Hofsós</i>	15.7	6.4	0
<i>Hólmavík</i>	10	1.4	0
<i>Húsafell</i>	7.9	2.9	0

<i>Húsavík</i>	27.1	16.0	0
<i>Hvammstangi</i>	9.2	2.8	0
<i>Hveragerði</i>	7.1	1.4	0
<i>Hveravellir</i>	17.7	3.0	0
<i>Hvolsvöllur</i>	11.8	1.5	0
<i>Höfn í Hornafirði</i>	98.3	95.8	74.5
<i>Ísafjörður</i>	4.6	1.4	0
<i>Keflavík</i>	4.3	1.4	0
<i>Kirkjubæjarklaustur</i>	65.1	54.2	14.1
<i>Kópasker</i>	31.5	15.7	0
<i>Króksfjarðarnes</i>	4.3	1.4	0
<i>Landeyjahöfn</i>	15.9	2.9	0
<i>Landmannalaugar</i>	40.7	12.6	1.4
<i>Laugarvatn</i>	9.8	2.4	0
<i>Mýri í Bárðardal</i>	42.1	24.6	5.7
<i>Neskaupstaður</i>	60.4	47.1	5.7
<i>Norðurfjörður á Ströndum</i>	11.4	2.8	0
<i>Nýidalur</i>	49.0	30.7	3.6
<i>Ólafsfjörður</i>	24.3	8.7	0
<i>Ólafsvík</i>	2.9	0	0
<i>Patreksfjörður</i>	2.9	0	0
<i>Raufarhöfn</i>	29.6	12.6	0
<i>Reyðarfjörður</i>	68.6	54.7	11.6
<i>Reykholt í Borgarfirði</i>	5.7	2.0	0
<i>Reykjahlið við Mývatn</i>	40.3	21.3	1.7
<i>Reykjavík</i>	5.7	1.4	0
<i>Sandgerði</i>	4.3	1.4	0
<i>Sauðárkrókur</i>	15.7	5.7	0
<i>Selfoss</i>	8.5	1.4	0
<i>Seyðisfjörður</i>	60.4	47.2	5.1
<i>Siglufjörður</i>	22.2	8.6	0
<i>Sigöldustöð</i>	34.3	9.7	1.4
<i>Skaftafell</i>	100	100	93.8
<i>Skagaströnd</i>	13.2	6.3	0
<i>Skógar undir Eyjafjöllum</i>	27.1	6.4	0
<i>Staðarskáli</i>	5.8	2.9	0
<i>Stykkishólmur</i>	4.3	1.4	0
<i>Stöðvarfjörður</i>	74.2	52.4	10.2
<i>Suðureyri í Súgandafirði</i>	2.9	1.4	0
<i>Tálknafjörður</i>	2.8	1.0	0
<i>Unaðsdalskirkja</i>	7.1	1.4	0
<i>Varmahlíð</i>	19.8	5.3	0
<i>Vík í Mýrdal</i>	35.2	11.7	0
<i>Vestmannaeyjar</i>	13.2	2.9	0

<i>Vopnaffjörður</i>	50.5	26.8	4.3
<i>Þingeyri</i>	3.4	1.4	0
<i>Þingvellir; þjónustumiðstöð</i>	5.9	1.4	0
<i>Þorlákshöfn</i>	7.1	1.4	0
<i>Þórshöfn</i>	34.5	18.2	0
<i>Þórsmörk; Básar</i>	26.8	8.3	0

7 Bibliography

- Ágústsdóttir, A. M. (2015). Ecosystem approach for natural hazard mitigation of volcanic tephra in Iceland: Building resilience and sustainability. *Natural Hazards*, 78(3), 1669–1691.
- Auker, M. R., Sparks, R. S. J., Jenkins, S. F., Aspinall, W., Brown, S. K., Deligne, N. I., Jolly, G., Loughlin, S. C., Marzocchi, W., Newhall, C. G. & Palma, J. L. (2015). Development of a new global Volcanic Hazard Index (VHI). In Loughlin, S., Sparks, S., Brown, S., Jenkins, S., & Vye-Brown, C. (Eds.), *Global Volcanic Hazards and Risk* (pp. 349–358). Cambridge University Press; Cambridge Core. doi.org/10.1017/CBO9781316276273.024.
- Barnard, S. T. (2004). Results of a reconnaissance trip to Mt. Etna, Italy: The effects of the 2002 eruption of Etna on the province of Catania. *Bulletin of the New Zealand Society for Earthquake Engineering*, 37(2), 47–61.
- Barsotti, S., Andronico, D., Neri, A., Del Carlo, P., Baxter, P., Aspinall, W. & Hincks, T. (2010). Quantitative assessment of volcanic ash hazards for health and infrastructure at Mt. Etna (Italy) by numerical simulation. *Journal of Volcanology and Geothermal Research*, 192(1–2), 85–96.
- Barsotti, S., Bignami, C., Buongiorno, M., Corradini, S., Doumaz, F., Guerrieri, L., Merucci, L., Musacchio, M., Nannipieri, L. & Neri, A. (2011). SAFER Response to Eyjafjallajökull and Merapi Volcanic Eruptions. In *Let's embrace space* (European Commission, DG Enterprise and Industry). European Union.
- Barsotti, S., Di Rienzo, D. I., Thordarson, T., Björnsson, B. B. & Karlsdóttir, S. (2018). Assessing Impact to Infrastructures Due to Tephra Fallout From Öraefajökull Volcano (Iceland) by Using a Scenario-Based Approach and a Numerical Model. *Frontiers in Earth Science*, 6. doi.org/10.3389/feart.2018.00196.
- Barsotti, S., Nannipieri, L. & Neri, A. (2008). MAFALDA: An early warning modeling tool to forecast volcanic ash dispersal and deposition. *Geochemistry, Geophysics, Geosystems*, 9(12).
- Barsotti, S. & Neri, A. (2008). The VOL-CALPUFF model for atmospheric ash dispersal: 2. Application to the weak Mount Etna plume of July 2001. *Journal of Geophysical Research: Solid Earth*, 113(B3).
- Barsotti, S., Neri, A. & Scire, J. (2008). The VOL-CALPUFF model for atmospheric ash dispersal: 1. Approach and physical formulation. *Journal of Geophysical Research: Solid Earth*, 113(B3).
- Barsotti, S., Parks, M., Pfeffer, M. A., Roberts, M., Ófeigsson, B., Gudmundsson, G., Jónsdóttir, K., Vogfjörð, K., Kristinsson, I., Bergsson, B. & Þrastarson, R. (2019). *Hekla volcano monitoring project. Report to ICAO*. Reykjavik: Icelandic Met Office. www.vedur.is/media/vedurstofan-utgafa-2019/VI_2019_003_ICAO_final_web.pdf
- Baxter, P. J. (1990). Medical effects of volcanic eruptions. *Bulletin of Volcanology*, 52(7), 532–544.
- Behnke, S., Thomas, R., Edens, H., Krehbiel, P. & Rison, W. (2014). The 2010 eruption of Eyjafjallajökull: Lightning and plume charge structure. *Journal of Geophysical Research: Atmospheres*, 119(2), 833–859.
- Bennett, A., Odams, P., Edwards, D. & Arason, Þ. (2010). Monitoring of lightning from the April–May 2010 Eyjafjallajökull volcanic eruption using a very low frequency lightning location network. *Environmental Research Letters*, 5(4), 044013.
- Berrisford, P., Dee, D., Fielding, K., Fuentes, M., Kallberg, P., Kobayashi, S. & Uppala, S. (2009). The ERA-interim archive. *ERA Report Series*, 1, 1–16.
- Biassé, S., Scaini, C., Bonadonna, C., Folch, A., Smith, K. & Höskuldsson, A. (2014). A multi-scale risk assessment for tephra fallout and airborne concentration from multiple Icelandic volcanoes—Part 1: Hazard assessment. *Natural Hazards and Earth System Sciences*, 14(8), 2265–2287.
- Blong, R. (1996). Volcanic hazards risk assessment. In *Monitoring and mitigation of volcano hazards* (pp. 675–698). Springer.

- Bonadonna, C., Connor, C. B., Houghton, B., Connor, L., Byrne, M., Laing, A. & Hincks, T. (2005). Probabilistic modeling of tephra dispersal: Hazard assessment of a multiphase rhyolitic eruption at Tarawera, New Zealand. *Journal of Geophysical Research: Solid Earth*, 110(B3).
- Bonadonna, C., Genco, R., Gouhier, M., Pistolesi, M., Cioni, R., Alfano, F., Hoskuldsson, A. & Ripepe, M. (2011). Tephra sedimentation during the 2010 Eyjafjallajökull eruption (Iceland) from deposit, radar, and satellite observations. *Journal of Geophysical Research: Solid Earth*, 116(B12).
- Bonasia, R., Scaini, C., Capra, L., Nathenson, M., Siebe, C., Arana-Salinas, L. & Folch, A. (2014). Long-range hazard assessment of volcanic ash dispersal for a Plinian eruptive scenario at Popocatepetl volcano (Mexico): Implications for civil aviation safety. *Bulletin of Volcanology*, 76(1), 789.
- Brasseur, G. & Granier, C. (1992). Mount Pinatubo aerosols, chlorofluorocarbons, and ozone depletion. *Science*, 257(5074), 1239–1242.
- Bursik, M. (2001). Effect of wind on the rise height of volcanic plumes. *Geophysical Research Letters*, 28(18), 3621–3624.
- Calder, E., Wagner, K. & Ogburn, S. E. (2015). Volcanic hazard maps. In Loughlin, S., Sparks, S., Brown, S., Jenkins, S., & Vye-Brown, C. (Eds.), *Global Volcanic Hazards and Risk* (pp. 335–342). Cambridge University Press; Cambridge Core. doi.org/10.1017/CBO9781316276273.022
- Casadevall, T. J. (1994). *Volcanic ash and aviation safety: Proceedings of the first international symposium on volcanic ash and aviation safety* (Vol. 2047). US Government Printing Office.
- Cashman, K. V. & Scheu, B. (2015). Magmatic fragmentation. In *The Encyclopedia of Volcanoes* (pp. 459–471). Elsevier.
- Cioni, R., Longo, A., Macedonio, G., Santacroce, R., Sbrana, A., Sulpizio, R. & Andronico, D. (2003). Assessing pyroclastic fall hazard through field data and numerical simulations: Example from Vesuvius. *Journal of Geophysical Research: Solid Earth*, 108(B2).
- Costa, A., Dell’Erba, F., Di Vito, M., Isaia, R., Macedonio, G., Orsi, G. & Pfeiffer, T. (2009). Tephra fallout hazard assessment at the Campi Flegrei caldera (Italy). *Bulletin of Volcanology*, 71(3), 259.
- Costa, A., Suzuki, Y., Cerminara, M., Devenish, B., Ongaro, T., Herzog, M., Van Eaton, A. R., Denby, L., Bursik, M. & Vitturi, M. de’Michieli. (2016). Results of the eruptive column model inter-comparison study. *Journal of Volcanology and Geothermal Research*, 326, 2–25.
- Damby, D. E., Horwell, C. J., Larsen, G., Thordarson, T., Tomatis, M., Fubini, B. & Donaldson, K. (2017). Assessment of the potential respiratory hazard of volcanic ash from future Icelandic eruptions: A study of archived basaltic to rhyolitic ash samples. *Environmental Health*, 16(1), 98.
- Dlugokencky, E., Dutton, E., Novelli, P., Tans, P., Masarie, K., Lantz, K. & Madronich, S. (1996). Changes in CH₄ and CO growth rates after the eruption of Mt. Pinatubo and their link with changes in tropical tropospheric UV flux. *Geophysical Research Letters*, 23(20), 2761–2764.
- Dufek, J. (2016). The fluid mechanics of pyroclastic density currents. *Annual Review of Fluid Mechanics*, 48, 459–485.
- Dutton, E. G. & Christy, J. R. (1992). Solar radiative forcing at selected locations and evidence for global lower tropospheric cooling following the eruptions of El Chichón and Pinatubo. *Geophysical Research Letters*, 19(23), 2313–2316.
- Esposti Ongaro, T., Clarke, A., Voight, B., Neri, A. & Widiwijayanti, C. (2012). Multiphase flow dynamics of pyroclastic density currents during the May 18, 1980 lateral blast of Mount St. Helens. *Journal of Geophysical Research: Solid Earth*, 117(B6).
- Esposti Ongaro, T., Neri, A., Todesco, M. & Macedonio, G. (2002). Pyroclastic flow hazard assessment at Vesuvius (Italy) by using numerical modeling. II. Analysis of flow variables. *Bulletin of Volcanology*, 64(3), 178–191.

- Favalli, M., Chirico, G. D., Papale, P., Pareschi, M. T. & Boschi, E. (2009). Lava flow hazard at Nyiragongo volcano, DRC. *Bulletin of Volcanology*, 71(4), 363–374.
- Favalli, M., Pareschi, M. T., Neri, A. & Isola, I. (2005). Forecasting lava flow paths by a stochastic approach. *Geophysical Research Letters*, 32(3).
- Folch, A. (2012). A review of tephra transport and dispersal models: Evolution, current status, and future perspectives. *Journal of Volcanology and Geothermal Research*, 235, 96–115.
- Gíslason, S. R., Stefánsdóttir, G., Pfeffer, M. A., Barsotti, S., Jóhannsson, Th., Galeczka, I., Bali, E., Sigmarsson, O., Stefánsson, A., Keller, N. S., Sigurdsson, Á., Bergsson, B., Galle, B., Jacobo, V. C., Arellano, S., Aiuppa, A., Jónasdóttir, E. B., Eiríksdóttir, E. S., Jakobsson, S., ... Gudmundsson, M. T. (2015). Environmental pressure from the 2014–15 eruption of Bárðarbunga volcano, Iceland. *Geochemical Perspectives Letters*, 1(0), 84–93. doi.org/10.7185/geochemlet.1509.
- Grönvold, K., Larsen, G., Einarsson, P., Thorarinnsson, S. & Sæmundsson, K. (1983). The eruption of Hekla 1980–1981. *Bulletin Volcanologique*, 46(4), 349–363.
- Gudmundsson, G. (2011). Respiratory health effects of volcanic ash with special reference to Iceland. A review. *The Clinical Respiratory Journal*, 5(1), 2–9.
- Gudmundsson, H. J. (1999). *Holocene glacier fluctuations and tephrochronology of the Oræfi district, Iceland* [PhD]. School of Geosciences, the University of Edinburgh, Edinburgh.
- Gudmundsson, M. T. & Larsen, G. (2016). Grímsvötn. In: Óladóttir, B., Larsen, G. & Guðmundsson, M. T. *Catalogue of Icelandic Volcanoes*. IMO, UI and CPD-NCIP. <http://icelandicvolcanoes.is/?volcano=GRV>.
- Gudmundsson, M. T., Larsen, G., Höskuldsson, Á. & Gylfason, Á. G. (2008). *Volcanic hazards in Iceland*. *Jökull*, 58, 251–268.
- Gudnason, J., Thordarson, T., Houghton, B. F. & Larsen, G. (2017). The opening subplinian phase of the Hekla 1991 eruption: Properties of the tephra fall deposit. *Bulletin of Volcanology*, 79(5), 34.
- Gudnason, J., Thordarson, T., Houghton, B. & Larsen, G. (2018). The 1845 Hekla eruption: Grain-size characteristics of a tephra layer. *Journal of Volcanology and Geothermal Research*, 350, 33–46.
- Guffanti, M., Mayberry, G. C., Casadevall, T. J. & Wunderman, R. (2009). Volcanic hazards to airports. *Natural Hazards*, 51(2), 287–302.
- Horwell, C. J. & Baxter, P. J. (2006). The respiratory health hazards of volcanic ash: A review for volcanic risk mitigation. *Bulletin of Volcanology*, 69(1), 1–24.
- Höskuldsson, Á., Janebo, M., Thordarson, T., Andrésdóttir, T. B., Jónsdóttir, I., Guðnason, J., Schmith, J., Moreland, W. & Magnúsdóttir, A. Ö. (2018). *Total Grain Size Distribution in Selected Icelandic Eruptions* (p. 2018). http://futurevolc.vedur.is/data/Gosva/Total_Grain_Size_Distribution_in_Selected_Icelandic_Eruptions_01.pdf.
- Höskuldsson, Á., Þórðarson, Þ., Schmith, J. & Larsen, G. (2018). *Um eðli Kötlugosa. Kötlurádstefna*. www.vik.is/files/124/201811141312374037aee756747e567afb885a3a85881a.pdf.
- Hurst, T. & Smith, W. (2004). A Monte Carlo methodology for modelling ashfall hazards. *Journal of Volcanology and Geothermal Research*, 138(3–4), 393–403.
- IVHNN. (2008). *Volcanic Gases and Aerosols Guidelines*. http://www.ivhnn.org/images/pdf/gas_guidelines.pdf.
- Janebo, M. H., Thordarson, T., Houghton, B. F., Bonadonna, C., Larsen, G. & Carey, R. J. (2016). Dispersal of key subplinian–Plinian tephra from Hekla volcano, Iceland: Implications for eruption source parameters. *Bulletin of Volcanology*, 78(10), 66.

- Jenkins, S., Barsotti, S., Hincks, T., Neri, A., Phillips, J., Sparks, R., Sheldrake, T. & Vougioukalakis, G. (2015). Rapid emergency assessment of ash and gas hazard for future eruptions at Santorini Volcano, Greece. *Journal of Applied Volcanology*, 4(1), 16.
- Jenkins, S., Magill, C., McAneney, J. & Blong, R. (2012). Regional ash fall hazard I: a probabilistic assessment methodology. *Bulletin of Volcanology*, 74(7), 1699–1712.
- Jónsdóttir, T. (2015). *Grain size distribution and characteristics of the tephra from the Vatnaöldur AD 871±2 and Katla 1918 eruptions, Iceland* [MS thesis]. University of Iceland.
- Jónsson, P. (2007). *Eyðing Bæjar í Öraefasveit í Öraefajökulsgosinu 1362* [BS thesis]. University of Earth Sciences, Iceland.
- Jørgensen, K. (1981). The Thórsörk ignimbrite: A review. In *Tephra Studies* (Self S., Sparks R.S.J., Vol. 75, pp. 347–354). Springer.
- Kavanagh, J. L., Engwell, S. L. & Martin, S. A. (2018). A review of laboratory and numerical modelling in volcanology. *Solid Earth*, 9(2), 531–571.
- Lacasse, C. (2001). Influence of climate variability on the atmospheric transport of Icelandic tephra in the subpolar North Atlantic. *Global and Planetary Change*, 29(1–2), 31–55.
- Larsen, G. (2000). Holocene eruptions within the Katla volcanic system, south Iceland: Characteristics and environmental impact. *Jökull*, 49, 1–28.
- Larsen, G. (2002). A brief overview of eruptions from ice-covered and ice-capped volcanic systems in Iceland during the past 11 centuries: Frequency, periodicity and implications. *Geological Society, London, Special Publications*, 202(1), 81–90.
- Larsen, G. & Eiríksson, J. (2008). Late Quaternary terrestrial tephrochronology of Iceland—Frequency of explosive eruptions, type and of tephra deposits. *J. Quat. Sci.*, 23, 109–120. doi.org/doi: 10.1002/jqs.1129.
- Larsen, G. & Gudmundsson, M. T. (2016a). Bárðarbunga. In: Óladóttir, B., Larsen, G. & Guðmundsson, M. T. *Catalogue of Icelandic Volcanoes*. IMO, UI and CPD-NCIP. <http://icelandicvolcanoes.is/?volcano=BAR>.
- Larsen, G. & Gudmundsson, M. T. (2016b). Katla. In: Óladóttir, B., Larsen, G. & Guðmundsson, M. T. *Catalogue of Icelandic Volcanoes*. IMO, UI and CPD-NCIP. <http://icelandicvolcanoes.is/?volcano=KAT>.
- Larsen, G., Róbertsdóttir, B., Óladóttir, B. A. & Eiríksson, J. (2019). A shift in eruption mode of Hekla volcano, Iceland, 3000 years ago: Two-coloured Hekla tephra series, characteristics, dispersal and age. *Journal of Quaternary Science*.
- Larsen, G. & Thordarson, T. (2016). Hekla. In: Óladóttir, B., Larsen, G. & Guðmundsson, M. T. *Catalogue of Icelandic Volcanoes*. IMO, UI and CPD-NCIP. <http://icelandicvolcanoes.is/?volcano=HEK>.
- Loughlin, S. C., Sparks, S., Brown, S. K., Jenkins, S. F. & Vye-Brown, C. (Eds.) (2015). *Global Volcanic Hazards and Risk*. Cambridge University Press; Cambridge Core. doi.org/10.1017/CBO9781316276273.
- Loughlin, S. C., Vye-Brown, C., Sparks, R. S. J., Brown, S. K., Barclay, J., Calder, E., Cottrell, E., Jolly, G., Komorowski, J.-C., Mandeville, C., Newhall, C. G., Palma, J. L., Potter, S. & Valentine, G. (2015). An introduction to global volcanic hazard and risk. In Loughlin, S., Sparks, S., Brown, S., Jenkins, S., & Vye-Brown, C. (Eds.), *Global Volcanic Hazards and Risk* (pp. 1–80). Cambridge University Press; Cambridge Core. doi.org/10.1017/CBO9781316276273.003.
- Macedonio, G. & Costa, A. (2012). Brief communication. Rain effect on the load of tephra deposits. *Natural Hazards and Earth System Science*, 12(4), 1229–1233.
- Macedonio, G., Costa, A. & Folch, A. (2008). Ash fallout scenarios at Vesuvius: Numerical simulations and implications for hazard assessment. *Journal of Volcanology and Geothermal Research*, 178(3), 366–377.

- Marzocchi, W., Sandri, L., Gasparini, P., Newhall, C. & Boschi, E. (2004). Quantifying probabilities of volcanic events: The example of volcanic hazard at Mount Vesuvius. *Journal of Geophysical Research: Solid Earth*, 109(B11).
- Mastin, L. G., Guffanti, M., Servranckx, R., Webley, P., Barsotti, S., Dean, K., Durant, A., Ewert, J. W., Neri, A. & Rose, W. I. (2009). A multidisciplinary effort to assign realistic source parameters to models of volcanic ash-cloud transport and dispersion during eruptions. *Journal of Volcanology and Geothermal Research*, 186(1–2), 10–21.
- McCormick, M. P., Thomason, L. W. & Trepte, C. R. (1995). Atmospheric effects of the Mt Pinatubo eruption. *Nature*, 373(6513), 399.
- Moles, J. D., McGarvie, D., Stevenson, J. A., Sherlock, S. C., Abbott, P. M., Jenner, F. E. & Halton, A. M. (2019). Widespread tephra dispersal and ignimbrite emplacement from a subglacial volcano (Torfajökull, Iceland). *Geology*, 47(6), 577–580.
- Moreland, W. M., Thordarson, T., Houghton, B. F. & Larsen, G. (2019). Driving mechanisms of subaerial and subglacial explosive episodes during the 10th century Eldgjá fissure eruption, southern Iceland. *Volcanica*, 2(2), 129–150.
- Negro, C. D., Fortuna, L. & Vicari, A. (2005). Modelling lava flows by Cellular Nonlinear Networks (CNN): Preliminary results. *Nonlinear Processes in Geophysics*, 12(4), 505–513.
- Neri, A., Aspinall, W. P., Cioni, R., Bertagnini, A., Baxter, P. J., Zuccaro, G., Andronico, D., Barsotti, S., Cole, P. D. & Ongaro, T. E. (2008). Developing an event tree for probabilistic hazard and risk assessment at Vesuvius. *Journal of Volcanology and Geothermal Research*, 178(3), 397–415.
- Newhall, C. & Hoblitt, R. (2002). Constructing event trees for volcanic crises. *Bulletin of Volcanology*, 64(1), 3–20.
- Newhall, C. & Self, S. (1982). The volcanic explosivity index (VEI) an estimate of explosive magnitude for historical volcanism. *Journal of Geophysical Research: Oceans*, 87(C2), 1231–1238.
- Óladóttir, B. A., Larsen, G. & Sigmarsson, O. (2011). Holocene volcanic activity at Grímsvötn, Bárðarbunga and Kverkfjöll subglacial centres beneath Vatnajökull, Iceland. *Bulletin of Volcanology*, 73(9), 1187–1208.
- Óladóttir, B. A., Larsen, G., Thordarson, T. & Sigmarsson, O. (2005). The Katla volcano S-Iceland: Holocene tephra stratigraphy and eruption frequency. *Jökull*, 55, 53–74.
- Óladóttir, B. A., Sigmarsson, O., Larsen, G. & Thordarson, T. (2008). Katla volcano, Iceland: Magma composition, dynamics and eruption frequency as recorded by Holocene tephra layers. *Bulletin of Volcanology*, 70(4), 475–493.
- Osman, S., Rossi, E., Bonadonna, C., Frischknecht, C., Andronico, D., Cioni, R. & Scollo, S. (2019). Exposure-based risk assessment and emergency management associated with the fallout of large clasts at Mount Etna. *Natural Hazards and Earth System Sciences*, 19(3), 589–610.
- Pagneux, E. P., Guðmundsson, M. T., Karlsdóttir, S. & Roberts, M. J. (2015). *Volcanogenic floods in Iceland: An assessment of hazards and risks at Öraefajökull and on the Markarfljót outwash plain*. Reykjavik: Icelandic Met Office.
- Palais, J., Taylor, K., Mayewski, P. A. & Grootes, P. (1991). Volcanic ash from the 1362 AD Oraefajokull eruption (Iceland) in the Greenland ice sheet. *Geophysical Research Letters*, 18(7), 1241–1244.
- Pallister, J., Papale, P., Eichelberger, J., Newhall, C., Mandeville, C., Nakada, S., Marzocchi, W., Loughlin, S., Jolly, G. & Ewert, J. (2019). Volcano observatory best practices (VOBP) workshops—a summary of findings and best-practice recommendations. *Journal of Applied Volcanology*, 8(1), 2.
- Pilcher, J., Bradley, R., Francus, P. & Anderson, L. (2005). A Holocene tephra record from the Lofoten Islands, arctic Norway. *Boreas*, 34(2), 136–156.

- Prata, A. & Tupper, A. (2009). Aviation hazards from volcanoes: The state of the science. *Natural Hazards* 51(2):239-244.
- Richter, N., Favalli, M., de Zeeuw-van Dalftsen, E., Fornaciai, A., Fernandes, R. M. da S., Pérez, N. M., Levy, J., Victória, S. S. & Walter, T. R. (2016). Lava flow hazard at Fogo Volcano, Cabo Verde, before and after the 2014-2015 eruption. *Natural Hazards & Earth System Sciences*, 16(8).
- Scaini, C., Folch, A. & Navarro, M. (2012). Tephra hazard assessment at concepción Volcano, Nicaragua. *Journal of Volcanology and Geothermal Research*, 219, 41–51.
- Scaini, C., Biasse, S., Galderisi, A., Bonadonna, C., Folch, A., Smith, K. and Höskuldsson, A., 2014. A multi-scale risk assessment for tephra fallout and airborne concentration from multiple Icelandic volcanoes—Part 2: Vulnerability and impact. *Natural Hazards and Earth System Sciences*, 14(8), pp.2289-2312.
- Scire, J. S., Robe, F. R., Fernau, M. E. & Yamartino, R. J. (2000). A user's guide for the CALMET Meteorological Model. *Earth Tech, USA*, 37.
- Scire, J. S., Strimaitis, D. G. & Yamartino, R. J. (2000). A user's guide for the CALPUFF dispersion model. *Earth Tech, Inc. Concord, MA*, 10.
- Scollo, S., Coltelli, M., Bonadonna, C. & Del Carlo, P. (2013). Tephra hazard assessment at Mt. Etna (Italy). *Natural Hazards and Earth System Sciences*, 13(12), 3221–3233.
- Selbekk, R. S. & Trønnes, R. G. (2007). The 1362 AD Öraefajökull eruption, Iceland: Petrology and geochemistry of large-volume homogeneous rhyolite. *Journal of Volcanology and Geothermal Research*, 160(1–2), 42–58.
- Sharma, K., Self, S., Blake, S., Thordarson, T. & Larsen, G. (2008). The AD 1362 Öraefajökull eruption, SE Iceland: Physical volcanology and volatile release. *Journal of Volcanology and Geothermal Research*, 178(4), 719–739.
- Sólnes, J., Sigmundsson, F. & Bessason, B. (2013). *Náttúruvá á Íslandi: Eldgos og jarðskjálftar*. Reykjavík: Viðlagatrygging Íslands, Háskólaútgáfan.
- Sparks, R., Aspinall, W., Crossweller, H. & Hincks, T. (2013). Risk and uncertainty assessment of volcanic hazards. *Risk and Uncertainty Assessment for Natural Hazards*, 364–398.
- Spence, R., Kelman, I., Baxter, P., Zuccaro, G. & Petrazzuoli, S. (2005). Residential building and occupant vulnerability to tephra fall. *Natural Hazards and Earth System Sciences*, 5(4), 477–494.
- Spinetti, C., Barsotti, S., Neri, A., Buongiorno, M., Doumaz, F. & Nannipieri, L. (2013). Investigation of the complex dynamics and structure of the 2010 Eyjafjallajökull volcanic ash cloud using multispectral images and numerical simulations. *Journal of Geophysical Research: Atmospheres*, 118(10), 4729–4747.
- Stewart, C., Johnston, D., Leonard, G., Horwell, C., Thordarson, T. & Cronin, S. (2006). Contamination of water supplies by volcanic ashfall: A literature review and simple impact modelling. *Journal of Volcanology and Geothermal Research*, 158(3–4), 296–306.
- Sutawidjaja, I. S., Prambada, O. & Siregar, D. (2013). The August 2010 Phreatic Eruption of Mount Sinabung, North Sumatra. *Indonesian Journal on Geoscience*, 8(1), 55–61.
- Thorarinsson, S. (1958). The Öraefajökull eruption of 1362. *Acta Naturalia Islandica*, 2(2).
- Thordarson, T. & Höskuldsson, Á. (2007). The Eruption of Öraefajökull 1362 and the Destruction of the District Herad, SE Iceland. *Shimabara: Cities on Volcanoes 5*. Japan, 19–23 November 2007.
- Thordarson, T. & Höskuldsson, Á. (2008). Postglacial volcanism in Iceland. *Jökull*, 58, 197–228.
- Thordarson, T. & Larsen, G. (2007). Volcanism in Iceland in historical time: Volcano types, eruption styles and eruptive history. *Journal of Geodynamics*, 43(1), 118–152.
- Thordarson, T. & Self, S. (1996). Sulfur, chlorine and fluorine degassing and atmospheric loading by the Roza eruption, Columbia River Basalt Group, Washington, USA. *Journal of Volcanology and Geothermal Research*, 74(1–2), 49–73.

- Thordarson, T. & Self, S. (2003). Atmospheric and environmental effects of the 1783–1784 Laki eruption: A review and reassessment. *Journal of Geophysical Research: Atmospheres*, 108(D1), AAC-7.
- Thordarson, Thorvaldur & Larsen, G. (2007). Volcanism in Iceland in historical time: Volcano types, eruption styles and eruptive history. *Journal of Geodynamics*, 43(1), 118–152.
- Tomlinson, E., Thordarson, T., Müller, W., Thirlwall, M. & Menzies, M. (2010). Microanalysis of tephra by LA-ICP-MS—strategies, advantages and limitations assessed using the Thorsmörk Ignimbrite (Southern Iceland). *Chemical Geology*, 279(3–4), 73–89.
- Walker, G. (1962). Tertiary welded tuffs in eastern Iceland. *Quarterly Journal of the Geological Society*, 118(1–4), 275–290.
- Wilson, T. M., Stewart, C., Sword-Daniels, V., Leonard, G. S., Johnston, D. M., Cole, J. W., Wardman, J., Wilson, G. & Barnard, S. T. (2012). Volcanic ash impacts on critical infrastructure. *Physics and Chemistry of the Earth, Parts A/B/C*, 45, 5–23.
- Witham, C., Barsotti, S., Dumont, S. et al (2020). Practising an explosive eruption in Iceland: outcomes from a European exercise. *J Appl. Volcanol.* 9, 1. doi.org/10.1186/s13617-019-0091-7.
- Porkelsson, B., Karlsdóttir, S., Gylfason, Á. G., Höskuldsson, Á., Brandsdóttir, B., Ilyinskaya, E., Guðmundsson, M. T. & Högnadóttir, Þ. (2012). *The 2010 Eyjafjallajökull eruption, Iceland*. [Report to ICAO].